Functional markers for cerebral norepinephrine deficiency in Alzheimer's disease

Dissertation

zur

Erlangung des Doktorgrades (Dr. rer. nat.)

der

Mathematisch-Naturwissenschaftlichen Fakultät

der

Rheinischen Friedrich-Wilhelms-Universität Bonn

vorgelegt von

Verena Maria Kiven

aus

Bedburg

Bonn, 2020

Angefertigt mit Genehmigung der Mathematisch-Naturwissenschaftlichen Fakultät
der Rheinischen Friedrich-Wilhelms-Universität Bonn

1. Gutachter: Prof. Dr. Klaus Fließbach

2. Gutachter: Prof. Dr. Michael Hofmann

Tag der Promotion: 22.01.2021

Erscheinungsjahr: 2021

Table of Contents

List of abbreviations

AB(1/2)	Attentional blink (with one target/two targets per trial)
ACC	Anterior cingulate cortex
AChEI	Acetylcholinesterase inhibitor
AD	Alzheimer's disease
AD-dementia	Alzheimer's disease with dementia
AD-MCI	Mild cognitive impairment due to Alzheimer's disease
APP	Amyloid precursor protein
BOLD	Blood-oxygen-level-dependent
CERAD	Consortium to establish a registry for Alzheimer's disease
Contrast T-D	Contrast analysed in the OB paradigm: target vs. distractor
Contrast T-S	Contrast analysed in the OB paradigm: target vs. standard
CSF	Cerebrospinal fluid
EEG	Electroencephalography
EOG	Electrooculography
ERP	Event-related potential
fMRI	Functional magnetic resonance imaging
FOV	Field of view
HC	Healthy control subjects
ICA	Independent component analysis
ISI	Interstimulus interval
LC	Locus coeruleus
LC-NE system	Locus coeruleus-norepinephrine system
L-DOPS	L-threo-dihydroxyphenylserine
M	Mean
Mdn	Median
MMSE	Mini Mental State Examination
MPRAGE	Magnetisation prepared rapid acquisition gradient echo
MRI	Magnetic resonance imaging
NE	Norepinephrine
NIA-AA	National Institute on Aging - Alzheimer's Association
No-target trial	Trial without any target presentation (in AB1 paradigm)
OB	Oddball
OFC	Orbitofrontal cortex
PDR	Pupil dilation response
PET	Positron emission tomography
PETT	Positron emission transverse tomograph
PFC	Prefrontal cortex
ROI	Region of interest
RSVP	Rapid serial visual presentation
RT	Reaction time
SD	Standard deviation
SE	Standard error
SEM	Standard error of the mean
SOA	Stimulus-onset asynchrony
T1	Target 1
T2	Target 2
TE	Echo time; parameter for MRI

List of figures

List of tables

Summary

Pathological alterations of the locus coeruleus (LC)-norepinephrine (NE) system occur early in the course of Alzheimer's disease (AD), and manifest in poor attention and distractibility. Cortical NE is released from the LC nucleus, located within the upper dorsolateral pontine tegmentum of the brainstem, and is substantially involved in the regulation of attentional processes. This interaction can be summed by the Yerkes-Dodson relationship describing that basic tonic LC activity during undirected attention is replaced by a short (100-200 ms) phasic LC response after occurrence of a novel, motivational relevant stimulus. This adaptation leads to a NE-mediated increase in signal processing to appropriate target regions. Effects of the impaired allocation of NE on cognitive deficits in AD are subject of extensive research. However, before the effectiveness of noradrenergic interventions can be proven, it is first necessary to identify behavioural and physiological correlates of NE-deficiency.

The electrophysiological P3 component and the non-luminance mediated pupil dilation response (PDR) are extensively discussed physiological parameters of the LC-NE system. Accuracy and reaction time obtained in Attentional blink (AB) and Oddball (OB) paradigms represent possible behavioural correlates. Aim of this thesis was to evaluate to what extent these non-invasive parameters can be established as markers for early NE deficiency in AD. To investigate potential disease-dependent alterations, the study included 24 patients with AD and 26 healthy controls (HC). Additionally obtained structural measures of LC volumes were used to analyse correlations with physiological and behavioural parameters of LC-NE system functionality.

Evaluation of task performances, electrophysiological data and the PDR revealed inconclusive outcomes. Accuracies obtained in OB and AB1 paradigms, as well as the PDR evoked by the OB paradigm were reliably decreased in early AD patients. Evidence for a statistical correlation of OB-accuracies with structural dimensions of the LC nucleus was admittedly missing. Previous studies, however, demonstrated that the target detection rate was highly associated with LC phasic responses. For this reason, it is assumed that the significantly lower OB-accuracy in AD patients reflected degenerative alterations of the LC-NE system. These conclusions justify the usage of the parameter OB-accuracy as behavioural correlate for early NE deficiency in AD.

Furthermore, LC volumes did not show robust correlations with AB1-accuracies in AD patients. But HC demonstrated improved performances in association with higher LC intensities and larger LC volumes. This outcome suggests that the LC nucleus plays an important role for task performance. It was previously shown that tasks requiring stimulus detection, novelty and motivational relevance evoke increased activity in the brain region comprising the LC nucleus. These attributes can be ascribed to the AB1 paradigm. Based on these considerations it is concluded that the measured group difference reflected a malfunctioning LC-NE system in the patient group. The AB1-accuracy is therefore advised to be used as behavioural marker for NE deficiency in AD.

The PDR evoked by the OB paradigm represents a physiological parameter that was sensitive for disease-related changes of the LC-NE system. The main parameter of interest was the entire pupillary deflection from baseline evaluated by using statistics correcting for the multiple comparison problem. Additional support for this conclusion is provided by significant relationships between PDR and structural LC dimensions. The PDR is therefore suggested to be an appropriate correlate for NE deficiency in AD patients.

The remaining investigated parameters were either not sensitive for degeneration of the LC-NE system or they indicated ambiguous outcomes. The AB2 paradigm induced floor effects that give rise to justified doubts about the validity of the test results. Based on the present data, it is not possible to evaluate the effects of the AD-related NE deficiency on the behavioural parameter AB2-accuracy. Performance of the AB1 paradigm failed to generate robust P3 components in both groups. The assumption is that the test conditions did not reliably activate the neural network that is involved in P3 generation. Some of the discrepancy concerning the electrophysiological P3 findings may be due to small statistical power.

In conclusion, the present study identified three different correlates of NE deficiency: OB-accuracy, AB1-accuracy and the PDR evoked by an OB paradigm. These markers can support diagnosis and proof the effectiveness of new drugs targeting the LC-NE-system. In particular, they provide an important requirement for further pharmacological interventions that are based on β-receptor agonists.

1. Introduction

1.1 Alzheimer's disease

The western society shows a continuous increase in life expectancy and there is a growing demand of understanding age-associated diseases. One relevant issue is formed by neurodegenerative processes which become manifest in neuronal cell death, and the reduction or the loss of function. Brain regions involved in cognitive functioning are often affected by neurodegeneration and the associated neurological symptoms might result in the psychiatric syndrome dementia. An estimated prevalence of 47 million people worldwide suffered from dementia in 2015 and around 60-70% of all cases represented the neurodegenerative disorder Alzheimer's disease (AD) (reviewed by World-Health-Organization, 2017).

In 1906, it was Alois Alzheimer who first reported the case of a patient, Auguste Deter, suffering from memory loss, progressive changes in personality and pronounced psychosocial impairment. After performing extensive post mortem brain studies, he hypothesized that the disease pattern might be a result of massive neuron loss and tiny foci of peculiar substances in the cerebral cortex (Cipriani *et al.*, 2011). Alzheimer summarized these findings in one independent medical condition that later on was named after him.

Today, extensive research shed further light on the underlying mechanisms of AD. The disease is pathologically characterized by cellular changes within the central nervous system that can be detected by *in vivo* measures around 20 years prior to the development of cognitive decline. Accumulations of extracellular β-amyloid plaques and intraneuronal formation of abnormal tau tangles are the main cause for failed nutrients transfer, and eventually for cell death (H. Braak *et al.*, 2011). These degeneration processes structurally and clinically manifest in the hippocampus which is, amongst others, involved in memory consolidation (H. Braak & Braak, 1991; reviewed by Turkington & Mitchell, 2010). While the disease progresses, the neuron loss also affects other brain regions like the amygdala, basal forebrain and the neocortex.

The extensive decline in neuronal density goes along with distorted functions and altered behaviour. Symptoms, however, emerge gradually over a longer time

period. Alzheimer's disease is a progressive disorder that shows various stages depending on the level of cognitive decline (clinical criteria) or biomarkers (research criteria). The symptomatic predementia phase of AD is characterized by a degree of cognitive impairment exceeding age-appropriate decline (Albert *et al.*, 2011). Patients demonstrate an objective deficit in one or more cognitive domains, but they largely perform their daily life independently. This phase is referred to as mild cognitive impairment due to AD (AD-MCI). The primary underlying pathophysiology is AD which is corroborated by various biomarkers: the rate of brain atrophy revealed by magnetic resonance imaging (MRI), positive amyloid positron emission tomography (PET), elevated cerebrospinal fluid (CSF) tau or low CSF β-amyloid ($A\beta_{42}$). Once the progressive cognitive impairment constrains work or daily life, the disease transitions from AD-MCI to the dementia phase of AD (AD-dementia) (Albert *et al.*, 2011; McKhann *et al.*, 2011). This stage is associated with objective, chronic decline in at least two cognitive domains including learning and recall of new information (McKhann *et al.*, 2011).

While the most obvious cognitive impairment in early AD concerns memory formation, in later stages neocortical functions like language, problem-solving, executive and visuospatial functions are also affected (reviewed by Perry & Hodges, 1999). Malfunctioning basic attentional processes, however, might be an underrated problem in early AD because it is difficult to detect the accompanying impairments in daily life. Many patients appear to have concentration problems or they are easily distractible. These symptoms are ascribed to attention deficits developing early in the course of the disease and being correlated with the severity of AD-associated pathology (Foldi, Lobosco, & Schaefer, 2002). In early AD, attention deficits represent the first cognitive indicator of neurodegeneration in neocortical brain regions (reviewed by Parasuraman & Haxby, 1993).

Attention is a cognitive domain that comprises of many component processes ranging from attentional modulation of visual stimuli to shifting spatial attention and to detection, filtering and inhibition of environmental stimuli. Although attentional focusing appears to be preserved in AD, there is growing evidence for an impaired selective attention early in the course of the disease (reviewed by Perry & Hodges, 1999). Selective attention includes various processes like visual object selection and response inhibition. In AD patients, a dysfunction of this attentional domain affects the ability to disengage and shift attention to different environmental stimuli with

discriminating characteristics like colour or shape (reviewed by Parasuraman & Haxby, 1993). These findings are supported by studies showing a decreased performance of AD patients in detection and discrimination tasks. It was concluded that tasks requiring selective attention are the most sensitive in detecting attentional deficits in early AD (Perry, Watson, & Hodges, 2000).

Recent studies point to the locus coeruleus-norepinephrine system (LC-NE system) as a mediator of selective attentional processes. There is reasonable suspicion that pathological alterations of this system induce attention deficits in AD. Before reflecting this potential link, it is necessary to get a deeper insight into the nature of the LC-NE system itself.

1.2 The locus coeruleus-norepinephrine system

1.2.1 Anatomy and neuronal connections of the locus coeruleus

The locus coeruleus (LC) is a small, tube-like shaped nucleus located deep within the upper dorsolateral pontine tegmentum of the brainstem. In humans, the rostrocaudal extension of the LC measures approximately 16 mm and comprises around 22000 – 51000 neurons per hemisphere (e.g. German *et al.*, 1988; Giorgi *et al.*, 2017; Mouton *et al.*, 1994). A stereotactic investigation of anatomical hallmarks of the LC did not find gender-specific variations of LC dimensions (Fernandes *et al.*, 2012). Due to its pigmented appearance resulting from neuromelanin storage, the LC is clearly detectable on macroscopic scale. The polymer neuromelanin is formed by oxidation of the catecholamine norepinephrine (NE) from its precursor dopamine and has been identified as a valid marker for noradrenergic neurons in the LC region (Baker *et al.*, 1989; Wakamatsu *et al.*, 2015). Within the central nervous system, LC neurons have been confirmed as the sole source of cortical NE (Dahlström & Fuxe, 1964; reviewed by Foote, Bloom, & Aston-Jones, 1983; reviewed by Moore & Bloom, 1979). A schematic overview of the anatomical location of the LC and its efferent NE pathways is shown in figure 1.

Norepinephrine shows modulatory effects on neurons within the LC and in widespread target regions. These effects are mediated via three types of NE receptors: α1, β and α2. The first two types are mainly located at the postsynaptic

neuron and have both excitatory and inhibitory effects. The group of α2 receptors is localized at pre- and postsynaptic neurons and inhibits the signal conduction to the postsynaptic neuron. Within the LC nucleus, the most important NE receptors are α2-receptors (Benarroch, 2009). Therefore, the LC-NE system shows manifold effects dependent on the type of NE receptors located in target regions (Del Tredici & Braak, 2013; Samuels & Szabadi, 2008).

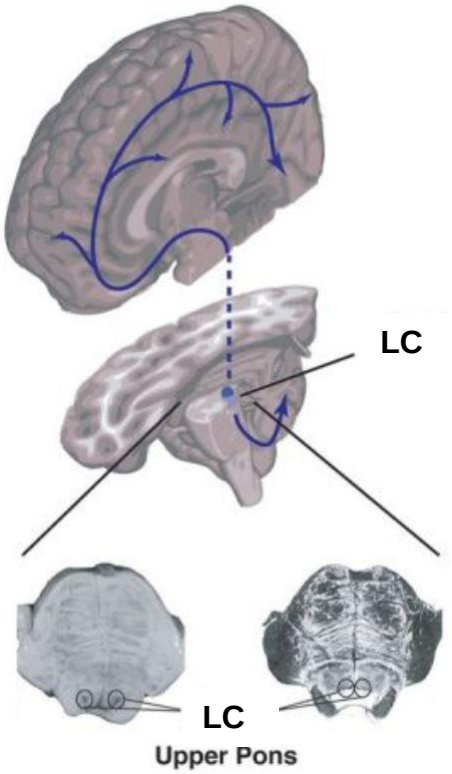

Figure 1. Anatomy and efferent pathways of the LC-NE system.
The human LC nucleus is bilaterally located in the posterior pons and its efferent neurons branch to the cerebral, cerebellar and hippocampal cortices. The pigmented appearance of the LC results from neuromelanin storage. Neuromelanin is a polymer accumulating from the oxidation of the catecholamine NE. The LC represents the sole source of cortical NE.

The figure was modified from Jenkins, Mehta, and Sharp (2016).

Extensive investigation of noradrenergic effects on cortical neurons revealed that NE increases the local inhibitory and excitatory signal propagation. At the same time NE also suppresses spontaneous activity of these neurons (Aston-Jones & Cohen, 2005b; Benarroch, 2009). In this way, NE actively contributes to an enhanced "signal-to-noise" ratio and eventually, to improved processing of incoming sensory signals (Sara, 2009).

Locus coeruleus neurons do not consistently release the same amount of NE; they rather adapt the allocation of NE to particular demands. Significant environmental stimuli have the potential to trigger NE release. Once the neurotransmitter is released into the synaptic cleft, it binds to α2-receptors with the

effect to inhibit the presynaptic neuron. This autoregulatory inhibition lasts for about 200-500 ms and in this time frame ("refractory period") no further action potential is propagated (Berridge & Waterhouse, 2003; Nieuwenhuis *et al.*, 2005).

Innervation of LC neurons is mediated by various brain regions maintaining excitatory connections to the nucleus. Therefore, the firing rate of LC neurons is controlled by the amygdala (Del Tredici & Braak, 2013), the orbitofrontal cortex (OFC) (Aston-Jones *et al.*, 2002) and the anterior cingulate cortex (ACC) (Aston-Jones *et al.*, 2002; Del Tredici & Braak, 2013; Rajkowski *et al.*, 2000).

The LC nucleus controls the NE concentration in other brain regions via wide axonal connections to the cerebral, cerebellar and hippocampal cortices (Foote, Bloom, & Aston-Jones, 1983; Moore & Bloom, 1979). The ACC is both a source of input to the LC and at the same time also a target region (Gompf *et al.*, 2010). The complex interaction between the LC and the distinct brain structures might be an important mediator of cognition. Evidence points to a noradrenergic contribution to complex cognitive processes like attention, behavioural flexibility, learning as well as working memory consolidation and retrieval (Borodovitsyna et al., 2017).

1.2.2 The locus coeruleus-norepinephrine system and cognition

Progress in research revealed that the LC-NE system is not only involved in increasing arousal and promoting the sleep/wake cycle (Berridge & Waterhouse, 2003; Devilbiss & Waterhouse, 2004; Waterhouse & Woodward, 1980). Beyond that, certain levels of NE contribute to the detection of environmental stimuli by priming sensory neurons. Application of pharmacological agents promoting the cortical NE supply provided evidence for facilitated processing of visual stimuli in primary sensory neurons (Borodovitsyna, Flamini, & Chandler, 2017; Navarra *et al.*, 2017; Zitnik, Clark, & Waterhouse, 2014). Experiments with auditory signals (Manunta & Edeline, 2004) and those activating the gustatory sense (Heath *et al.*, 2006) also demonstrated that NE increased the neuronal sensitivity for relevant information in the domain-specific cortical target regions. At the same time, irrelevant information processing appears to be inhibited. These results fit in with the previously described NE-mediated facilitation of the local "signal-to-noise" ratio that results in improved stimulus discrimination (Sara, 2009).

Recently, there are indications that functioning of LC neurons exceeds simple sensory processing. If the LC non-specifically enhanced the neuronal sensitivity in response to all environmental information, it would be impossible to detect relevant stimuli. Therefore, the working mechanism of the LC-NE system is potentially more flexible than originally assumed. Two distinct, fundamental modes of information processing are involved: tonic and phasic neuronal activity. The tonic mode is characterized by a continuous, long-lasting firing pattern that shows variations in frequency. In the phasic mode, signal transmission occurs via short activity increases that are limited in time. There are some theories that LC neurons hold the ability to adapt the neuronal firing mode to individual environmental situations (e.g. reviewed by Aston-Jones & Cohen, 2005b). In accordance with these conclusions are studies pointing to a correlation between cortical NE concentrations, the firing rate of LC neurons and attention.

These findings suggest that an adaptive behaviour of the LC activity contributes to the selective processing of relevant stimuli. Filtering of incoming sensory information is a necessary requirement for the proper functioning of attention processes. It involves the inhibition of irrelevant information while simultaneously relevant stimuli are focused and processed. The adaptive gain theory explains how alterations of LC-NE system activity are correlated to modulated cognitive performance.

1.2.3 The adaptive gain theory

Previous studies show that the LC-NE system actively regulates sustained and flexible attention that exceeds the promotion of simple stimulus processing (reviewed by Aston-Jones & Cohen, 2005a; Corbetta, Patel, & Shulman, 2008; Del Tredici & Braak, 2013). Presumably, a sort of filter controlled by the LC or its target regions is responsible for specific LC responses to relevant information. According to Aston-Jones and Cohen (2005b) the underlying mechanism of action can be explained by the adaptive gain theory. This theory postulates that the adaptation of the LC-NE system is implemented by switching the neuronal activity between tonic and phasic firing modes.

The tonic mode of LC neurons is related to flexible and undirected attention while exploring the environment for new tasks. The subject is not focused on a

certain behavioural goal, and the LC-NE system functions as an attentional filter that is temporary specific and spatially global. Therefore, the subject's ability for perceiving important stimuli is increased. The tonic mode is associated with basic activity of LC neurons that is consistent and does not show single, prominent increases in the firing rate. Variations of the firing frequency result in different levels of tonic arousal. These levels determine the subject's sensitivity for detecting new information: intermediate arousal is related to optimized, focused attention while higher or lower levels produce less efficient attentive behaviour (reviewed by Aston-Jones & Cohen, 2005b; Aston-Jones, Rajkowski, & Cohen, 1999). The resulting inverted-U relationship between LC activity and optimization of performance is represented in figure 2.

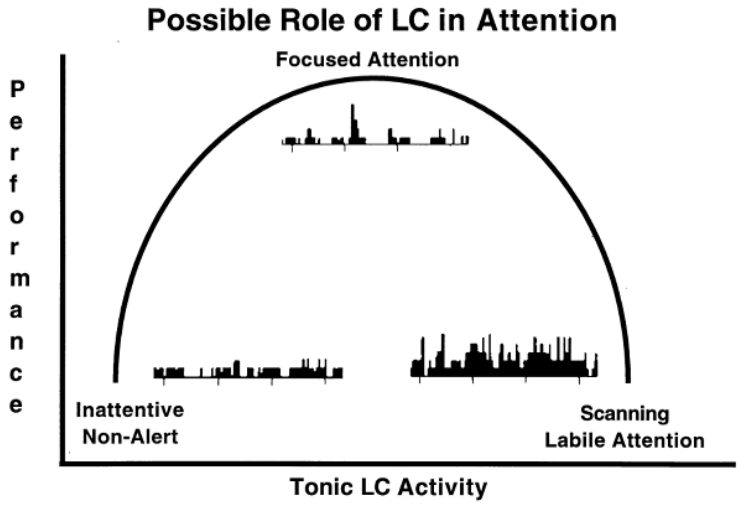

Figure 2. Relationship between tonic LC activity and attention.
The arousal curve representing the inverted-U relationship between activity of LC neurons and performance on a task requiring focused attention. Low levels of tonic LC activity are related to a non-alert, inattentive state and result in poor cognitive performance. Moderate tonic and prominent phasic firing rates of LC neurons optimize the behavioural performance. This state of focused attention can be triggered by the occurrence of a motivational relevant target stimulus. High levels of tonic LC activity without any phasic bursts cause poor performance levels.

Reprinted from Aston-Jones, Rajkowski, and Cohen (1999).

Intermediate tonic arousal increases the probability for a shift in the phasic mode to optimize task engagement respectively exploitation of the environment. Appearance of a novel, task-relevant stimulus elicits fast, phasic firing rates of LC neurons. According to the adaptive gain theory, this mode leads to a NE-mediated increase in signal processing to appropriate target regions. As a result, behavioural attention increases within 100-200 ms so that the performance is optimized. About 200-500 ms after stimulus appearance, LC neurons enter the refractory period and do not indicate any responsiveness at all.

Adaptation of the LC firing mode is controlled by prefrontal brain areas. As previously mentioned, the ACC and the OFC maintain neuronal connections to the LC nucleus. Both prefrontal structures are highly involved in rating the benefit that comes along with fulfilling of a task and accordingly, they selectively innervate LC neurons to evoke a certain response (reviewed by Aston-Jones & Cohen, 2005b). Thus, the LC-NE system regulates the balance between exploration and exploitation, and induces the behaviour which is most appropriate for the individual situation.

Human studies (Gilzenrat *et al.*, 2010; reviewed by Nieuwenhuis, Aston-Jones, & Cohen, 2005) and those with monkeys (Aston-Jones *et al.*, 1994; Clayton *et al.*, 2004) support the adaptive gain theory and report a correlation of high performance levels with phasic activation of LC neurons. Clayton *et al.* (2004) investigated the impulse activity of monkey LC neurons during performance of a simple discrimination task. In accordance with the adaptive gain theory, two modes of LC activity were identified. Phasic LC activation preceded both correct and incorrect responses, but this pattern was only observed after presentation of task-related stimuli. After presentation of stimuli that did not require a response, there was only a slightly elevated tonic LC activity without any phasic bursts. Therefore it was concluded that the phasic LC response is an important antecedent to optimized performance levels in stimulus detection tasks (Clayton *et al.*, 2004).

In summary, the LC-NE system integrates attentional processing by controlling the sensitivity of target neurons according to the relevance of incoming information. This effect is mediated by switching from intermediate tonic activity to phasic LC firing in response to the perception of salient stimuli. Bursts of NE released to target regions, like hippocampus and prefrontal cortex (PFC), increase the activity of excitatory inputs and decrease the activity of inhibitory inputs. As a result, the

adaptive LC functionality optimizes the processing of salient stimuli and eventually, task performance.

1.3 The locus coeruleus-norepinephrine system in Alzheimer's disease

Although episodic memory deficits characterize the first clinical stage of AD, attentional deficits are also common or may even precede memory deficits. At an early disease stage, this deficit manifests in poor concentration or in easy distractibility (reviewed by Perry & Hodges, 1999).

A growing number of studies support the hypothesis that alterations in LC-NE system functionality contribute to cognitive deficits in AD (Heneka et al., 2010; Kelly et al., 2017; Wilson et al., 2013). Evidence for pathological alterations of the LC-NE system is provided by structural imaging as well as cythopathological and animal studies using models of AD.

1.3.1 Structural imaging of the locus coeruleus

Due to the small dimensions of the LC and its location in the dorsal pons of the brainstem, structural imaging of the nucleus poses a major challenge. However, there are recent attempts to visualize the nucleus by using the neuromelanin stored within LC neurons as an endogenous contrast agent. This approach is based on the ability of neuromelanin to bind heavy metals such as iron (Trujillo Diaz *et al.*, 2016).

The LC is visualized by the adaptation of a T1-weighted turbo spin echo scan sequence for MRI which is sensitive to neuromelanin (Keren *et al.*, 2015; Sasaki *et al.*, 2006). Using this method, bilateral hyperintense signals were found in those brain regions that correspond with areas of higher neuromelanin storage (Keren *et al.*, 2015; Naidich *et al.*, 2009; Sasaki *et al.*, 2006). An exemplary MRI scan based on this method is presented in figure 3A. A recent study showed that a high density of intracellular water protons interacting with neuromelanin is the source of the high MR signal located in the LC region (Watanabe *et al.*, 2019). However, other paramagnetic ions than neuromelanin could also be involved in generation of the obtained signal since brain areas with low neuromelanin content have similar MR

signals than LC regions (reviewed by Betts, Kirilina*, et al.*, 2019; Cassidy *et al.*, 2019; Watanabe *et al.*, 2019).

Validating LC images by comparing MR signals with histological samples faces some problems. Tissue fixation (Dusek *et al.*, 2019), post mortem redistribution of iron (N. Krebs *et al.*, 2014; Shima *et al.*, 1997) and a scanning temperature that differs from body temperature (Birkl *et al.*, 2014) are some aspects that could result in differences between MR signal and histology (reviewed by Betts, Kirilina*, et al.*, 2019). A combined approach of histology and post mortem MRI provides further insights into the validation of LC imaging. A specific template can be used to standardize individual brainstem images while maintaining individual variations in LC signal intensity (Keren *et al.*, 2009). The LC hyperintensities obtained by this approach are highly correlated with number and location of LC neuromelanin cells in post mortem tissue samples (Keren *et al.*, 2015).

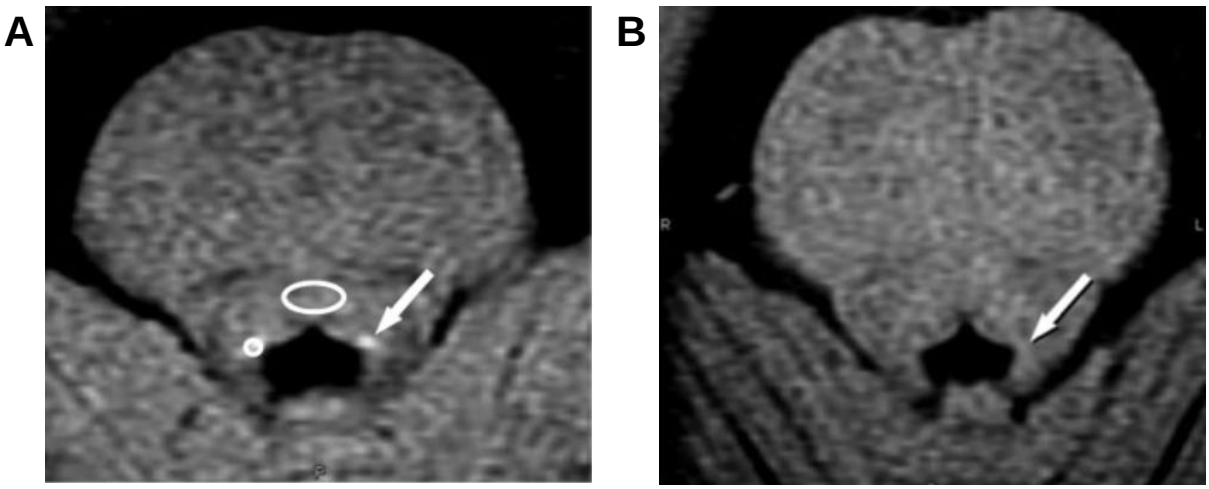

Figure 3. Neuromelanin-sensitive MRI scans.
The images show the pons and midbrain acquired from a healthy control subject (A) and a patient with AD (B). The arrows point to hyperintensity areas at locations corresponding to the LC. The small circle highlights the region of interest for measuring signal intensity in the LC and the large circle indicates the region of interest for the pontine tegmentum. The latter was used to calculate LC contrast ratios. In comparison to the control subject, the AD patient shows severely reduced hyperintensity areas. Underlying reason for this observation might be the decreased neuromelanin content due to neuronal depletion in the course of the disease.

The figure was modified from Takahashi *et al.* (2015).

Although more research is necessary to understand the processes contributing to neuromelanin-driven contrasts, this approach of *in vivo* LC visualization has the potential to support diagnosis and evaluate novel treatments. The obtained LC signals are moderately consistent for scan-rescan reliability (Betts *et al.*, 2017; Dahl *et al.*, 2019; Langley *et al.*, 2017; Tona *et al.*, 2017) and achieve reliability indexes that are similar to those of bigger structures in less susceptible brain regions (Tona *et al.*, 2017). Therefore, neuromelanin-sensitive MRI represents a promising, non-invasive method to determine structural alterations of the LC nucleus related to ageing or neurodegeneration.

Since neuromelanin-driven MRI strongly depends on the content of intracellular neuromelanin, it is important to keep in mind that neuromelanin concentrations stored in LC neurons vary with age (Manaye *et al.*, 1995; Mann & Yates, 1974). Younger adults could possibly not have reached the maximum neuromelanin concentration, yet. Therefore, neuromelanin does not represent a suitable marker for LC imaging in this age cohort (Liu *et al.*, 2019; Manaye *et al.*, 1995). Older adults show a stagnated rate of neuromelanin accumulation so that the obtained hyperintensities potentially correspond to the actual number of LC neurons. In the course of further ageing, LC neurons are lost and therefore, the neuromelanin content and the obtained LC signal intensity decrease (Liu *et al.*, 2019). These variations across the lifespan result in an inverted U-shaped relationship between LC signal intensity and age (Shibata *et al.*, 2006).

Recently, neuromelanin-sensitive MRI was used to investigate the relationship between memory performance and LC integrity. Dahl *et al.* (2019) reported that older participants showed better episodic memory when they had higher LC integrity. When comparing these results with data obtained in younger participants, functionally relevant age differences were found in the rostral LC. This segment maintains important connections to other brain areas that are involved in memory performance. It was concluded that the integrity of the LC-NE system represents an important aspect of successful cognitive ageing (Dahl *et al.*, 2019).

To date, there are only few attempts to use neuromelanin-sensitive MRI sequences to detect structural LC changes associated with neurodegenerative disorders. Patients suffering from pathological processes that come along with LC degeneration (such as Parkinson’s disease) show decreased LC intensities

compared to healthy controls (HC) (reviewed by Liu *et al.*, 2017; Ohtsuka *et al.*, 2013; Sasaki *et al.*, 2006).

One of the first studies using neuromelanin-sensitive MRI to examine LC volumes in patients with AD-MCI and AD-dementia was performed by Takahashi *et al.* (2015). Both patient groups indicated significantly reduced LC contrast ratios in comparison with HC. Figure 3B shows the neuromelanin-sensitive MR image obtained in an AD patient. This finding is in accordance with AD-related decrease of neuromelanin concentration as a result of neuronal loss in the LC. The researchers concluded that the parameters used for this measurement can be reliably applied in AD research to visualize LC degeneration. Recent studies further investigated the complex relationship between neuromelanin-driven MR images and AD pathology. The obtained LC contrast ratios are modulated by both CSF amyloid in early AD (Betts, Cardenas-Blanco*, et al.*, 2019) and the tau pathology at higher levels of amyloid burden (Jacobs *et al.*, 2018). The latter result was demonstrated by using tau and amyloid PET.

Neuromelanin-sensitive MRI scanning protocols reliably show reduced LC intensity ratios in neurodegenerative diseases that are associated with LC neuron loss. Because neuromelanin is stored within cell bodies of neurons, this approach provides further insights into disease-related changes in cell density, but not in synaptic density or in cell activity (reviewed by Betts, Kirilina*, et al.*, 2019). Although further research is necessary to conclusively elaborate on pathological alterations in AD, there are convincing indications for AD-associated decreased LC volumes in patients.

1.3.2 Cytopathological alterations in Alzheimer's disease

Alzheimer's disease manifests in manifold cytopathological alterations of the LC-NE system. Post mortem studies demonstrated degeneration and decline in neuronal density within the LC region of AD patients (Grudzien *et al.*, 2007; Kelly *et al.*, 2017; Lyness, Zarow, & Chui, 2003). Stereological estimates reveal 30% loss of total LC neurons in AD-MCI and additional 25% loss in AD-dementia (Kelly *et al.*, 2017). These observations might be the result of long lasting pathological processes beginning many years before the onset of the first clinical AD symptoms.

It is specifically the pathology of the microtubule-associated protein tau that is closely related to the loss of LC neurons. In AD patients, the protein is abnormally phosphorylated which results in aggregation of neurofibrillary tangles in neuronal cell bodies (Bancher *et al.*, 1989; E. Braak, Braak, & Mandelkow, 1994). These tangles are hypothesized to be spread to other brain regions via axonal connections (Goedert, 2015; Mohamed *et al.*, 2013). Abnormal tau deposits precede the degeneration of LC neurons by many years (Giorgi *et al.*, 2017; Theofilas *et al.*, 2017). H. Braak and Del Tredici (2011) discovered intraneuronal lesions in noradrenergic LC neurons in subjects younger than 30 years old. Malfunctioning LC-derived proximal axons interfere with proper transport of nutrients and could therefore be involved in the development of AD (H. Braak *et al.*, 2011). There is evidence for a positive correlation between the degree of hyperphosphorylated tau accumulation within the LC and the stage of AD (Theofilas *et al.*, 2017).

Another study points to a positive relationship between LC neuron loss or NE deficiency, respectively, and pathological β-amyloid accumulation in LC projection areas like hippocampus and frontal cortex (Heneka *et al.*, 2006). Additionally notable were the increased inflammatory processes in these brain regions. This finding supports the theory that NE is an essential regulator of inflammation by increasing microglial migration and phagocytosis of β-amyloid (reviewed by Feinstein *et al.*, 2002; reviewed by Giorgi *et al.*, 2019). The reduced supply of NE in LC target regions encouraged local inflammation and eventually accumulation of β-amyloid (Heneka *et al.*, 2010; Heneka *et al.*, 2006). Based on the complex relationship between NE loss, increased inflammation and β-amyloid plaques in LC target regions the researchers concluded that LC degeneration plays an essential role in the development of AD (Heneka *et al.*, 2006).

Further effects of the AD-associated pathology are altered concentrations of adrenergic receptors. In fact, the observed changes were rather inconsistent ranging from decreased α1 receptor densities in the PFC (Kalaria, 1989), hippocampus and cerebellum (Shimohama *et al.*, 1986), to slightly increased α1 binding sites in sublayers of the PFC (Szot *et al.*, 2007) and the hippocampus (Szot *et al.*, 2006). Increased densities of α2 receptors were found in the PFC (Kalaria *et al.*, 1989), the dentate gyrus (Szot *et al.*, 2006) and in microvessels (Kalaria *et al.*, 1989) that are innervated by LC neurons (Kalaria, Stockmeier, & Harik, 1989). Gannon *et al.* (2015)

reviewed the diverse AD-related changes in NE receptor concentrations for each subtype separately.

The described cytopathological alterations suggest that the LC nucleus plays an essential key role in the development and expression of AD. To date, there is no evidence for the underlying mechanism mediating this observation and the effects on specific functional deficits in AD remain unclear.

1.3.3 The locus coeruleus-norepinephrine system in animal models

Only few studies used animal models to explain the functional consequences of the impaired LC-NE system in AD. Established animal models in AD research are transgenic mice. They are characterized by overexpression of mutant amyloid precursor protein (APP) resulting in the development of extensive β-amyloid pathology. Additional AD-like impairment of the LC-NE system is induced by the neurotoxin N-(2-chloroethyl)-N-ethyl-bromo-benzylamine, or dsp4, which selectively depletes NE in LC neuron terminals. This results in a significant loss of NE in LC projection areas. These manipulations come along with enhanced inflammation, β-amyloid plaque accumulation and mnemonic deficits (Heneka *et al.*, 2006). The protecting characteristics of NE are probably based on NE functioning as a positive regulator of microglial β-amyloid clearance (Heneka *et al.*, 2010; Jardanhazi-Kurutz *et al.*, 2011).

To investigate the consequences of selective NE deficiency, Hammerschmidt *et al.* (2013) triggered a further gene manipulation leading to dopamine β-hydroxylase deficiency in an APP mouse model. In doing so, the NE synthesis was interrupted while the LC nucleus itself stayed intact. Double mutant mice showed impaired long-term potentiation and spatial memory deficits exceeding the deficits observed in single mutant mice. The behavioural deficits were partly reversed by treatment with the NE precursor drug L-threo-dihydroxyphenylserine (L-DOPS) (Hammerschmidt *et al.*, 2013). The positive effect of increased NE levels on cognition was observed in ageing rats (Luo *et al.*, 2015) and in other transgenic mice models of AD (Kalinin *et al.*, 2012; Kummer *et al.*, 2014). Although treatment with L-DOPS partially restored the memory deficits, it did not affect the β-amyloid deposition (Kummer *et al.*, 2014).

Another hallmark of AD, the tau pathology, represents a further target for the development of animal models. Tau transgenic mice show mutations that induce massive accumulation of hyperphosphorylated tau leading to a deficient assembly of microtubules (Bugiani *et al.*, 1999). Iba *et al.* (2015) unilaterally injected synthetic preformed tau fibrils into the LC of tau transgenic mice. This so-called tau-seeding approach enabled to investigate the distribution of the tau pathology from the LC region to anatomically connected brain areas (Clavaguera *et al.*, 2009). First, they discovered that the tau pathology was not only spread to afferent and efferent terminals of LC neurons, it was also transneuronally propagated to neurons located in widespread LC projection areas like the amygdala and frontal cortex. The resulting pathology was closely related to AD, while the un-injected control mice showed fewer similarities with AD. The researchers concluded that the tau pathology in the LC region is an essential factor for the development of neurodegeneration. Second, after six months they found significant cell loss in the LC ipsilateral to the injection site. In contrast, neurons were preserved for up to 12 months in the contralateral LC. This outcome revealed that the tau pathology was partially cleared as long as the burden did not exceed a certain value. Third, the LC-injected mice did not develop tau pathology in the hippocampus and entorhinal cortex, which poses a major difference to the pathology in early AD patients. The researchers suggested miscellaneous explanations for this finding, amongst others: neuronal connections from LC to these target regions had degenerated before pathological tau was propagated, other structures than the LC were involved in spreading tau to these regions, or the propagation of overexpressed tau in transgenic mice or synthetic tau, respectively, could differ from that of naturally developed pathological tau in AD (Iba *et al.*, 2015).

Ahnaou *et al.* (2019) replicated this tau-seeding approach in tau transgenic mice, but additionally they used multichannel electrodes for recording intracranial EEG. In this way they were able to investigate potential alterations in functional connectivity as a result of tau pathology. Interestingly, the brain area that had previously lacked tau pathology, the hippocampus (Iba *et al.*, 2015), showed robust dysfunctional networks. Neuronal activity significantly decreased in the ipsilateral hippocampus, while the contralateral hippocampus exhibited increased activity, possibly due to compensation. Thus, the tau accumulation in the LC was able to cause functional disturbances in brain areas that did not suffer from tau pathology, yet (Ahnaou *et al.*, 2019).

To summarize, these findings emphasize the important role of NE for normal cognitive functioning. Locus coeruleus degeneration, the accompanying NE deficit and the AD-associated pathology directly contribute to neuropathological changes and cognitive deficits in AD. Further knowledge of the consequences of LC degeneration is crucial for understanding AD and for providing a treatment target. Therefore, there is a great demand for identifying behavioural and functional correlates that might be utilized as surrogate markers for the functionality of the LC-NE system in AD patients.

1.4 Behavioural correlates of locus coeruleus-norepinephrine system functionality

To investigate behavioural effects of LC-NE deficiency, it is necessary to identify cognitive processes that are highly driven by noradrenergic action. The human brain is exposed to a huge load of environmental information. Because not all input can be efficiently processed, a selective attention system is required to filter relevant stimuli. Study results showed that the LC-NE system plays an important role in the modulation of the attention system (adaptive gain theory, reviewed by Aston-Jones & Cohen, 2005b).

Maintenance of attention and a vigilant state is associated with increased brain activity in the PFC, responsible for holding the task demands, and the superior parietal cortex (Pardo, Fox, & Raichle, 1991). Modulated NE release to the PFC is potentially controlled by the ACC and the OFC, which are both involved in monitoring task-related utility (reviewed by Aston-Jones & Cohen, 2005b; Cohen, Botvinick, & Carter, 2000; Han, Eaton, & Marois, 2018). These observations are in line with the model of a fronto-parietal control network that is essential for working memory and attention control. Performance related to the active maintenance of task goals when interfering and distracting stimuli occur is highly dependent of the activation of this network (Niendam *et al.*, 2012).

Pharmacological manipulations in monkeys (Arnsten, Steere, & Hunt, 1996), rats (Jentsch, Aarde, & Seu, 2009) and humans (Coull *et al.*, 1999) reveal the importance of NE for proper functioning of the fronto-parietal attention network. Noradrenergic antagonists reduced the detection rate of salient stimuli, while

noradrenergic agonists improved the functional integration of brain systems that are involved in attentional processes (Arnsten, Steere, & Hunt, 1996; Coull *et al.*, 1999; Jentsch, Aarde, & Seu, 2009).

According to the previously described adaptive gain theory (see chapter 1.2.3) NE is not released continuously to its target regions. The LC firing mode is rather adapted to individual environmental situations (e.g. reviewed by Aston-Jones & Cohen, 2005b). The tonic mode of LC neurons is characterized by undirected attention. In this mode, the LC functions as a temporary specific and spatially global filter for relevant stimuli that are salient in terms of frequency, novelty and motivational or emotional relevance (Berridge & Waterhouse, 2003; Sara, 2009). Variations of the firing frequency result in different levels of tonic arousal. Only the intermediate level optimizes focused attention by increasing the probability of switching into the phasic mode (reviewed by Aston-Jones & Cohen, 2005b; Aston-Jones, Rajkowski, & Cohen, 1999). Phasic activity is related to fast firing rates of LC neurons and leads to a NE-mediated increase in signal processing to its target regions. In this way, the selective attention for task-related stimuli increases and the behavioural performance is optimized (e.g. reviewed by Aston-Jones & Cohen, 2005b). For more details see chapter 1.2.3 “The adaptive gain theory”.

In summary, it is the modulated and flexible release of NE that contributes to selective processing of relevant stimuli. This leads to the theory that the LC-NE system poses a relevant key component for the regulation of attentional behaviour. Therefore, selective attention represents a suitable cognitive domain for investigating the functionality of the LC-NE system. Two neuropsychological tasks that potentially reflect the working mechanism of the LC-NE system are the “Oddball (OB) paradigm” and the “Attentional blink (AB) paradigm” investigated within the context of a rapid serial visual presentation (RSVP). Both tasks highly involve the attentional system and they require the complex NE-mediated balance between complexity and efficiency.

1.4.1 Target detection

Description of the task

The Oddball (OB) paradigm is a stimulus discrimination task that has been designed in different variants so far. A classical task design comprises of two different stimuli that are presented in a random order. Characteristically one of those stimuli occurs less frequently than the other one and is defined as a target. During the continuously on-going stimulus presentation, the participant is required to detect the target, typically by pressing a button or by mentally counting (e.g. Kiat, 2018; Polich, 1989; Verleger & Berg, 1991). The frequently occurring stimuli (standards) need to be ignored. The 2-stimulus variant of the OB paradigm can be extended to a 3-stimulus task. In this approach, an additional infrequent non-target stimulus (distractor) is presented within the stimulus stream and does not require a reaction. Perception of the involved stimuli can be mediated by different sensory systems since experimental setups vary across auditory (Cecchi *et al.*, 2015; Polich, 1989; Verleger & Berg, 1991), visual (Bledowski *et al.*, 2004) or tactile (Bolton & Staines, 2014) stimuli.

The low number of targets demanding a participant's reaction and the minimal response output suggest that the task difficulty is quite low. However, performance of the OB paradigm still requires a constant vigilant state and considerable effort is necessary since the involved neuronal mechanisms are quite complex. Processing of the presented stimuli may induce different neural responses dependent on predictability and motivational relevance of the perceived stimulus type. The LC neurons fire in a tonic activity pattern while perceiving standard stimuli because they appear frequently and are not relevant for fulfilling the task. In this mode, the system efficiently scans the stimulus stream for task relevant events. The perception of infrequent stimuli (targets and distractors) selectively triggers phasic release of NE to LC projection areas for a fast and efficient processing (e.g. Aston-Jones *et al.*, 1994; Rajkowski, Kubiak, & Aston-Jones, 1994). Further evaluation of salient stimuli leads to optimized behavioural responses by either detecting targets or ignoring distractors.

Explanation of the oddball effect

Previous findings show that the visual perception of a novel, unexpected stimulus (target) presented within a stream of repeated stimuli subjectively appears to persist

for a longer time compared to standards (Pariyadath & Eagleman, 2008; Tse *et al.*, 2004). There are thoroughly discussed attempts to explain this so-called oddball effect. Theories focused on a decreased attention level in response to standard presentation as underlying cause (Tse *et al.*, 2004). Continuously repeated standards fulfil the expectation of perceiving that certain type of stimulus. To reduce metabolic costs, this prediction results in a more efficient neural processing of repeated stimuli (Grill-Spector, Henson, & Martin, 2006). This view is in line with a reduced neuronal response to repeated stimuli as assessed by cortical brain imaging (Henson & Rugg, 2003) and EEG (Grill-Spector, Henson, & Martin, 2006). The concept of the adaptive gain theory (e.g. reviewed by Aston-Jones & Cohen, 2005b) is consistent with these findings. Standard stimuli are not relevant for task performance and therefore, they do not address the attention system. The resulting intermediate tonic activity of LC neurons functions as a filter for finding the task relevant targets (Berridge & Waterhouse, 2003; Sara, 2009).

According to the context-updating hypothesis (Donchin, 1981; Donchin & Coles, 1988), the working memory system is highly involved in the evaluation of incoming stimuli: once a stimulus has entered the processing system, working memory compares this stimulus with the previously detected stimuli. In case the stimulus is congruent with the prediction, the neural mode of the stimulus environment remains stable. When the prediction of an upcoming stimulus presentation is violated, as it is the case by perceiving a novel target, the sensory processing serves as an alert. Neural activity increases in response to the changed environmental circumstances which is indicated by an increased brain activity elicited by novel stimuli (Grill-Spector, Henson, & Martin, 2006; Henson & Rugg, 2003). In terms of the adaptive gain theory it means that LC neurons temporally switch into the phasic firing mode to enhance NE release to brain regions involved in stimulus evaluation (e.g. reviewed by Aston-Jones & Cohen, 2005b). Attentional resources are shifted towards the appropriate target stimulus and the goal-relevant information is updated in accordance with the currently processed target.

Eventually, it is the combination of predictive coding and neural adaptation that optimizes attention and stimulus processing in a stimulus discrimination task, such as the OB paradigm (Desimone & Duncan, 1995; Grill-Spector, Henson, & Martin, 2006). The flexibility of the LC-NE system enables the neural mode to switch into a phasic firing pattern once a target stimulus was perceived. As a result, the sensitivity

to changing sensory input is increased so that novel stimuli more likely attract attention (Hawkins *et al.*, 1990; Schindel, Rowlands, & Arnold, 2011). This incidence explains the occurrence of the oddball effect: the apparently elongated target presentation is based on an increased attentional level that is spent on the target in comparison with standards.

Neuronal correlates involved in the oddball paradigm

Research has been engaged in finding the neuronal correlates that are involved in the attentional shift towards salient stimuli. Pardo, Fox, and Raichle (1991) investigated the brain activity during performance of a simple stimulus detection task requiring sustained attention. Simultaneously, they used the intravenous $H_2{}^{15}O$ technique (Herscovitch, Markham, & Raichle, 1983; Raichle *et al.*, 1983) with a positron emission transverse tomograph (PETT VI) system (Yamamoto, Ficke, & Ter-Pogossian, 1982). This approach measured changes in local tissue radioactivity during task performance. The obtained changes were synonymously associated with changes in regional blood flow because they were linearly related to each other (Pardo, Fox, & Raichle, 1991). The study showed increases in local blood flow in the prefrontal and superior parietal cortex. The effect was independent of the sensory modality. Other studies also report sensitivity of the PFC to changes in the probability of an event (Casey *et al.*, 2001; McCarthy *et al.*, 1997).

It is important to distinguish between brain areas involved in visual attention modulations (e.g. extrastriate cortex) and the potential sources of such modulation (e.g. frontal cortex) (Posner & Driver, 1992). These distinct brain areas were activated during performance of a stimulus discrimination task that focused the attention on changes in shape, colour and speed of visual stimuli (Corbetta *et al.*, 1991). Simultaneously, they obtained PETT VI recordings after administration of $H_2{}^{15}O$ as blood flow tracer. The researchers found increased brain activity not only in the extrastriate cortex but a.o. also in the ACC, part of the basal ganglia and the right lateral frontal cortex. Presumably, the latter brain regions are responsible for extrastriate amplifications, which is in line with other studies revealing the importance of the ACC for target detection and the preparation of an appropriate response (Ardekani *et al.*, 2002; Posner *et al.*, 1988).

These study results suggest that frontal and parietal brain regions are activated during performance of a stimulus discrimination task. Once a stimulus is

detected, both regions fulfil diverse functions: while the more anterior regions, like the ACC, are involved in target detection and response preparation, the parietal lobe induces the orientation to visual locations (Posner & Driver, 1992; Posner & Petersen, 1990).

The locus coeruleus-norepinephrine system and the oddball paradigm

Already early in the course of LC research, the LC was proposed to be a major regulator of alertness. Animal research showed that NE enhanced the "signal-to-noise" ratios in sensory neurons. Based on this finding, Servan-Schreiber, Printz, and Cohen (1990) developed a "top-down" neural network model which proposed that an increased "signal-to-noise" ratio improves signal detection (e.g. reviewed by Berridge & Waterhouse, 2003; Sara, 2009).

Because direct assessment of LC activity is challenging due to its small dimensions and its location in the brainstem, there are only few human studies investigating LC activity during performance of a stimulus detection task. However, by using functional magnetic resonance imaging (fMRI) it has been demonstrated that the brain region comprising the LC nucleus shows increased activity in paradigms requiring attention, prediction and stimulus detection (e.g. Kahnt & Tobler, 2013; Minzenberg *et al.*, 2008; Murphy *et al.*, 2014). Other studies have tested the effects of novelty (R. M. Krebs *et al.*, 2013) and motivational relevance (Mohanty *et al.*, 2008) on stimulus processing and found target-related increased neuronal activity in the LC and its associated projection areas.

A recent approach obtained LC activity during performance of an OB paradigm containing different types of salient stimuli: novel neutral targets, novel emotional targets, and familiar targets (R. M. Krebs *et al.*, 2018). As assessed by fMRI, the researchers found a lineally increasing LC activity from standard trials to familiar targets, to novel neutral targets and to novel emotional targets. Further analyses indicated that, compared to standard stimuli, only both categories of novel targets elicited robust LC activity increases. The result was independent of the target modalities "neutral" and "emotional". This finding suggests that it is the relative stimulus novelty within an OB task that recruits the LC-NE system, rather than emotional saliency, task relevance or contextual novelty (R. M. Krebs *et al.*, 2018).

The conclusion is that salient stimuli in an OB paradigm represent an ideal trigger for recruiting the LC-NE system. Especially stimulus novelty, as it is

characterized by rare targets embedded into frequently occurring standards, elicits LC-mediated phasic bursts of NE to its projection areas. Therefore, the OB paradigm represents a suitable task to investigate the functionality and degeneration of the LC-NE system in AD.

Behavioural correlates reflecting a norepinephrine deficiency

Parameters obtained during performance of an OB paradigm can be taken as an indirect measure of LC-NE system activity. Especially accuracy levels and the reaction time (RT) necessary for target identification are of great interest as behavioural correlates. Pharmacological manipulations with clonidine, a noradrenergic autoreceptor agonist which reduces LC-NE system activity, resulted in decreased neuronal responses during performance in an auditory OB paradigm. On behavioural level, participants showed decreased performance accuracy with simultaneously increased RT after receiving clonidine (Coull *et al.*, 1995; Lovelace, Duncan, & Kaye, 1996). This observation is in concordance with animal studies reporting correlations of accuracy levels with changing NE concentrations that were either natural (Aston-Jones *et al.*, 1994; Usher *et al.*, 1999) or pharmacologically induced (Ivanova *et al.*, 1997; Sirvio *et al.*, 1993). Norepinephrine depletion resulted in reduced phasic responses of LC neurons and thus, in reduced stimulation of brain areas that are involved in target processing. Eventually, both the target detection rate and the RT are highly dependent on LC phasic responses (reviewed by Nieuwenhuis, Aston-Jones, & Cohen, 2005).

Insufficient NE supply to target regions decreases the task-focused performance in an OB paradigm; in other words, the insufficiency shows direct impact on the behavioural correlates, accuracy and RT. Based on this theory, the previously described disturbances of the LC-NE system in AD might also result in altered behavioural responses obtained in an OB paradigm. There are only few studies reporting behavioural performance results of AD patients.

Polich and Corey-Bloom (2005) tested different modalities of OB paradigms in AD patients and compared the performance with that of healthy elderly subjects. They presented both auditory and visual tasks, each with various difficulty levels. The overall effect was that an increased task difficulty came along with increased error rates and RT. This correlation was especially evident in the AD group which also indicated a significantly lower accuracy and a longer RT compared to HC. Both

groups produced lower accuracy and longer RT in the visual task modality than in the auditory task. These experiments demonstrated that the OB paradigm produces behavioural effects on accuracy and RT that discriminate AD from healthy subjects (Polich & Corey-Bloom, 2005).

This result was further investigated in an auditory OB paradigm by comparing the performance of subjects with different stages of AD: AD-MCI and AD-dementia (Tsolaki *et al.*, 2017). For both groups, there was a stage-dependent decrease in target accuracy: AD-dementia was associated with the lowest accuracy, AD-MCI with an intermediate level and controls with the highest level. The RT was significantly longer in AD-dementia than in healthy elderly but did not differ in AD-MCI.

Apparently, both parameters are sensitive to task difficulty and early cognitive decline. Accuracy levels and RT obtained in an OB paradigm may thus represent behavioural correlates of NE deficiency in AD patients.

1.4.2 Attentional blink

A well investigated phenomenon in the human signal processing is the attentional blink (AB). It describes a deficit in visual selective attention that occurs when two motivational relevant stimuli need to be processed in close temporal proximity. There is strong evidence for the involvement of the LC-NE system in the development of the AB.

The rapid serial visual presentation task

The RSVP task uses alternating visual stimuli at the same position in rapid succession (Raymond, Shapiro, & Arnell, 1992). Typically, stimuli are presented with an interval of approximately 100 ms. Embedded into these stimuli are two targets that are distinguishable from distractors (e.g. two letters amongst digits), and need to be selected and processed by the subject. Targets are stimuli that are relevant for fulfilling the task while distractors have to be neglected. Below, both targets involved in the RSVP are referred to as target 1 (T1) and target 2 (T2). The subject's visual attention is examined by varying the number of distractors separating both targets: lag 1 corresponds to no intervening distractor while lag 2 means one intervening distractor, and so on.

Task performance is rated in terms of accuracy rates for correct identification of T2 at varying lag categories. While the performance on T1 identification is generally relatively accurate, identification of T2 strongly depends on the number of intervening distractors. There is a higher accuracy in correctly reporting T2 when the presentation of T1 and T2 is separated by a longer time interval (which equals a longer lag). However, the accuracy rate of T2 decreases when T2 presentation occurs only a few intervening distractors after T1 (Broadbent & Broadbent, 1987; Raymond, Shapiro, & Arnell, 1992). The AB occurs most frequently when both targets are presented with a temporal distance in the range of 200-500 ms (Jolicoeur, 1999a). After this time window, the performance of T2 identification gradually recovers.

Another interesting phenomenon related to the performance of the RSVP task is a so-called “lag 1 sparing”. This means that the correct identification of T2 is characteristically preserved when there is no intervening distractor between T1 and T2. Hence, the name of this effect derives from its temporally specific occurrence at lag 1 (Potter *et al.*, 1998).

The AB is typically obtained in a RSVP task of sequentially presented alphanumerical stimuli, but there are also designs obtaining an AB by using words (Luck, Vogel, & Shapiro, 1996), symbols (Chun & Potter, 1995), pictures (Evans & Treisman, 2005), auditory (J. Duncan, Martens, & Ward, 1997) or tactile (Hillstrom, Shapiro, & Spence, 2002) stimuli. From these findings it can be inferred that the AB represents an ubiquitous phenomenon in perceptual attention (reviewed by Martens & Wyble, 2010).

Explanations for the attentional blink

Though there were many studies investigating at what processing stage the blinked target is lost, no definite explanation for the physiological mechanisms has been reported, yet. Electrophysiological studies provide strong indications for the AB being a post-perceptual deficit (Dux & Marois, 2009). Situations without correct target identification reliably elicit EEG potentials that are associated with early perceptual (Vogel, Luck, & Shapiro, 1998) and semantic (Luck, Vogel, & Shapiro, 1996; Pesciarelli *et al.*, 2007) processing. Presumably, both targets are correctly assessed and semantically processed but some dysfunction afterwards prevents the conscious

access to the perceived information. One thoroughly discussed theory has been emerged to explain this phenomenon.

The interference model hypothesizes that a limited-processing capacity is involved in the development of the AB (Dux & Marois, 2009; Isaak, Shapiro, & Martin, 1999; Martens & Wyble, 2010). Processing of both targets leads to a competition for limited attentional resources. During task performance an attention filter efficiently selects T1 for further processing. The increased attention for T1 binds a high load of processing capacity which results in lacking capacities for successful T2 detection. Subsequently, conscious identification and storage of T2 is either postponed or incorrect (Dell'Acqua, Pascali*, et al.*, 2003; Jolicoeur, 1999b). This effect is only observed when the stimulus-onset asynchrony (SOA) is smaller than about 500 ms, while the temporal distance of larger SOAs prevents interference from T1. The interference model also provides an explanation for the observed “lag 1 sparing”: if T2 follows T1 in close temporal proximity at lag 1, processing of T2 appears within the attention filter for T1 and can be easily detected.

A limited-processing capacity as underlying mechanism for the AB is supported by studies using EEG (Martens, Elmallah*, et al.*, 2006) and magnetoencephalography (Shapiro *et al.*, 2006). Both techniques identify increased potentials associated with attention and working memory, such as the P3 respectively M3, in response to successful T1 identification when T2 is missing. The same potentials are decreased in response to T2 in AB trials (Martens, Elmallah*, et al.*, 2006).

In summary, the AB poses a deficit in the storage of T2 into working memory because the limited processing resources are already used to full capacity by T1 storage. The attention filter selecting the information being processed by the limited resources is controlled by a widespread neuronal system involving the complex LC-NE system.

Neuronal correlates of the attentional blink

Research has been engaged in finding the neuronal correlates that are involved in the attentional deficit. Studies using fMRI (Kranczioch *et al.*, 2005; Marcantoni *et al.*, 2003; Marois, Yi, & Chun, 2004) and EEG (Sergent, Baillet, & Dehaene, 2005) provided evidence for a reduced neuronal activity in the ACC, the lateral PFC and the posterior parietal cortex when T2 was not identified. These brain regions provide

relevant functions for target detection: lateral-frontal regions are related to processing and maintenance of goals, posterior-parietal regions are important for target selection and occipital regions are responsible for stimulus perception (Hommel *et al.*, 2006). Marois and Ivanoff (2005) suggested that the limited processing capacity observed in an RSVP stream can be traced back to a fronto-parietal network as neuronal base.

Two temporary long-range synchronization networks have been observed: brain regions that are involved in stimulus processing in a RSVP stream on the one hand and brain regions related to target processing on the other hand (Gross *et al.*, 2004). Synchronization within these networks was decreased in trials with AB compared to trials with correct T2 identification. There are indications that the LC-NE system is involved in controlling these networks to optimize attention.

The locus coeruleus-norepinephrine system mediating the attentional blink

To elaborate how the LC-NE system is involved in the AB, it is necessary to have a closer look on the mechanisms regulating the release of NE to according brain regions. Alterations between phasic and tonic activity modes of LC cells promote selective attention or behavioural flexibility and attentiveness, respectively (Aston-Jones, Rajkowski, & Cohen, 1999; see also figure 2). This flexible activity pattern of the LC poses a potential mechanism explaining the AB (Nieuwenhuis *et al.*, 2005). Perception of salient stimuli, such as a target amongst distractors, is facilitated by an increased LC activity and subsequent phasic bursts of LC neurons. Those bursts augment the release of NE to target areas resulting in an enhanced responsiveness to their afferent input (Berridge & Waterhouse, 2003; Nieuwenhuis *et al.*, 2005). In this condition the attentional system can correctly process the perceived T1 to working memory and eventually, consciousness.

However, a neurobiological mechanism limits the benefit of NE for T2 processing. The underlying reason becomes evident when having a deeper look into the adaptive nature of the LC-NE system. The promoting effect of NE bursts to target brain areas is temporarily limited to less than 200 ms (Dux & Marois, 2009; Nieuwenhuis *et al.*, 2005). As soon as the NE concentration exceeds a certain value, an autoinhibitory process of the LC nucleus reduces its activity to subbaseline levels (Berridge & Waterhouse, 2003). This refractory period peaks approximately 50-100 ms after the phasic response of LC activity and lasts up to 200-500 ms after stimulus

onset. The temporal characteristics of the refractory period correspond notably well with the temporal occurrence of the AB (Usher *et al.*, 1999). During the refractory phase the attention system is limited in its response to subsequent targets and in recruiting further phasic LC bursts (Papesh & Guevara Pinto, 2019). A second target presented during this time period does not benefit from the supportive effect of NE which results in an impeded T2 processing.

These findings considerably suggest that the LC-NE system plays a crucial role in the development of the AB. Adaptation of the activity mode of the LC and the corresponding amount of NE release, are significant parameters for successful stimulus processing. Therefore, the AB characterizes a suitable paradigm for investigating the functionality of the LC-NE system.

The attentional blink as behavioural correlate for a norepinephrine deficiency

Based on this theory, the previously described degeneration of the LC-NE system might result in an altered AB effect in AD patients. Already early in the course of the disease patients require more time for letter recognition and show a reduced speed of central visual processing (Schlotterer, Moscovitch, & Crapper-McLachlan, 1984). This finding is independent of the age-appropriate visual acuity.

Peters *et al.* (2012) investigated the magnitude of the AB during performance of a RSVP task in AD patients. Two different task versions were presented to the participants: a single target condition and a dual target condition with one respectively two targets embedded into a sequence of digit distractors. The distance between the two targets, and therefore the task difficulty, varied by the number of intervening distractors. Performance in the single target condition did not show significant differences between AD patients and the control group. In the dual target condition, the patient group presented a more pronounced and prolonged AB effect than healthy elderly. The performance in the AD group approximated the performance of control subjects as the distance between both targets increased. This study provided evidence for a reduced ability to deal with two concurrent targets in AD patients. The finding of an elongated AB effect has previously been reported by two other studies examining stimulus processing in either a classical RSVP task with AD-dementia patients (Kavcic & Duffy, 2003) or a RSVP task requiring visuospatial orientation with AD-MCI subjects (Perry & Hodges, 2003).

These studies suggest that pathological disturbances of the LC-NE system, like those in AD, possibly exaggerate the deficit in detecting T2 shortly after T1 appearance (the AB). A potential underlying reason is the decreased release of NE in target regions and the resulting limited processing capacity. Presumably, this leads to an enhanced inter-target competition in AD patients compared to healthy age-matched controls and ends up in abnormal temporal dynamics of visual selective attention (Kavcic & Duffy, 2003). Therefore, the AB effect is a potential behavioural correlate of a dysfunctional LC-NE system in AD patients.

1.5 Potential measures of locus coeruleus-norepinephrine system functionality

In order to investigate the effects of NE deficiency in AD, it is necessary to identify correlates reflecting the functionality of the LC-NE system. Because size and location of the LC nucleus impede the direct assessment of neuronal activity, alternative methods for assessing brain activity need to be considered. Two non-invasive, feasible methods are EEG and pupillary recordings.

1.5.1 Electroencephalography: the P3 component

Electroencephalography represents an established tool for understanding neurophysiological and pathological processes. Brain activity is assessed by electrodes that are placed on different locations on the surface of the scalp. Due to the functional organization of the cortex, the detected electrical potentials vary in dependence of the location of the recording electrodes. The activity from deep sources is too small to be accurately measured by extracranial electrodes. Therefore, electrical currents produced within the cerebral cortex are most important for EEG recordings (reviewed by Siuly, Li, & Zhang, 2017).

To gain useful information about cognitive processes, cortical brain activity is measured in response to environmental stimuli. The so-called event-related potentials (ERP) are generated when the voltage fluctuations in the EEG are time-locked to sensory, motor or cognitive events. Event-related potentials are composed of a series of peaks that are called components. Electroencephalography data

generated in a single trial do not contain the ERP waveform only, but also random noise like muscle activity and electromagnetic interference. Further processing steps, like averaging and filtering, are required to isolate the signal of interest (reviewed by Huang, Chen, & Zhang, 2015; reviewed by Sanei & Chambers, 2007).

In comparison with background EEG activity, the ERPs appear rather small with voltages in the range from 1-30 µV. For this reason, it is necessary to average a large number of ERPs for extracting the signal of interest from the general electrophysiological activity. The more trials are included into the averaging, the more random noise is filtered out. This approach is based on the assumption that across a large number of trials, the ERP remains identical in shape and phase. In contrast, the random noise is largely independent of the time-locking stimulus and varies from trial to trial. While the averaging process diminishes the noise, a characteristic ERP waveform is retained (reviewed by Kamel & Malik, 2014; reviewed by Sanei & Chambers, 2007).

The nomenclature of the individual components of an ERP complies with two different parameters describing the particular voltage deflection: a letter (P, N) corresponding to the polarity (positive, negative) and digits representing either the latency in milliseconds after stimulus onset or the component's ordinal position in the waveform. It is assumed that the components occurring within the first 100 ms after stimulus onset can be ascribed to physical characteristics of the stimulus like intensity and frequency (exogenous components). Components evoked at later latencies are attributed to cognitive processes that are induced by stimulus detection (endogenous components) (reviewed by Sanei & Chambers, 2007).

A well investigated ERP component is the P300 or P3. In psychophysiological research, this component has been established as a reliable tool for the detection of attentional processes in stimulus detection tasks. There are also strong indications for the LC-NE system being involved in the generation of the P3.

The electrophysiological P3 associated with attention processes

The occurrence of P3 components has been observed after the conscious detection of infrequent, rare and task-relevant events. In young adults, the P3 peak latency averages at approximately 300-400 ms after target detection so that it represents the third major positive peak in an ERP waveform. The phenomenon was first observed by Sutton *et al.* (1965). They reported that a subject's degree of uncertainty with

respect to the sensory modality of the presented stimulus modulates ERP waveforms. This effect was also generated by the predictability of the sensory modality (Sutton *et al.*, 1965) and by an omitted but informative stimulus (Sutton *et al.*, 1967). Shortly after, the P3 was elicited in a visual and auditory OB paradigm for the first time (Ritter & Vaughan, 1969). The study identified a late positive component with a peak around 450 and 550 ms that was associated with the detection of a change in stimulating signals and that was only evident after successful target identification. This effect was independent of motor responses as the authors proved by further variations of their experiments. Investigation of the spatial distribution of the P3 component revealed a predominant occurrence over the parieto-central area of the scalp (Vaughan & Ritter, 1970).

Since then, the OB paradigm has become the most common task for investigating the P3 (reviewed by Nieuwenhuis, Aston-Jones, & Cohen, 2005). Profound research revealed two subcomponents that may be ascribed to the P3: P3a and P3b. The first subcomponent is associated with the detection of rare or alerting stimuli in situations demanding focussed attention. Using the terminology of the OB paradigm, the P3a is evoked by the discrimination between target/distractor and standard stimuli (Pardo, Fox, & Raichle, 1991; Posner, 1992; Posner & Petersen, 1990). For this reason the P3a is also referred to as “novelty P3” and peaks about 60-80 ms earlier than the P3b (reviewed by Nieuwenhuis, Aston-Jones, & Cohen, 2005). Its spatial distribution shows maximum deflections in electrodes covering the fronto-central cortex. This observation is in line with a fMRI study reporting frontal lobe activity in response to novelty (McCarthy *et al.*, 1997).

The P3b subcomponent is elicited by targets demanding event-categorization and memory updating of the stimulus representation (Donchin & Coles, 1988; Kok, 2001). The appearance probability of a task-related event also shows impact on the P3b amplitude: less probable events evoke larger amplitudes compared to more frequent events. Maximum positive deflections are generated by the parietal cortex (Donchin, 1981; Simson, Vaughan, & Ritter, 1977). In neurocognitive research, the use of the general term P3 usually addresses the P3b. Therefore, this subcomponent is also named the “classic P3”.

In summary, it can be assumed that the P3a is related to frontal activations while the subsequently emerging P3b is associated with temporal/parietal activations. This is in concordance with the thesis that rare stimuli induce top-down attentional

control and bottom-up memory-driven processes that control response output (Debener *et al.*, 2005; Huang, Chen, & Zhang, 2015). When incoming stimuli demand attention (both targets and distractors), the P3a-related frontal activity is linked to increased activity in the ACC and the subsequent transmission of the novel information to hippocampal regions. At this location, the attentional resources allocate memory updating and in case of processing target stimuli, the transmission of the particular output to the parietal cortex. Thereby, the P3b response can be obtained in an EEG. It is important to note that the hippocampus itself is unlikely to be directly involved in P3 generation because its electrical potentials cannot be measured by scalp electrodes (reviewed by Nieuwenhuis, Aston-Jones, & Cohen, 2005). Generally speaking, the P3 occurrence is a result of the interaction between frontal lobe and hippocampal/temporal-parietal functioning (reviewed by Huang, Chen, & Zhang, 2015).

Amplitude and latency of the maximum ERP deflection are reliable parameters for investigating the P3 component. Amplitudes are associated with the degree of allocated cognitive resources and the cognitive performance; P3 latencies potentially reflect the speed of information processing and, rather indirectly, cognitive performance (van Dinteren *et al.*, 2014). Previous research has shown that the amplitude, latency and the scalp topography of the P3 component are modulated by parameters that also affect cognition, like learning (Carrión & Bly, 2008) and age (Fjell, Walhovd, & Reinvang, 2005). In association with normal ageing, the P3 latency progressively increases with 1 to 2 ms/year, the P3 amplitude decreases and the spatial topography slightly shifts to frontal areas (Horvath *et al.*, 2018). Since smaller P3 amplitudes are related to a decreased task performance, they are suggested to represent age-related cognitive decline (Polich, 1996; van Dinteren *et al.*, 2014).

The P3 generated in the oddball and attentional blink paradigms

The P3 deflections are modulated by frequency and motivational significance of the eliciting stimulus (Kamp & Donchin, 2015; reviewed by Nieuwenhuis, Aston-Jones, & Cohen, 2005). For instance, emotionally task-relevant stimuli, both positive and negative, evoke larger P3 amplitudes than emotionally neutral events (Keil *et al.*, 2002). The stimulus modality presented in the paradigm also shows differential effects on the P3 deflection. Katayama and Polich (1999) reported that P3 amplitudes and latencies induced by a 3-stimulus OB paradigm using visual stimuli

were larger and longer, respectively, compared to those induced by auditory stimuli. Nevertheless, both stimulus modalities activated similar brain regions. Another parameter affecting the P3 is the amount of attention attributed to the stimulus. Only attended stimuli elicit a robust P3 component, while the same unattended stimuli fail to evoke such a response. This effect becomes evident when investigating dual task studies (Kok, 2001; Wickens *et al.*, 1983) or AB paradigms (Kranczioch, Debener, & Engel, 2003).

The study of Vogel, Luck, and Shapiro (1998) used a classic AB paradigm to investigate task-related ERPs. Components associated with early perceptual processing (P1 and N1) were largely unaffected by the attentional deficit following correct T1 identification. In contrast, the P3 component was completely suppressed in this time window (Nieuwenhuis *et al.*, 2005). This finding was explained by other studies observing P3 components in relation to T1 and T2 detection. Correct identification of T2 was related to a robust P3 generation while the unidentified T2 did not elicit the P3 component (e.g. Dell'Acqua, Jolicoeur*, et al.*, 2003; Kranczioch, Debener, & Engel, 2003; Shapiro *et al.*, 2005). Thus, the conscious perception of target stimuli influences the P3 deflection in an AB paradigm. But also the distance between both targets shows significant effects: a shorter temporal distance between T1 and T2 presentation is associated with a decreased P3 amplitude (Luck, 1998).

Additionally, P3 latencies shed light on the neural processing of targets in an AB paradigm. Martens, Munneke*, et al.* (2006) investigated the ERPs measured in 'blinkers' (showing a strong AB) and 'non-blinkers', separately. In comparison with the group of blinkers, non-blinkers indicated shorter P3 latencies after successful T1 and T2 detection. This result points to a quicker consolidation process in the non-blinker group which provides evidence for the P3 latency being a promising correlate of target processing.

Manifold studies showed that the electrophysiological P3 component poses a reliable physiological correlate of the processing of environmental events. Amplitude and latency of the P3 are modulated by different parameters like target frequency, relevance and the degree of cognitive demand necessary for task performance. These effects are evident in OB and AB paradigms. Therefore, the P3 represents a promising parameter for investigating target processing in both tasks.

Role of the locus coeruleus-norepinephrine system in P3 generation

To investigate the cognitive consequences of an AD-related NE deficiency, it is necessary to identify functional correlates of the LC-NE system. Evidence suggests that the electrophysiological P3 is a result of phasic bursts of NE in response to stimulus evaluation and decision making (reviewed by Nieuwenhuis, Aston-Jones, & Cohen, 2005). Similar antecedent conditions point to a correlation between P3 components and LC phasic responses. Both responses are closely related to motivational or emotional significance of an environmental stimulus (Berridge & Waterhouse, 2003; reviewed by Nieuwenhuis, Aston-Jones, & Cohen, 2005). Furthermore, the target probability shows direct modulatory effects on the P3 amplitude and the magnitude of LC responses: lower probability corresponds with both larger P3 amplitude and larger LC neuron firing (Alexinsky *et al.*, 1990).

These findings are integrated in the LC-P3 hypothesis stating that phasic activity of LC neurons and the subsequent release of NE play a decisive role in generating the P3. Evidence derived from neurophysiological research demonstrates that NE target regions are largely consistent with brain areas involved in P3 generation (reviewed by Nieuwenhuis, Aston-Jones, & Cohen, 2005). But there are also similarities between the temporal frame of the LC response and the time course of the typical P3 latency (300-550 ms): phasic neuron activity (equals approximately 150-200 ms poststimulus) plus NE physiological effects (equals approximately 150 ms postdischarge) plus the slow signal transmission velocity of NE fibers (Aston-Jones, Segal, & Bloom, 1980; Berridge & Waterhouse, 2003; Foote, Bloom, & Aston-Jones, 1983; reviewed by Nieuwenhuis, Aston-Jones, & Cohen, 2005).

The LC-P3 hypothesis is also corroborated by psychopharmacological studies using drugs that affect LC activity. One commonly used agent is clonidine, a noradrenergic autoreceptor agonist, which decreases the LC firing rate and thereby reduces NE release to target regions. Depending on the presentation modality of the OB paradigm, inconsistent effects were reported. Decreased P3 areas or amplitudes, respectively, were detected using an auditory OB design in animals (Swick, Pineda, & Foote, 1994) and in humans (Brown *et al.*, 2015; C. C. Duncan & Kaye, 1987; Joseph & Sitaram, 1989; Lovelace, Duncan, & Kaye, 1996). In contrast, the area and amplitude of the P3 component remained stable when elicited by visual OB stimuli in animals (Pineda & Swick, 1992) and humans (Lovelace, Duncan, & Kaye, 1996). The

effect of this modality asymmetry, however, is not robust since Halliday *et al.* (1994) demonstrated a decreased visual P3 component after clonidine treatment.

Lesion studies with monkeys (Pineda, Foote, & Neville, 1989) and rats (Ehlers & Chaplin, 1992) during performance of OB tasks provided further evidence for a reduced P3 potential as a result of LC neuron damage and NE reduction, respectively. The lesions did not affect the levels of dopamine or serotonin. Early ERPs associated with sensory processing did not indicate decreased deflections; they were rather increased on cortical level. These findings suggest that the LC-NE system specifically regulates neuronal processes that contribute to the electrophysiological P3 component.

There are only few studies investigating the correlation between the LC-P3 hypothesis and the AB. As explained previously, the activation dynamics of the LC-NE system and the subsequent refractory period after T1 detection correspond to the temporal profile of the behavioural attentional deficit (200-500 ms after T1). Since the P3 is suggested to pose an electrophysiological correlate of the LC-NE system, it is hypothesized that the occurrence of the P3 component and the AB show a similar temporal pattern. This assumption was confirmed for both targets: while the detection of T1 elicits a robust P3 (McArthur, Budd, & Michie, 1999), T2 presented during the AB fails to evoke a P3 (Vogel, Luck, & Shapiro, 1998). The latter effect is only observed for T2 stimuli that were not correctly identified; consciously detected T2 stimuli elicited normal P3 responses (Rolke *et al.*, 2001). These results indicate that the refractory period of LC neurons and the subsequent decreased NE supply to target areas lead to the absence of a subsequent P3 component. Thus, the neuronal refractory period provokes a complementary refractory period in P3 elicitation (reviewed by Nieuwenhuis, Aston-Jones, & Cohen, 2005). Correct T2 detection at lag 1 does not generate a robust P3, although the performance is often preserved ("lag 1 sparing") (Kranczioch, Debener, & Engel, 2003). According to Nieuwenhuis *et al.* (2005), this phenomenon might be explained by a benefit from remaining NE concentrations associated with T1 processing. While it shows positive effects on the behavioural accuracy for T2, the refractory period of LC neurons inhibits the generation of a second P3.

To summarize the results, the electrophysiological P3 is triggered by attention demanding processes that are controlled by the LC-NE system. Several studies showed that manipulated NE concentrations directly affect the occurrence of the P3

component. Based on these results, the P3 may be regarded as a non-invasive, physiological correlate of the LC activity. The combined use of attention tasks recruiting the LC-NE system and the electrophysiological P3 provide a promising approach for investigating the cognitive consequences of NE deficiency in AD.

The electrophysiological P3 in Alzheimer's disease

With respect to the demonstrated noradrenergic contribution to P3 generation and the previously described altered LC-NE system related to AD pathology, it can be hypothesized that AD patients produce altered P3 components compared to healthy elderly. A number of studies investigated this theory. Cecchi *et al.* (2015) used an auditory OB paradigm to elicit P3 components in patients with mild AD. The patient group exhibited lower P3 amplitudes and longer latencies compared to healthy age-matched controls. Follow-up analyses of the midline electrodes revealed that the disease-related changes were most prominent at central and parietal electrodes. These physiological alterations were accompanied by lower accuracy in target detection and longer RT. Other studies testing an auditory (Hedges *et al.*, 2016; Lai *et al.*, 2010; reviewed by Morrison *et al.*, 2018) or visual (Parra *et al.*, 2012) OB paradigm confirmed the results of the decreased amplitude and the longer latency of the P3 component in AD patients.

The separate analysis of patients with AD-MCI and AD-dementia sheds light on the progressive development of AD-related changes. Subjects with AD-MCI show prolonged P3 latencies compared to healthy controls, but still shorter latencies compared to AD-dementia patients (Horvath *et al.*, 2018; Morrison *et al.*, 2018). Thus, the stage of neurodegeneration in AD was correlated with P3 latencies. A meta-study confirmed these results for the P3 amplitude which appears larger in AD-MCI compared to AD-dementia (Jiang *et al.*, 2015). Therefore, the P3 component poses a reliable parameter for differentiating between symptomatic states of AD and for predicting the progression from AD-MCI to AD-dementia (Morrison *et al.*, 2018). Especially the P3 latency appears to represent a sensitive correlate of the patient's cognitive abilities (Lai *et al.*, 2010; Morrison *et al.*, 2018) and attention deficits (Lee *et al.*, 2013). These findings suggest that the electrophysiological P3 might be a reliable marker for detecting (preclinical) impaired attentional functioning in AD patients (Lee *et al.*, 2013; Parra *et al.*, 2012).

Event-related potential data show significant changes in AD patients that are consistent with cognitive deficits in memory and attention. This can be related to the disease-associated degeneration of brain areas that are relevant for P3 generation, such as parietal and frontal cortex, and hippocampus. However, it remains unclear to what extent the substantial alterations of the LC-NE system contribute to these effects. Studies investigating a potential correlation between the noradrenergic deficiency in AD and alterations of the P3 occurrence are still missing so that conclusive remarks are not possible.

1.5.2 Pupil dilation response

The pupil size is controlled by the autonomic nervous system with reciprocal innervations of sympathetic and parasympathetic neurons (reviewed by Beatty & Lucero-Wagoner, 2000). This complex interaction enlarges the pupil by directly stimulating the dilator muscles (sympathetic pathway) and by inhibiting the Edinger-Westphal complex to relax the sphincter muscles (parasympathetic pathway). Alterations of the pupil size can be elicited by different parameters like changes in environmental luminance, accommodation of the lens and sensory stimuli such as pain (reviewed by Beatty & Lucero-Wagoner, 2000).

There is evidence for an indirect noradrenergic control of the pupil size mediated via the sympathetic pathway in dimly lit environments (Szabadi, 2013). The LC-NE system effectively adapts the pupil size (Samuels & Szabadi, 2008) while it also plays a crucial role in mediating attentional processes (Aston-Jones & Cohen, 2005a, 2005b). Pupil sizes acquired in a dimly lit environment and associated with attention demanding stimuli might represent reliable physiological correlate for the LC-NE system.

The pupil dilation response associated with attention processes

The occurrence of motivational relevant events is associated with the so-called orienting response comprising a set of autonomic, physiological changes like a rise in skin conductance or a transient change in heart rate (Nieuwenhuis, De Geus, & Aston-Jones, 2011). Another well-established orienting response is the temporary dilation of the pupils which is often discussed in the context of the electrophysiological P3. Both parameters are elicited by the same environmental

stimuli, so it stands to reason that they involve the same or similar neurocognitive processes (Kamp & Donchin, 2015).

Pupil dilation in response to environmental stimuli may provide significant information about the occurrence and timing of attentional processes in the human brain. The parameters amplitude and latency are important parameters for investigating the pupil dilation response (PDR). As it was observed for the P3, the PDR is sensitive for stimulus novelty. An early study investigated the effects of an auditory OB paradigm on the pupil size (Qiyuan *et al.*, 1985). The event-related PDR to both targets and standards was inversely proportional to their probability. In multimodal task designs recording pupil diameter and EEG simultaneously an inverse relationship between target probability and the PDR amplitude respectively P3 amplitude was found (Friedman *et al.*, 1973; Steinhauer & Hakerem, 1992). The maximum pupil dilation occurred 1000-2000 ms after stimulus onset. More recent studies confirmed that the PDR is elicited by infrequent events in OB paradigms (Gilzenrat *et al.*, 2010; Murphy *et al.*, 2011).

Other studies investigated the PDR during performance of an AB paradigm. The effort necessary for processing T1 influences the accuracy of processing T2 (the AB phenomenon). This effect is mirrored in the pupil size which varies as a function of task-induced mental effort (Alnæs *et al.*, 2014; Porter, Troscianko, & Gilchrist, 2007; van Rijn *et al.*, 2012; Wolff *et al.*, 2015). By applying statistical models Wierda *et al.* (2012) and Zylberberg, Oliva, and Sigman (2012) estimated the load of mental effort that is necessary to consciously perceive both targets in an AB paradigm. The PDR showed that the more effort was invested in T1 processing, the lower were the accuracy and the PDR for T2. Additionally, they found a larger PDR at lag 1 compared to later lags. This effect might be elicited by the competition of two successive targets for processing capacity. Alternatively, it represents an indicator for the cost of temporal integration of two successive targets (Wolff *et al.*, 2015). Another study investigated the temporal dynamics of “lag 1 sparing” in AB paradigms. Wolff *et al.* (2015) demonstrated that an increased PDR after correctly identifying two successive targets might be due to the enhanced mental effort that was necessary to recruit a sufficient amount of processing capacities. Thus, the more mental effort is necessary to complete a task, the larger appears to be the PDR.

Although the electrophysiological P3 and the PDR often co-occur and show similar eliciting parameters, there are inconsistent results whether they correlate with

each other: while Friedman *et al.* (1973) reported a relationship between both parameters, there was no evidence for a correlation in the studies conducted by Murphy *et al.* (2011) and Kamp and Donchin (2015). The authors suggested that both parameters are associated with distinct functions since the PDR appears to be more closely linked to responding and the P3 is associated with stimulus evaluation (Kamp & Donchin, 2015).

These findings show that the PDR provides reliable information about attentional processes. The PDR is sensitive to novelty, motivational relevance and mental effort, and is most often elicited in OB paradigms. The LC-NE system might play a regulatory role in the adaptation of attention-dependent pupil sizes.

Role of the locus coeruleus-norepinephrine system in the pupil dilation response

Although LC neurons do not directly innervate pupil muscles, growing evidence points to the LC-NE system as potential regulator of event-related PDRs (Murphy *et al.*, 2014). This suggestion is based on single-cell recordings in animals. The pupil diameter significantly correlated with the monkey LC tonic activity and the behavioural performance (Joshi *et al.*, 2016; Rajkowski, 1993). Another animal study demonstrated a strong relationship between non-luminance mediated variations in pupil size and cortical arousal state (McGinley *et al.*, 2015). Given the evidence derived from animal studies, the phasic arousal of LC neurons might be measured in terms of the PDR.

Studies investigating human subjects reliably confirmed these results (Aston-Jones & Cohen, 2005b; Gilzenrat *et al.*, 2010; Jepma & Nieuwenhuis, 2011). The adaptive gain theory postulates that good performance is related to intermediate tonic LC activity with phasic bursts in response to infrequent, relevant stimuli. Poor performance and distractibility are associated with high tonic and low phasic LC activity. This activity pattern is also reflected by pupil sizes which show intermediate baseline (tonic) diameters and large phasic PDRs in correlation with optimized performances (Kamp & Donchin, 2015). Thereby, baseline pupil sizes and behavioural performance appear in a strong inverted U-relationship (Gilzenrat *et al.*, 2010; Murphy *et al.*, 2011). This finding suggests that the PDR reflects the pure phasic LC activity when the baseline pupil diameter is subtracted from the signal.

Further evidence for a correlation between LC-NE system activity and the PDR was obtained by pharmacological manipulations. The agent modafinil is a psychostimulant that inhibits NE transporters and results in increased synaptic NE, consistent with enhanced phasic LC responses. In contrast, clonidine is a noradrenergic autoreceptor agonist which presumably reduces NE release by binding the inhibiting α2-receptors. Hou *et al.* (2005) used both pharmacological agents in human subjects and found augmented LC-mediated pupil dilation in response to modafinil while the pupil diameter was reduced after clonidine. The researcher concluded that increased pupil diameters might be associated with enhanced activity of the LC-NE system (Minzenberg *et al.*, 2008).

One of the first human studies directly assessing the functional relationship of the LC-NE system with pupil sizes was reported by Murphy *et al.* (2014). During the performance of a 2-stimulus OB task the participants' brain activity was assessed using combined pupillometry and fMRI. The result was a strong positive correlation between target-induced LC activity as demonstrated by the blood-oxygen-level-dependent (BOLD)-contrast and the PDR. This outcome was confirmed by a recent study which additionally showed that fluctuations of LC responses are robustly coupled to fluctuations in the PDR amplitude (de Gee *et al.*, 2017). Typically, the pupillary responses are measured in terms of dilation amplitude and latency. The maximum amplitude is suggested to represent the proportion of NE release (reviewed by Beatty & Lucero-Wagoner, 2000), while the baseline pupil diameter is associated with tonic LC activity (Gilzenrat *et al.*, 2010; Rajkowski, 1993).

These study results provide substantial evidence for an attention-related noradrenergic modulation of the pupil diameter. Pharmacological manipulations of the NE availability and environmental conditions associated with increased LC-NE activity show noradrenergic effects on the PDR. In conclusion, the PDR obtained during performance of an OB paradigm might be used as a reliable, non-invasive marker of LC-NE system activity and potentially, noradrenergic deficiency.

The pupil dilation response in Alzheimer's disease

As described above, pupillary responses obtained during attention-demanding tasks are linked to the functioning of the LC. Early degenerative changes of the LC-NE system in AD might therefore result in altered PDRs in patients. To date, only one study investigated the effects of NE deficiency on the PDR. Dragan *et al.* (2017)

obtained the rates of changes in pupil size due to stimulus onset (pupil response velocity) in subjects at risk for developing AD, patients with AD and HC. To elicit the pupillary response, all participants performed a cognitive task requiring goal-directed search and memory. The study showed that memory effects were reflected by pupillary responses, but only in healthy participants. Stimulus onset elicited a general pupillary response that decreased with age and, in particular, with AD-related cognitive impairment. The researchers proposed that the observed pupillary changes were mediated by the LC system. However, it is important to note that a small sample size (n=9) was included in the group of early AD patients (Dragan *et al.*, 2017).

Although this study investigated pupil sizes in response to mnemonic processes rather than attention, this result provides important information about the general context of mental effort. Several studies suggest that pupillary responses that are modulated by mental effort might be used as a correlate for cognitive decline even before the task performance is affected (Ahern & Beatty, 1979; Beatty, 1982; Granholm *et al.*, 1996; van Der Meer *et al.*, 2010). An increasing pupil diameter is linked to increasing cognitive demands and inversely related to individual cognitive abilities. From this it follows that subjects with cognitive deficits show larger PDRs and maintained performance which probably reflects compensatory effort (Granholm *et al.*, 1996; Granholm *et al.*, 2017). Decreased pupil diameters and a poor task performance are the result of exceeding compensatory capacities. The latter thesis is in line with the study reporting decreased pupillary responses and performance in AD patients (Dragan *et al.*, 2017).

Based on these findings Granholm *et al.* (2017) investigated the PDR during a digit span task in AD-MCI patients indicating different stages of cognitive impairment. As predicted, the PDR differentiated the AD-MCI group from control subjects. Patients with moderate cognitive impairment showed larger PDRs while maintaining the same performance as the HC group. The task-induced increased pupil diameter possibly reflects the compensatory effort that was necessary to achieve the same performance as healthy subjects. This effect was limited to low and moderate levels of cognitive load. At high processing loads, pupil diameters decreased in those subjects that exceeded the limit of individual cognitive capacities. Patients with severe cognitive impairments presumably did not modulate resource allocation according to processing load as it is indicated by decreased PDRs and poor performances. So this group could have exceeded their capacities to compensate the

cognitive deficit. The authors proposed that this finding probably represents dysfunctions in the LC-NE system and related brain areas that are involved in cognitive effort allocation.

The investigated relationship between pupil size and modulatory actions of the LC-NE system on the one hand, and the early degeneration of the LC-NE system in AD on the other hand, suggest that the PDR might be used as a correlate for noradrenergic dysfunctions. However, to date no study with AD patients investigated the PDR during performance of attention tasks, such as the OB paradigm, and showed the direct relationship of the disease-associated LC degeneration and the PDR.

1.6 Aim of this thesis

The early detection of AD is inevitable for preventing, slowing and stopping the disease (reviewed by Alzheimer's Association Report, 2015). Therefore, research has been increasingly engaged in identifying markers that enable early diagnosis and the discovery of new drugs. Potential preclinical markers in dementia are parameters reflecting the functionality of the LC-NE system.

Cognitive processing of environmental stimuli is highly related to the allocation of NE and its modulatory effects in target brain areas. However, the system controlling NE release is affected in AD and distortions of the LC-NE system even contribute to the development of the AD-associated pathology. It remains elusive to what extent the NE deficiency contributes to cognitive deficits in AD. Before appropriate therapies targeting the LC-NE system can be developed, it is first necessary to identify markers of NE-deficiency and to find evidence for a causal relationship with LC degeneration. Especially the electrophysiological P3 and the PDR have been proposed as physiological correlates for the functioning of the LC-NE system.

Several studies indicated that the P3 component shows characteristic alterations associated with AD. To date, the non-luminance mediated PDR in AD patients is not well investigated. The previous studies reporting on this issue are either based on a small sample size (n=9) or AD-MCI patients only. None of these studies investigated the PDR elicited by target stimuli in an OB paradigm since pupil

dilations were rather based on mnemonic processes. The consistent relationship between both physiological parameters and the LC degeneration in AD remains elusive.

This study investigates the direct effects of AD-related NE deficiency on attention in a number of AD patients that is sufficient to perform correlation analyses between reliable behavioural, physiological and anatomical parameters of the LC-NE system. Within the scope of this thesis the following correlates were analysed and compared in AD patients and appropriate HC:

1) Behavioural correlates:
    a) RT and accuracy obtained in a 3-stimulus OB paradigm
    b) accuracy obtained in a simplified AB task (AB1 modality)
    c) the attentional deficit (AB) for T2 after detection of T1 (AB2 modality)
2) Physiological correlates:
    a) the electrophysiological P3b elicited during performance of a 3-stimulus OB paradigm and a simplified AB task (AB1 modality)
    b) the PDR elicited under the same conditions
3) Correlation analysis between all parameters and LC volumes.

This study aims to demonstrate to what extent these non-invasive parameters might be established as correlates for early NE deficiency in AD. In future clinical studies, the P3 and PDR could support diagnosis and the evaluation of noradrenergic interventions.

2. Methods

The following section describes the methodological approach to investigate the aims of this thesis. All experimental procedures were approved by the regional medical ethics committee (Ethik-Kommission Bonn, Germany, 12th June 2013) and conducted in accordance with the guidelines of the Declaration of Helsinki. All participants provided written informed consent after receiving detailed information about the experimental procedure.

2.1 Recruitment of subjects

All control subjects were recruited from a pool of interested healthy adults informed about the possibility to take part in the scientific work by advertisements in local newspapers, public talks or events organized by the German Center for Neurodegenerative Diseases. The group of patients with AD was recruited from the Memory Clinic (Klinisches Behandlungs- und Forschungszentrum für neurodegenerative Erkrankungen) at the University Hospital of Bonn, Germany. Prior to enrolling into the study all participants underwent a detailed medical interview conducted by the investigator to clarify exclusion criteria (see 2.2 Description of subjects) and to give an overview of the study procedures. Detailed written information was handed to the participants. All subjects received 70 Euros expense allowance for participation in the study.

2.2 Description of subjects

The study involved a between-subject design with 24 AD patients and 24 control subjects. Following the recommendations from the National Institute on Aging - Alzheimer's Association (NIA-AA) (Jack *et al.*, 2011), the study pooled patients in the clinical states of the disease: AD-MCI and AD-dementia. The NIA-AA defined the following clinical hallmarks for the AD-MCI group (Albert *et al.*, 2011): objective deficit in one or more cognitive domains without constraints in daily life; and for the AD-dementia group (McKhann *et al.*, 2011): objective, chronic decline in cognitive

functions with impairment of daily life. All AD patients were able to independently provide written consent and to understand the tasks. To get a homogeneous pool of patients, only those with a typical, amnestic type of AD were included. All AD patients were biomarker-tested and indicated, as a marker for cerebral amyloid deposit, either a decreased Aβ1-42/Aβ1-40-quotient in liquor or alternatively, a positive amyloid-PET. Alzheimer's disease patients did not suffer from other neurological or psychiatric diseases and indicated impaired cognitive functioning according to the consortium to establish a registry for Alzheimer's disease (CERAD) test battery (Morris *et al.*, 1989). To ensure the feasibility of the experiments for all participants within the AD group, the lower Mini Mental State Examination (MMSE) cut off score was set to 17.

Control subjects did not suffer from memory decline according to self-report, they were living at home independently and had unimpaired cognitive functioning as assessed by the CERAD test battery (within ± 1.5 standard units) and MMSE (cut off score 26).

For both groups, the age threshold was between 55 and 80 years. During data acquisition, all participants had normal or corrected visual acuity. All participants taking drugs affecting the NE system, such as certain antidepressiva and antihypertensives, were excluded from the study (see appendix-list 1). However, patients were allowed to take AD-related medication, such as acetylcholinesterase inhibitors (on average 9.37 mg/day).

2.3 Group comparisons

Detailed demographic and clinical characteristics are presented in table 1. Group comparisons of demographic data revealed no significant differences in sex distribution. The educational level of all participants was rated based on the German educational system. Participants were asked for the time passed to complete school (excluding revisions) and the first professional education. Thus, the educational level ranged between seven years (no graduation at all) and 20 years (university-entrance diploma, university degree and graduation), and did not show any differences between both groups. However, the AD group was older compared to the controls ($t(46) = -2.96$, $p \leq 0.01$, $r = 0.45$). To correct for this incidence, statistical analyses

were required to include the covariate age (see 2.7 Statistical analyses). The group of AD patients indicated a lower MMSE level compared to the group of healthy elderly ($U = 70.50$, $z = -4.53$, $p \leq 0.001$, $r = 0.65$).

Table 1. Demographic and clinical characteristics.

	N	Age (y) M (SD)*	Male (%)	Education (y) M (SD)	MMSE M (SD)**	AChEI (mg/day) M (SD)
HC	26	67.88 (5.72)	50.00	15.08 (3.60)	28.71 (1.23)	n/a
AD	24	72.29 (4.56)	62.50	15.00 (3.23)	24.17 (3.07)	9.37 (4.50)

Note. M = mean; SD = standard deviation; MMSE = Mini Mental State Examination; AChEI = acetylcholinesterase inhibitor; HC = healthy controls; AD = Alzheimer's disease; n/a = not applicable. * $p \leq .01$ and ** $p \leq .001$ significant group differences according to independent t-test and Mann-Whitney U test.

2.4 Behavioral paradigms

Two behavioural paradigms were used to investigate physiological processes in response to activation of the subject's attention system: an AB paradigm with two different difficulty levels and a visual, three-stimulus OB paradigm. In total, participation in all experimental procedures took between five and six hours per subject (incl. preparing of EEG acquisition). The paradigms were performed in the same order as described in the following sections.

All behavioural paradigms were presented on a 22 inch LCD display (Viewsonic VX2268wm) with a refresh rate of 100 Hz, a screen resolution of 1680x1050 and a colour depth of 32 bit. To ensure a moderate screen luminance, the background colour was grey (RGB code: 200/200/200) in all paradigms. The experiments were programmed and controlled by the software Presentation (version 17.103.15.14, Neurobehavioral Systems, San Francisco, CA, USA).

2.4.1 Visual 3-stimulus oddball paradigm

The OB paradigm comprised three different categories of visual stimuli. The first stimulus type was presented frequently (75 % of all stimuli) whereas the remaining two types of stimuli did each occur with a frequency of 12.5 %: distractors and

targets. This probability pattern of the three stimulus categories was established in previous physiological studies (O'Connell *et al.*, 2012; Schröder *et al.*, 2016). All stimuli were presented as black, geometric symbols with a height of three centimetres. The subjects' task was to press, as fast as possible, a button with their index finger when perceiving the predefined target stimulus. The remaining stimuli, standards and distractors, did not require any action. To reduce a bias effect of the predefined target stimulus, two different versions of the experiment were programmed: first, a triangle was defined as target and in the second version the target was the symbol of a circle. Both versions were assigned to the participants of both groups in a counterbalanced distribution process.

The stimuli were presented with variable, randomly selected ISIs (1500 ms, 1750 ms and 2000 ms) and in random order. Taking into account that some physiological responses last longer than the presented ISI of maximum 2000 ms, the stimulus sequence was programmed with one restriction: every target was required to be followed by at least two standard stimuli. In this way, the probability of measuring the effect of a second target at the end of the analysis window was reduced. Stimulus presentation lasted for 500 ms and recording of responses was active for 1000 ms after stimulus occurrence. In total, a number of 320 stimuli were presented within two main experimental blocks.

The instructions were presented on screen and possible questions were answered verbally. All subjects conducted 25 practice trials including subsequent feedback before beginning with the experiment. The main task did not provide any feedback on performance accuracy. An overview of the experimental procedure is shown in figure 4.

The accuracy of correct stimulus identification was analysed as behavioural parameter. For calculation of the accuracy, the amount of correctly identified target trials (hits; in %) was subtracted by the amount of false alarms (in %) in identification of the remaining stimulus types. The same approach was evaluated for the accuracy rate of correctly identified distractors and standard stimuli (correct rejection, in %), respectively. An additional behavioural parameter was the reaction time respectively the required time to press the button after target presentation (RT).

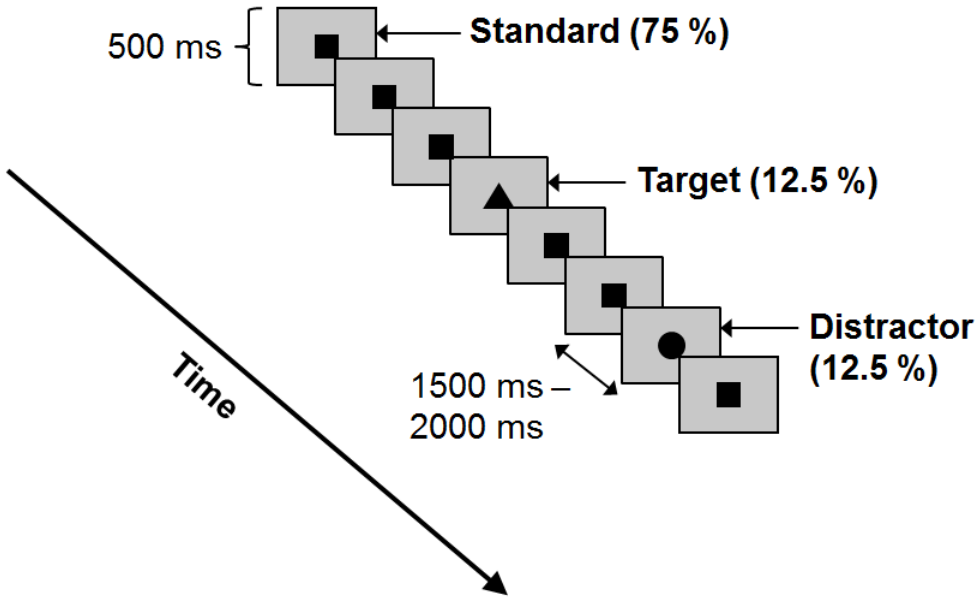

Figure 4. Experimental procedure of the visual three-stimulus OB paradigm.
Stimuli were presented in variable time intervals (1500-2000 ms). One rarely presented stimulus was defined as target. The task was to react by pressing a button while a target was presented and ignore all remaining stimuli.

2.4.2 Attentional blink: single task

This approach of an AB1 paradigm was based on a classical attentional blink task (see 2.4.3 Attentional blink: dual task (AB2)) and was a well suited method to examine a less demanding stimulus detection task (Kranczioch, Debener, & Engel, 2003; Peters *et al.*, 2012). Here, a randomly selected sequence of 50 visual stimuli was presented with the only restriction to never display two identical stimuli at adjacent positions. The trial length was longer compared to common AB designs (Kranczioch, Debener, & Engel, 2003; Peters *et al.*, 2012) to enable the simultaneous recording of the relatively slow pupil dilation before trial completion. The presented stimuli were mainly composed of digits ranging from two to nine (excluding zero and one to avoid ambiguity) and functioned as distractors. Embedded into these numbers, a single target was displayed which was randomly picked from a pool of letters (excluding M, N, I and O to avoid ambiguity). For all characters the font “Courier New” in size 48 and the colour black was used, and stimuli were presented at the centre of the screen. Target onset within one trial varied between positions eight, nine and ten which equals a time frame of 840–1080 ms after trial onset. The stimuli appeared in a rapid serial visual presentation (RSVP). To keep the experiment

feasible for AD patients and to avoid floor effects the stimulus presentation time was chosen slightly longer compared to commonly applied attentional blink designs for younger and/or healthy participants (Kranczioch, Debener, & Engel, 2003; Peters *et al.*, 2012; Warren *et al.*, 2009). As suggested by Peters *et al.* (2012), all stimuli were displayed for 120 ms and occurred without a blank screen in between (ISI: 0 ms). This approach compromises feasibility for AD patients and challenge for healthy subjects. An overview of the AB1 procedure is shown in figure 5.

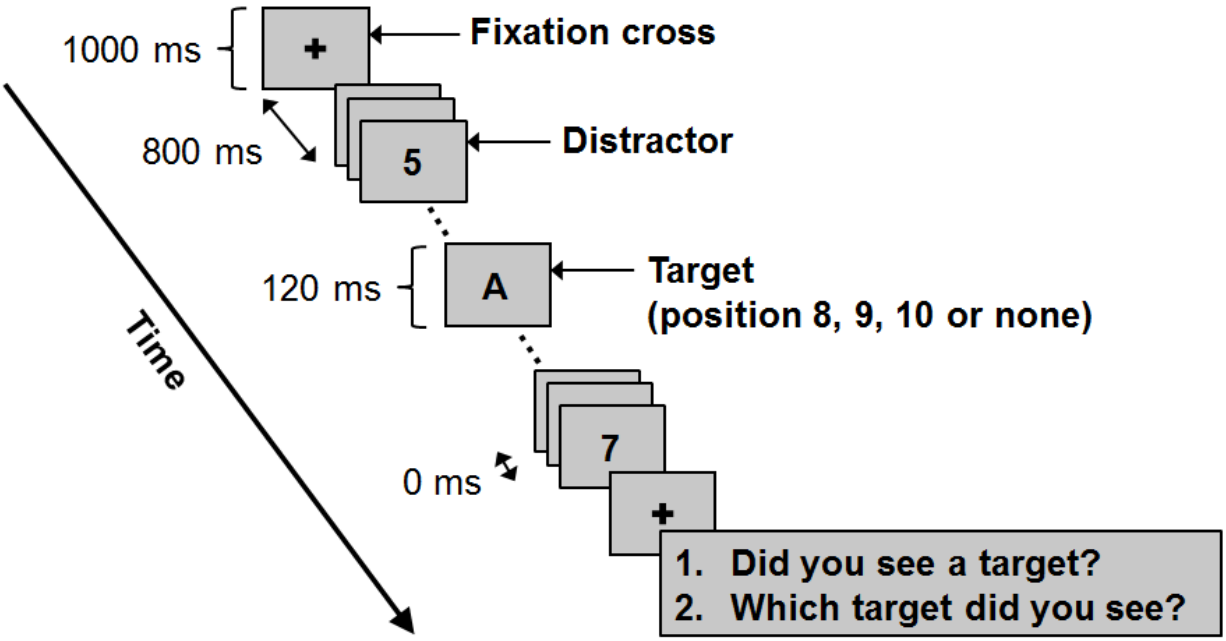

Figure 5. Experimental procedure of the AB1 paradigm.
Randomly selected distractor stimuli (numbers) were presented in a rapid sequence. Embedded into these stimuli, a target (letter) occurred at a randomly selected position. However, not all trials contained a target stimulus. Target and no-target trials were presented in random order. After completion of each trial, the participants' task was to verbally identify the target stimulus. The investigator noted all answers within the presentation software.

In total, 50 trials containing one target were presented to the subjects. To form a baseline contrast to target-induced attention, additionally 50 trials with no target at all (thus, only distractors) were randomly mixed with target trials. A fixation cross preceded each trial to focus attention at the beginning of the new trial. After completion of every trial two tasks were displayed on screen. The participants were required to verbally report to the investigator 1) if they detected a target and 2) in case they detected the target, to identify it. There was no time limit for answering.

Behavioural parameter for statistical analysis was the accuracy in percent: the amount of correctly identified targets with respect to the total amount of presented target-trials.

After reading the instructions presented on the screen, the participants had the opportunity to ask questions. Subsequently, all subjects conducted one introductory training block (ten trials) including feedback and two main experimental blocks of 50 trials each.

2.4.3 Attentional blink: dual task

Unless stated otherwise, details were taken over from the AB1 procedure. In contrast to the AB1 experiment, the dual task version of the AB procedure contained two targets (T1 and T2) per trial. Target letters were picked randomly with the restriction to show two different targets per trial. The distance between both targets was built by intervening distractors. Figure 6 shows the experimental procedure of the AB2 design.

Previously, the AB2 procedure had been tested in an unpublished pilot study with three AD patients and five control subjects. The AB2 experiment had been presented with a distance of 120 – 720 ms between both targets. Pilot results had indicated the AB effect with “lag 1 sparing“ in both groups with a slightly elongated effect in some participants (appendix-figure 1). Accordingly, for the current study it was decided to include a longer maximum distance between both targets to ensure that the performance of all subjects returned to baseline. Here, the distance randomly varied between zero (lag 1), one (lag 2), two (lag 3), four (lag 5) and six (lag 7) distractors. These values corresponded to a temporal distance of 120 – 840 ms.

There were no trials without targets. Twenty trials were presented per lag category and in total the AB2 procedure contained 100 trials. After each trial, participants were asked to verbally identify both targets. The order of target identification was not included into evaluation.

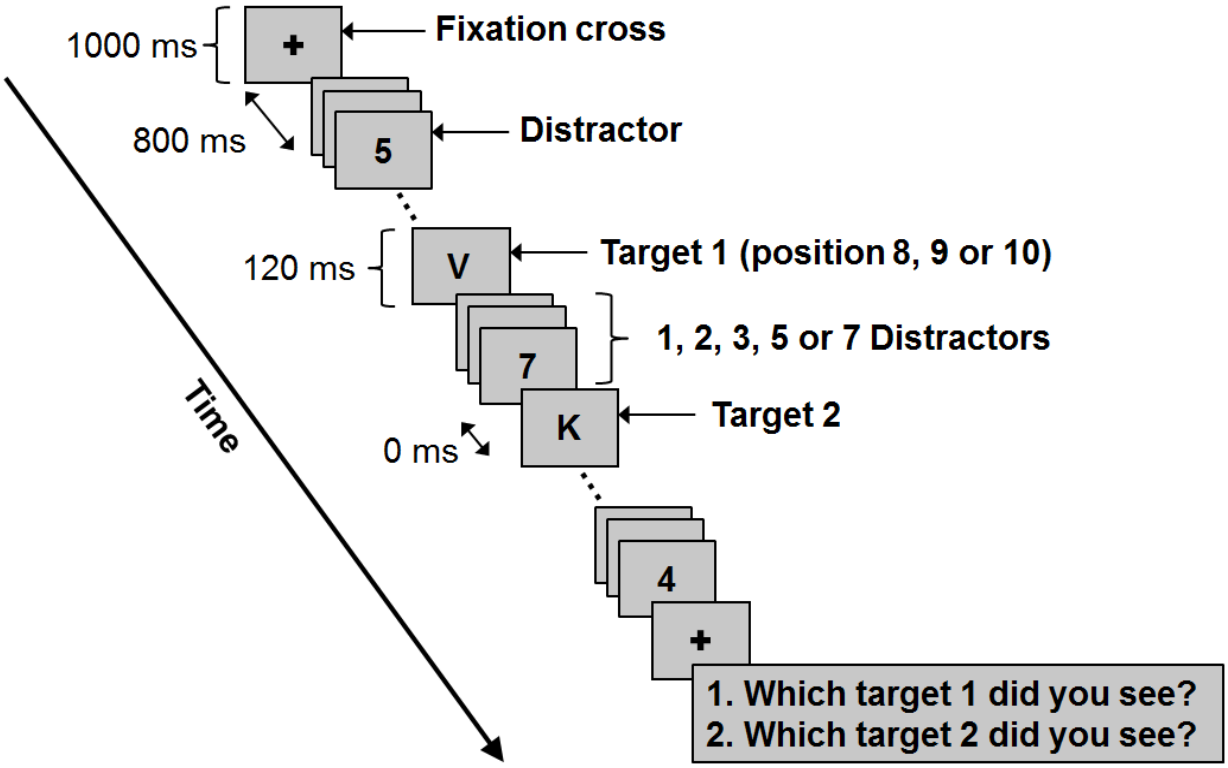

Figure 6. Experimental procedure of the AB2 paradigm.
Each trial was composed of a rapid sequence of distractors (numbers) combined with two different targets (letters) on random positions. The distance between both targets was defined by the number of distractor stimuli in between and varied randomly across trials. After completion of each trial, the participants' task was to verbally identify both target stimuli. The investigator noted all answers within the presentation software.

To measure the AB effect, the obtained parameter was the T2 identification rate in trials with correctly identified T1 stimuli. Therefore, the probability of reporting T2 given that T1 was reported correctly was calculated per lag category according to the following formula 1:

$$X_{T2\ identification\ rate\ (i)} = \frac{X_{T1\ corr.\ (i)\ +\ T2\ corr.\ (i)}}{X_{T1\ corr.\ (i)}} \quad \text{(formula 1)}$$

Here, $X_{T1\ corr.\ (i)}$ represents the amount of trials with correctly identified T1 in the lag category i. The amount of trials with T2 identification after correct T1 identification is described by $X_{T1\ corr.\ (i)\ +\ T2\ corr.\ (i)}$. This approach takes into account that the AB is defined as a deficit in the T2 identification rate as a consequence of T1

detection. Subjects with no correctly identified AB trial at all were excluded from analyses.

2.5 Physiological methods

Performance of both paradigms was accompanied by simultaneous recordings of EEG signals and pupillary responses. One exception was the dual task version of the AB paradigm: only behavioural data were analysed. The underlying reason for this decision was that the analysis of physiological, event-related data requires a higher amount of trial repetitions to generate a robust waveform. However, a sufficient amount of trials covering five different AB2 lag categories would have involved too many trial repetitions in total. For feasibility reasons of the complete experimental programme, especially concerning the AD patients, it was decided to forgo the analysis of physiological data obtained during performance of the AB2 task.

Data processing was performed off-line using the software MATLAB (The MathWorks Inc, 2013b and 2016b). Data were acquired within a dimly lit room and no distractions through external noise signals, like mobile phones, were possible.

2.5.1 The P3 component

Data acquisition

Electroencephalographic activity was recorded from 64 data channels and gel-based Ag/AgCl active electrodes (actiCAP, Brain Products GmbH, Germany) that were connected to the BrainAmp amplifier (Brain Products GmbH, Germany). The electrodes detected the underlying electrical charges transmitted by active brain cells. The brain's cortical surface is functionally organized and the processed activities might vary per location. Thus, it was important to place the electrodes on standardized scalp positions to make electrode recordings comparable between all subjects. One well established method was to relate electrode positions to known skull landmarks: from nasion to inion and side to side from the two ear lobes (reviewed by Kamel & Malik, 2014). Nasion meant the point between forehead and nose on eye level whereas inion stood for the bony prominence at the central base

skull at the back of the head. In the current study, all electrodes were placed according to the international 10-20 localization system including intermediate sites. This indicated that the distances between neighbouring electrodes were kept at either 10% or 20% of the total front-back or right-left distance (reviewed by Siuly, Li, & Zhang, 2017). An electrode placement system is a so-called montage. The montage used in the current study is displayed in appendix-figure 2.

Higher skin-electrode impedances decreased signal quality and it was necessary to optimize the contact for better recordings. Therefore, all electrodes were filled with an electrolyte gel (SuperVisc, Brain Products GmbH, Germany) that was supposed to get in contact with the skin. The high salt concentration in the gel and the low salt concentration inside the body caused the gel to diffuse into the skin and in this way minimize impedance values. According to the actiCAP operating instructions (version 007, Brain Products GmbH, Germany) a resistance of 25 to 35 kΩ is required for measurements with the actiCAP system. Here, scalp impedances were kept below 15 kΩ to assure proper data acquisition.

The software used for data recording was the BrainVision recorder (Brain Products GmbH, Germany). During recording, all channels were referenced to the FCz electrode and the ground electrode was anterior to Fz.

The sampling rate of data recording was 1000 Hz. No filter was applied during data acquisition. To temporally align continuous EEG data to stimulus presentation, the presentation software sent event markers reflecting stimulus onsets to the EEG recording software using a parallel port.

Preprocessing

Analyses of EEG data were accomplished by using the open-source MATLAB toolbox FieldTrip (version 20141203) (Oostenveld *et al.*, 2011). At first, a time epoch of 1400 ms was defined for each trial. By means of event markers within continuous EEG data, the temporal information of each stimulus onset was noted. Subsequently, an epoch of 200 ms prestimulus (Bledowski *et al.*, 2004; Kranczioch, Debener, & Engel, 2003) and 1200 ms poststimulus was selected. All analysis windows were locked to target and stimulus onset, respectively. Non-target trials of the AB1 paradigm required an alternative approach for selection of the analysis window. Therefore, the time value corresponding to the average presentation time of the target stimulus within target trials (960 ms) was added to the time of the first

distractor presentation in non-target trials. The analysis window was selected around this time point in the same way as in target trials. In doing so, the analysis window was selected in a temporal frame comparable to that of target trials.

After this, all epochs were visually inspected for artefacts, which are electrical signals originating from non-cerebral sources (reviewed by Siuly, Li, & Zhang, 2017). Trials containing artefacts with large amplitudes relative to the amplitude size of cortical responses were completely excluded from further analyses. Biological artefacts like those induced by contraction of muscles, eye movements and blinks, and heart activity produce characteristic waveforms within the EEG data (reviewed by Kamel & Malik, 2014). Electromyography artefacts were identified by automatic algorithms of the FieldTrip software and appropriate trials were rejected. Additionally, trials including electrooculography (EOG) artefacts during baseline or within 700 ms after stimulus occurrence were manually removed. The remaining EOG artefacts were removed using ICA. This technique is mainly used under the assumption that a (biological) signal is independent from the remaining part of the data (reviewed by Michel, 2009). Independent component analysis (ICA) mathematically identified and subtracted components containing the EOG waveform from EEG signals. Those artefacts, occurring as a slow, positive wave with a big amplitude, were most prominent in frontal electrodes and thus, could be easily detected by ICA (reviewed by Siuly, Li, & Zhang, 2017). This approach of EOG artefact rejection did not require the presence of periocular channels to assess the corresponding noise components (reviewed by Dickter & Kieffaber, 2014). Additionally, under the assumption of independent and characteristically waveforms, ICA was also used to remove electrocardiography artefacts. Then all epochs were visually checked for artefacts caused by ICA-dependent software failures. Only trials that indicated correct responses by the participant were included into further analyses.

After artefact rejection, the following percentage of all epochs was retained: for the OB paradigm 66.8 % (HC) respectively 70.0 % (AD) and for the AB1 paradigm 69.0 % (HC) respectively 68.4 % (AD). For further analyses, only subjects with at least ten remaining epochs per stimulus type were considered.

Bad channels were repaired by interpolation using the average values of neighbouring channels. All epochs of each channel were re-referenced off-line using the average signal of all channels which was previously described as the ideal

reference method (reviewed by Dickter & Kieffaber, 2014; reviewed by Kamel & Malik, 2014; reviewed by Siuly, Li, & Zhang, 2017).

Several filters were applied to the data to improve the signal-to-noise ratio of the event-related responses. Power line artefacts originating from the experimental equipment were filtered out at 50 Hz, 100 Hz and 150 Hz using a notch filter (reviewed by Kamel & Malik, 2014). Some filters have the potential to exclude a certain frequency spectrum to clean the data of interest and to highlight a certain component (reviewed by Dickter & Kieffaber, 2014). Particularly low-pass filters are involved in the identification of ERP waveforms (reviewed by Nieuwenhuis, Aston-Jones, & Cohen, 2005). In this study, a low-pass filter at 15 Hz was applied to the data (Bledowski *et al.*, 2004; Bougrain, Saavedra, & Ranta, 2012). This means that frequency components lower than 15 Hz were mainly included for further analyses while the higher frequency components were attenuated. Application of a high-pass filter was renounced because it would delimitate the development of the P300 waveform. There were previous studies on P300 components that also did not apply a high-pass filter (Kamp & Donchin, 2015; Schröder *et al.*, 2016).

Event-related potential analysis

Calculation of ERP waveforms was based on the difference between the post-stimulus signal and the mean signal chosen in a prestimulus period. The ERP was computed on top of a baseline measurement which was constant across all types of stimuli (reviewed by Michel, 2009). In this study, baseline correction was performed using the time period of 200 ms before stimulus onset (Bledowski *et al.*, 2004; Kranczioch, Debener, & Engel, 2003).

ERPs were calculated by averaging time-locked EEG data to external events to gain characteristic waveforms with relatively stable latencies and polarities (reviewed by Michel, 2009). To compute the P300 component, in each single channel all stimulus-locked epochs were averaged separately for targets, distractors and standard stimuli. The effect of interest was defined as the difference between the investigated stimuli. Difference waveforms (contrasts) were calculated in the following way: for the AB1 paradigm the ERP waves of non-target trials were subtracted from that of target trials (= contrast); for the OB paradigm the ERP waves of standard stimuli and distractors, respectively, were subtracted from that of target trials (contrast T-S respectively contrast T-D). The advantage of analysing contrasts was

that they represent the pure contribution of the motivational relevant target detection to the evoked physiological responses. This approach excluded a basic activation pattern produced by the tonic attentional system from the investigated signal.

To avoid the multiple comparison problem and to increase statistical power, not all electrodes could be considered for statistics. Since the P3b waveform is characteristically most prominent in centroparietal regions (Horvath *et al.*, 2018; reviewed by Nieuwenhuis, Aston-Jones, & Cohen, 2005), further analyses were restricted to the three midline electrodes covering the parietal cortex: CPz, Pz and POz (appendix-figure 2). Event-related potential waveforms of these electrodes were averaged per subject and per contrast condition. No lateralization effects were considered.

Parameterization

Parameterization of the ERP components is typically based on the peak amplitude and the latency of the waveform of interest (reviewed by Dickter & Kieffaber, 2014). To assign those parameters individually per subject, it was necessary to define an appropriate analysis window within the investigated epoch. Therefore, the time of the most positive deflection within the entire epoch was determined for each subject. These data were visualized within a histogram (appendix-figure 3) which revealed a bimodal distribution pattern. To reduce the influence of outliers, the analysis window was set based on the data achieved by most participants: 72.7 % of the data representing the most positive deflections were included within a time window of 300-800 ms after stimulus onset. According to published literature, the P3b component is described with a positive peak anywhere between 250 ms and 700 ms (reviewed by Luck, 2005), which is similar to our defined analysis window.

So in this study, the investigated amplitude of the P3b component was defined as the most positive peak within 300-800 ms after stimulus onset. The latency was defined as the time from stimulus onset to the corresponding P3b peak amplitude. To take into account that both groups potentially differ in the time needed to reach the maximum peak of the P3b amplitude, the slope of the ERP signal was calculated in all subjects per group. Therefore, as a further parameter, the amplitude was divided by the corresponding latency. The group's grand average was accomplished by averaging the ERPs from each subject and per contrast condition.

In fact, more parameters were analysed: the average amplitude within the defined time window between 300-800 ms poststimulus, the area under the curve within the same temporal frame as well as the distance between maximum P3b amplitude and the most negative deflection within the time window of 0-300 ms poststimulus. However, these additional calculations did not reveal findings that exceed the results of amplitude and latency respectively slope analyses. Thus, the following sections do not include these parameters.

2.5.2 The pupil dilation response

Data acquisition

On-going recording of the pupil dilation during performance of the experimental paradigms was performed by the Eyelink 1000 eye tracker-system (SR-Research Ltd, Ontario, Canada). Data were acquired within a dimly lit room. The infrared camera of this system, installed below the screen, was tracking the subjects' pupil size of the right eye with a sample frequency of 1000 Hz. The pupil size was measured in terms of an area in arbitrary units. Comparable to EEG data acquisition, portcodes containing temporal information of stimulus onset were sent to Eyelink 1000 software and implemented into continuous data recording.

All participants were seated on a chair with adjustable height and with their chin placed on an adjustable chin rest. According to the individual body height both devices were adjusted in such a way that the subject was able to focus the central desktop surface. The distance from chin rest to the desktop and camera was 70 cm and 50 cm, respectively. During measurements the light was turned off and the windows were dimmed with the only light source coming from the experimental desktop.

Before the experiments started, the eye tracker system was calibrated. Threshold values for detection of the pupil were defined automatically by the system. After calibration, measurements as basis for a range correction were performed: participants were asked to look at a fixation cross on screen while the background colour was changing in luminance. At first, the background had the same colour as during the actual experiment. After 6000 ms, alternately a white screen (RGB Code 250, 250, 250) with a black fixation cross and a black screen (RGB Code 0, 0, 0) with

a white fixation cross were presented each with 6000 ms duration. This alternation was repeated for four times and in the meantime, maximal pupil dilation (black screen) and minimal pupil contraction (white screen) were measured. As a result, there were four subject-dependent values for the maximal possible pupil size and four for the minimal possible pupil size. For each subject, the average difference in those pupil sizes was calculated and this range was used to standardize pupil data to their physiological maximum (see section “Standardization” for detailed description).

Preprocessing

Time epochs were defined by means of portcodes within continuous data. Because the epochs containing the stimulus-induced pupil sizes were selected slightly differently for both paradigms, the corresponding procedure is described separately.

AB paradigm:

Time epochs for the AB paradigm were primarily defined as the time interval from onset of the first distractor within each trial to the end of the trial: 0 – 6000 ms. Then the position of the T1 stimulus was detected. Analogue to the procedure of EEG data preprocessing, in non-target trials the time value corresponding to the average presentation time of the target stimulus within target trials (960 ms) was added to the time of the first distractor presentation. Further analyses of AB-derived pupil size data were restricted to the time interval between T1 stimulus onset and 4802 ms poststimulus. Furthermore, baseline pupil data were gained from the time window 300 ms before onset of each first distractor presentation to the onset of the corresponding trial presentation. This procedure was an established method in previous studies combining AB paradigms with pupillometry (Wierda *et al.*, 2012; Zylberberg, Oliva, & Sigman, 2012).

OB paradigm:

Time epochs for the OB paradigm were selected with a 3000 ms poststimulus interval and, to ensure proper artefact rejection, with 500 ms prestimulus data. However, prestimulus data were revised after data correction. Baseline pupil data were gained from the 300 ms time window preceding each stimulus onset. In a previous study, this approach of baseline selection was established for combining OB paradigms with pupillometry (Kamp & Donchin, 2015).

Summarized, in both paradigms the analysed pupil sizes were locked to stimulus respectively target onset. Comparable to EEG preprocessing, the baseline pupil data were used to control for the same origin conditions in all trials and additionally, it was used as a parameter for the tonic activation of the LC (Gilzenrat *et al.*, 2010). Changes in pupil size after stimulus presentations could be related to this basic activation.

In a next step the selected pupil data were cleaned from artefacts. Eye blinks, a very common cause for artefacts, were detected automatically by the Eyelink 1000 software. Eye blinks affect pupil sizes also shortly before and after the actual blink since the pupil dilates when the eyelid is closed. For this reason, a time interval of 100 ms before and after each eye blink is additionally rejected from further analyses (Einhauser *et al.*, 2008). The removed pupil data were linearly interpolated. Furthermore, all time epochs were inspected manually for remaining artefacts which were also linearly interpolated. Trials and baselines, containing less than 50 % of the pupil data due to artefacts or software failures, were excluded from analyses (Siegle *et al.*, 2003).

After artefact rejection, for the OB paradigm 91.2 % (HC) respectively 90.7 % (AD) and for the AB1 paradigm 91.1 % (HC) respectively 94.5 % (AD) of all epochs retained for further analyses. A minimum of five to ten trials per stimulus type were required to obtain reliable stimulus-induced waveforms per subject (Marchak & Steinhauer, 2011). Hence, epochs were averaged separately per stimulus type to reduce random perturbations.

Standardization

As previously mentioned, the Eyelink 1000 system calculates pupil sizes in arbitrary units. For this reason it was not possible to compare pupil sizes between subjects. Therefore, a standardization procedure was required before the statistical analyses were performed. For the current study, it was important to take into account that the aged pupil only shows reduced vegetative reactivity. The procedure of a range correction was the appropriate standardization process to correct for this fact (Piquado, Isaacowitz, & Wingfield, 2010).

As already described in the section “Data acquisition”, each experiment started with a measurement of the minimal constricted and the maximal dilated pupil

size to obtain an averaged, maximal possible range of the individual pupil response. These range values were calculated for each subject individually and subsequently, the event-related pupil data were related to this range according to Lykken (1972). Standardization of pupil sizes during baseline measurements was performed using the following formula 2:

$$x_{standardized\ (i)} = \frac{x_{baseline\ (i)} - x_{minimum}}{x_{maximum} - x_{minimum}} \quad \text{(formula 2)}$$

In this formula, $x_{baseline(i)}$ described the pupil size at a point of time i during the time interval defined as baseline. Maximal and minimal pupil sizes are represented by $x_{maximum}$ and $x_{minimum}$. To standardize the event-related pupil dilation ($x_{pupil\ dilation(i)}$) the following formula 3 was used:

$$x_{standardized\ (i)} = \frac{x_{pupil\ dilation\ (i)} - x_{averaged\ baseline}}{x_{maximum} - x_{minimum}} \quad \text{(formula 3)}$$

The standardized baseline was defined by $x_{averaged\ baseline}$, and $x_{maximum}$ respectively $x_{minimum}$ were equivalent to the definition described for formula 2.

Parameterization

Analogue to the investigated ERP parameters, contrasts between the different stimulus types were calculated in the following way: for the AB1 paradigm, pupil sizes measured within non-target trials were subtracted from those of target trials (= contrast); for the OB paradigm, pupillary responses to standard stimuli and distractors, respectively, were subtracted from those in response to target presentation (= contrast T-S respectively contrast T-D).

Parameters for statistical analyses were the peak amplitude, latency and slope of the target-induced pupillary responses. The amplitude was defined as the most positive deflection within a time window of 700 – 2000 ms after stimulus onset. This

temporary frame was chosen to exclude the influence of possible biphasic pupillary responses. The latency was defined as the time from stimulus onset to the first positive peak of target-induced pupil dilation. Because both groups potentially differ in the time needed to reach the maximum positive pupillary response, the slope of the curve progression was additionally calculated per group. The amplitude was divided by the corresponding latency.

2.6 Structural imaging of the locus coeruleus

Magnetic resonance imaging is a commonly used non-invasive technique in neuroscience and provides a detailed overview of brain structures and neurodegenerative processes. All participants of this study underwent MRI examination to obtain structural measures of the LC. However, the analysis of structural imaging data was performed by a student within the scope of an unpublished Master project and is not subject of this thesis. Because the processed MRI data were used as covariates in the statistical analyses of behavioural and physiological data (see 2.7 Statistical analyses), this section provides a brief overview of MRI data acquisition and processing.

Structural imaging of the LC region was performed at a three tesla MRI scanner (Skyra, Siemens Healthcare, Erlangen, Germany). Neuromelanin-sensitive MRI data were obtained using a turbo spin echo sequence with 0.5 mm in-plane resolution and a slice thickness of 2.5 mm. The following sequence parameters were applied: repetition time=634 ms, time echo (TE)=10 ms, flip angle: 180 deg, field of view (FOV) of 192 mm x 192 mm in plane over 16 slices, 220 Hz bandwidth per pixel, turbo factor 3, 8 averages. Positioning of the FOV was optimized for the LC region by using T1-weighted magnetisation prepared rapid acquisition gradient echo (MPRAGE) scans (R=2500 ms, inversion time=1100 ms, TE=4.37 ms, flip angle: 7 deg, 1 mm isotropic resolution over a FOV of 256 mm x 256 mm x192 mm).

Preprocessing steps, like correction for field inhomogeneities, cropping and extraction of the brain, were applied to MPRAGE scans. Final data analysis was performed on unprocessed neuromelanin sensitive images. Coregistration was optimized for the brainstem region and executed by an automated routine based on MATLAB. The individual MPRAGE scans were coregistered with the neuromelanin-

sensitive MRI scans and a standardized atlas mask for the LC (Keren *et al.*, 2009). In doing so, a region of interest (ROI) containing the LC and the surrounding tissue was defined. Each type of tissue induced a particular intensity level which can be approximated as a Gaussian distribution. Intensity histograms extracted from the ROI show three different Gaussian distributions: one with high mean intensity representing hyperintense LC voxels, another one with low mean intensity representing the surrounding tissue and the third one with intermediate intensity modelling partial volume effects like voxels containing both noradrenergic cells and surrounding tissue. Parameters for statistical analyses were the maximum intensity measured in the LC and the number of voxels (volume) that were assigned to the LC.

2.7 Statistical analyses

Unless stated otherwise, statistical analyses were performed using IBM SPSS statistics version 23.0. All data were tested for normality of distribution by using the Shapiro-Wilk test. If the assumption of homogeneity of variance and linearity was violated, variables were transformed in order to fulfil the statistical requirements. Details about the type of transformation are described within the concerned section. For all analyses a two-tailed significance level of $\alpha=0.05$ was selected.

To take account of the significant age difference between both groups, the variable “age” was added as a potential nuisance in the regression analyses. Additionally, the covariates LC intensity left and right, LC volume left and right, group, gender and education were used.

2.7.1 Behavioural data

As expected, accuracy levels for reactions to standard and distractor stimuli in the OB paradigm and in no-target trials in the AB1 experiment had low within-group variance due to ceiling effects. For this reason the assumption of a normal distribution was not achieved. Accordingly, these parameters were not subject of the statistical analyses.

Group differences of the remaining behavioural parameters from the AB1 and OB paradigms were analysed by linear regression analysis. Since the accuracy of

target identification in the OB paradigm did not meet the assumptions of homogeneity of variance and linearity, this variable was transformed by a square root transformation before applying linear regression analysis. The result was additionally confirmed by the nonparametric, distribution-free Mann-Whitney U test. Group differences in accuracy levels of all lag categories within the AB2 paradigm were tested by mixed-model regression analysis.

For each group, the main effect of lag latencies in the AB2 paradigm was statistically tested by using mixed-model regression analysis.

2.7.2 Physiological data

Group differences in electrophysiological and pupillary data were analysed using a cluster-based random permutation procedure proposed by Maris and Oostenveld (2007), and embedded within the FieldTrip toolbox in MATLAB. This method is effectively controlling for multiple comparisons so that it represents a very robust test statistic for evoked (electro-)physiological responses. The procedure evaluates the averaged waveforms by testing each adjacent time-sample for differences between both groups. For every time-sample, an independent t-test is performed and all t-values exceeding the α-level of 0.05 are clustered based on temporal adjacency. All individual t-values within one cluster are summed and the largest of the cluster-level statistics is noted. The multiple comparison problem is solved by evaluating this procedure on data sets that are randomly derived from both groups of participants. This randomization process and the subsequent cluster-level statistic on these distributions are repeated 1000 times by using the Monte Carlo method. For each randomization, the largest cluster-level statistic is entered into a null distribution. The actually observed test statistic is compared to the null distribution and the proportion of randomizations resulting in a larger test statistic than the observed one is called the p-value. Clusters indicating a *p*-value below 0.025 are considered significant. More details of this test procedure are described by Maris and Oostenveld (2007). However, in this study only significant cluster temporally located within the defined analysis window were taken into account.

The cluster-based random permutation procedure was applied not only on group level but additionally in a within-subject design to test differences of the individual waveforms from a baseline (“zero-line”). Here, the cluster analysis was not

restricted to the analysis window to proof evidence for the general development of task-induced deflections.

The described cluster-based random permutation procedure indicated a comparatively modern statistical approach. To complement data analysis by more conservative statistics and to take account of the age difference between both groups, additional calculations were performed. All physiological parameters (amplitude, latency and slope) were examined by linear regression analysis including the covariates described above.

2.7.3 Correlations between parameters and locus coeruleus volumes

Because part of the data was not normally distributed, the test statistic used to evaluate correlations between all investigated parameters was required to be non-parametric. Basically, two non-parametric correlation methods were suited for evaluation: Spearman's and Kendall's correlation coefficient. Because the present study investigated only small sample sizes and contained many values with the same score, Kendall's tau was the preferred method to analyse correlations (Field, 2009).

3. Results

The following section describes the results of the present thesis separately for each investigated parameter.

Sample sizes were not equal in all data sets because of missing values (for further details see chapter “2. Methods”). Drop out of MRI sessions at the request of participants and incomplete acquisition of pupil sizes/EEG data further reduced sample sizes. In correlation analyses, the sample size was additionally decreased because complete data sets per participant were required. Therefore, sample sizes are stated separately for all analyses.

3.1 Locus coeruleus volumes

Structural measures of the LC nucleus were obtained in 20 AD patients and control subjects, respectively. Based on neuromelanin sensitive MRI data, the following parameters were analysed separately for both sides: maximum LC intensity and LC volumes according to the number of voxels that were assigned to the LC (within the ROI). These parameters were used as covariates in the remaining statistical analyses to account for potential effects of LC volumes on the investigated behavioural and physiological correlates of LC-NE system functionality.

For the sake of completeness, the LC nuclei were tested for structural alterations in AD patients. The effect of the two groups on MRI parameters was investigated by performing a linear regression analysis. Mean LC volumes and statistical results are summarized in table 2. The regression analysis did not reveal any significant differences in LC volumes or intensities between AD patients and HC.

Table 2. Structural MRI data.
Intensities and volumes of the left and right LC, and statistical overview of the group comparison between AD patients (n=20) and the control group (n=20).

		M (SD)	R-Square	Regression Coefficient B	SE	*p*-value
Intensity left	HC AD	1.18 (0.09) 1.19 (0.09)	0.07	0.01	0.03	ns
Intensity right	HC AD	1.19 (0.08) 1.19 (0.08)	0.03	0.01	0.03	ns
Volume left	HC AD	9.90 (7.18) 11.05 (7.60)	0.02	0.68	2.70	ns
Volume right	HC AD	13.00 (10.02) 18.30 (13.57)	0.07	3.79	4.33	ns

Note. M = mean; SD = standard deviation; HC = healthy controls; AD = Alzheimer's disease; SE = standard error; ns = not significant.
The predictor "group" has no significant effect on LC volumes and intensities.

3.2 Visual 3-stimulus oddball paradigm

The participant's task was to actively distinguish visual target stimuli from distractors and standards. Functioning of the LC-NE system during performance of the task was assessed by the target accuracy and the corresponding RT (behavioural correlates), and by the simultaneously recorded stimulus-related P3 and PDR (physiological correlates).

3.2.1 Behavioural correlate

Statistical evaluation of the behavioural performance obtained in the visual 3-stimulus OB paradigm contained the data of 24 HC and AD subjects, respectively. The mean accuracy rates for the three stimulus types and the according target RT are summarized in table 3. As expected, the false alarm rates in the standard and distractor conditions were (close to) zero in both groups. Hence, these parameters were not subjected to statistical analyses. To test whether target accuracy (HC: mean (M) = 99.58 %, standard deviation (SD) = 1.59; AD: M = 94.79 %, SD = 12.62) and the corresponding RT (HC: M = 510.67 ms, SD = 70.49; AD: M = 549.53 ms, SD = 65.17) were predicted by group, a linear regression analysis was performed (table 3).

Table 3. Behavioral data obtained in the OB paradigm.
Presented are mean accuracy and reaction time (with standard deviation in parenthesis), and statistical overview of the group comparison.

	N	Accuracy (in %)			Reaction time (in ms)
		Target *	Distractor	Standard	
HC	24	99.58 (1.59)	100 (0)	100 (0)	510.67 (70.49)
AD	24	94.79 (12.62)	99.90 (0.51)	99.79 (0.32)	549.53 (65.17)
R-Square		0.30	n/a	n/a	0.23
Regression coefficient B		1.15	n/a	n/a	45.01
SE		0.55	n/a	n/a	25.80
p-value		< 0.05	n/a	n/a	ns

Note. OB = Oddball; HC = healthy controls; AD = Alzheimer's disease; SE = standard error; n/a = not applicable; ns = not significant.
* *These data were square root transformed before performing regression analysis*.

Residuals of the measured target accuracy did not meet the assumption of homogeneity of variance and linearity. For this reason, the data were square root transformed. The calculation of exemplary inverse transformations for an imaginary participant in each group (appendix-equation 1 and appendix-equation 2, respectively) assumed the characteristics summarized in appendix-table 1. The predictor "group" had an impact on the target identification rate such that the accuracy was significantly lower in AD patients than in HC ($p<0.05$). The regression analysis provided the benefit of including the age difference into statistical evaluation, but calculations were based on transformed data. Therefore, nonparametric statistics were additionally used to validate the conclusion of the linear regression analysis. The Mann-Whitney U test supported the previous result by showing a significantly lower target accuracy in the group of AD subjects (median (Mdn)=99) compared to HC (Mdn=100), $U=169.00$, $p<0.01$.

Residuals of the RT met the assumption of homogeneity of variance and linearity. Statistical analysis of the RT did not reveal significant group effects. The covariates describing the LC volume did not exert a significant effect on the behavioural correlates.

3.2.2 The electrophysiological P3 component

The P3 component was measured in response to the correct detection of target, distractor or standard stimuli in 22 AD subjects and controls, respectively. Characteristically, the electrodes covering the centroparietal regions show the most prominent P3b deflections (Horvath *et al.*, 2018; reviewed by Nieuwenhuis, Aston-Jones, & Cohen, 2005). To avoid the multiple comparison problem, waveform analyses were restricted to the three midline electrodes covering the parietal cortex: CPz, Pz and POz (appendix-figure 4). Event-related potential waveforms of these electrodes were averaged per subject and per contrast condition.

For statistical analyses the individual ERPs were calculated as contrast waveforms between target and standard (= contrast T-S), and between target and distractor (= contrast T-D) (figure 7). In doing so, analyses evaluated the phasic activation of the LC-NE system only, while the tonic activity was widely excluded. The maximum amplitudes, latencies and slopes assessed by this method are presented in table 4.

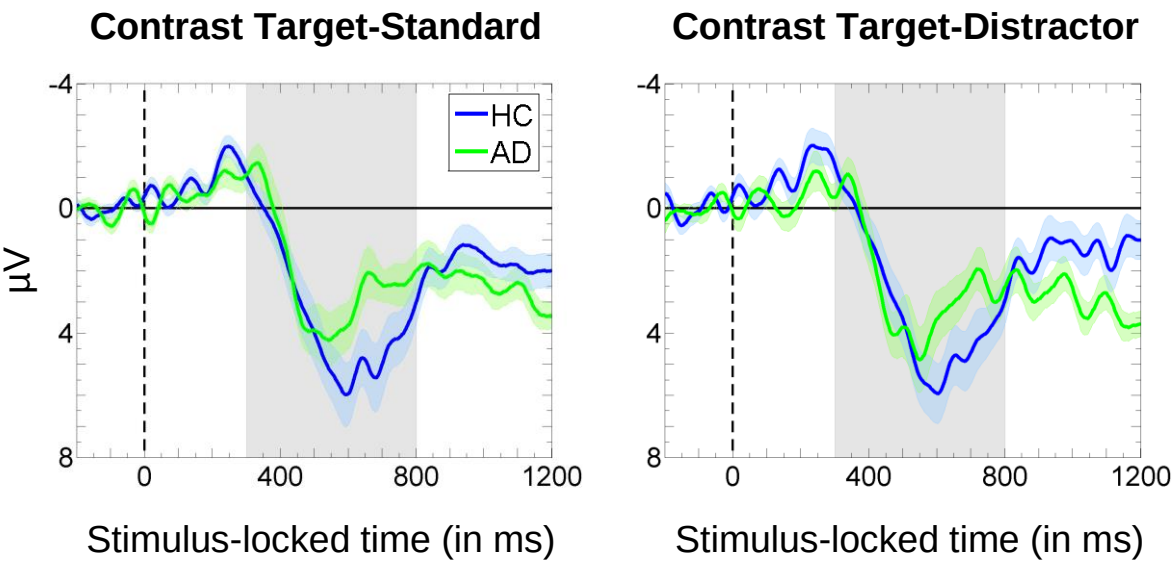

Figure 7. EEG waveforms acquired during performance of the OB paradigm.
Data are averaged over centroparietal electrodes CPz, Pz and POz. The dashed line indicates the appearance of the stimulus. The grey rectangle highlights the defined analysis window for the P3b component (300-800 ms). The shaded color areas show the SEM for each waveform.

To take account of the age difference between both groups, the effect of the predictor “group” on P3 parameters was evaluated by linear regression analysis including the covariate “age” (table 4). In both contrasts, the parameters amplitude, latency and slope did not differ between AD patients and HC.

The left LC intensity, however, indicated a trend for significant effects in both contrasts. Within the contrast T-S, the amplitude (regression coefficient B = -16.17, SE = 8.01, p=0.05) and slope (regression coefficient B = -0.03, standard error (SE) = 0.02, p=0.07) were affected by the left LC intensity. The covariate also had an impact on the parameter amplitude (regression coefficient B = -15.69, SE = 7.97, p=0.06) within the contrast T-D. In summary, the average predicted amplitudes decreased 16.17 µV respectively 15.69 µV, and the average predicted slope decreased 0.03 µV/ms per mm^3 of the left LC intensity.

In addition to the rather conservative regression analysis, waveform differences were also statistically tested by applying cluster-based random permutations (table 5). This is a reliable approach to control for the multiple comparison problem. In both contrasts and within the defined analysis window 300-800 ms, the stimulus evoked electrophysiological deflections did not differ between AD patients and control subjects.

The additionally performed within-subject design investigated the difference between the individual deflections after target detection from tonic baseline activity. Both groups indicated significant electrophysiological responses in the contrast T-S condition (HC: 411-1201 ms, $p < 0.01$; AD: 421-1201 ms, $p \leq 0.001$) and in the contrast T-D condition (HC: 428-902 ms, $p \leq 0.001$; AD: 412-1201 ms, $p \leq 0.001$).

Table 4. EEG data obtained during performance of the OB paradigm.
Overview of mean EEG data (with standard deviation) and statistical results gained from regression analyses.

		N HC/AD	HC (M (SD))	AD (M (SD))	R-Square	Regression Coefficient B	SE	*p*-value
Target vs. Standard	Amplitude (in µV)	22/22	8.01 (4.38)	7.02 (3.50)	0.21	-1.41	1.47	ns
	Latency (in ms)	22/22	579.36 (112.23)	585.41 (124.49)	0.12	25.52	45.73	ns
	Slope (in µV/ms)	22/22	$1.39*10^{-2}$ ($0.68*10^{-2}$)	$1.29*10^{-2}$ ($0.78*10^{-2}$)	0.16	$-0.20*10^{-2}$	$0.30*10^{-2}$	ns
Target vs. Distractor	Amplitude (in µV)	22/22	7.96 (3.92)	8.04 (3.97)	0.20	0.05	1.46	ns
	Latency (in ms)	22/22	592.59 (85.39)	604.18 (146.70)	0.08	22.46	47.96	ns
	Slope (in µV/ms)	22/22	$1.36*10^{-2}$ ($0.63*10^{-2}$)	$1.43*10^{-2}$ ($0.83*10^{-2}$)	0.17	$0.10*10^{-2}$	$0.30*10^{-2}$	ns

Note. OB = Oddball; HC = healthy controls; AD = Alzheimer's disease; M = mean; SD = standard deviation; OB = Oddball; SE = standard error; ns = not significant.
Linear regression analysis did not show significant group differences.

Table 5. Cluster-based random permutation test for EEG data (OB paradigm).

			N	Time window (in ms)	*p*-value
Target vs. Standard	HC vs. AD			/	/
	Within-subject	HC	22	411-1201	<0.01
		AD	22	421-1201	≤0.001
Target vs. Distractor	HC vs. AD			/	/
	Within-subject	HC	22	428-902	≤0.001
		AD	22	412-1201	≤0.001

Note. OB = Oddball; HC = healthy controls; AD = Alzheimer's disease.
In both conditions, no significant group difference was found within the analysis window.
Statistics for the within-subject design was performed for the difference between the individual physiological deflections from the baseline.

3.2.3 The pupil dilation response

The PDR was calculated in response to correct detection of target, distractor or standard stimuli in 21 AD patients and 20 healthy control subjects. Contrast waveforms between target and standard (= contrast T-S), and between target and distractor (= contrast T-D) were calculated and are depicted in figure 8. Maximum amplitudes, latencies and slopes derived from the PDR are noted in table 6.

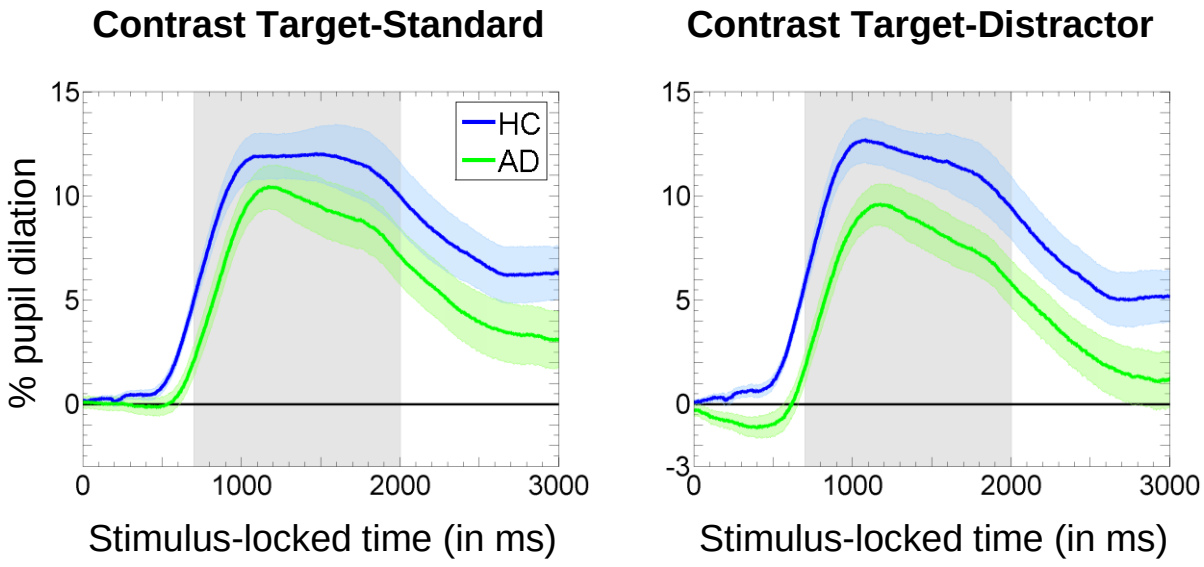

Figure 8. Pupil dilation acquired during performance of the OB paradigm.
Pupil dilations are presented in response to stimulus detection. The grey rectangle highlights the defined analysis window for the PDR (700-2000 ms). The shaded color areas show the SEM for each waveform.

A linear regression analysis was used to evaluate the effect of the different groups of participants on the PDR (table 6). In both contrasts, no significant group effects were detected. Within the contrast T-D the parameter slope indicated a group difference on trend level (p=0.05, two-tailed significance level). The average predicted slope decreased $3.38*10^{-5}$ %/ms in case the PDR was measured in AD patients compared to HC.

Multiple MRI covariates predicted PDR parameters that were calculated in both conditions. The PDR within the contrast T-S was significantly or on trend level influenced by the left (amplitude: regression coefficient B = -0.003, SE = 0.001, p<0.05; slope: regression coefficient B = $-2.75*10^{-6}$, SE = $0.1*10^{-5}$, p<0.05) and the right (amplitude: regression coefficient B = -0.002, SE = 0.001, p=0.05; latency: regression coefficient B = -5.30, SE = 2.81, p=0.07) LC volumes. Within the contrast T-D, the PDR was also significantly or on trend level affected by the left (amplitude: regression coefficient B = -0.003, SE = 0.001, p<0.05; slope: regression coefficient B = $-2.42*10^{-6}$, SE = $0.1*10^{-5}$, p<0.05) and the right (amplitude: regression coefficient B = -0.001, SE = 0.001, p=0.05) LC volumes. In summary, the following information was derived from the regression equations: the average predicted…

- … amplitude decreased 0.003 % respectively 0.002 % per additional mm³ of the left respectively right LC volume (contrast T-S).
- … amplitude decreased 0.003 % respectively 0.001 % per additional mm³ of the left respectively right LC volume (contrast T-D).
- … latency decreased 5.30 ms per additional mm³ of the right LC volume (contrast T-S).
- … slope decreased $2.75*10^{-6}$ %/ms per additional mm³ of the left LC volume (contrast T-S).
- … slope decreased $2.42*10^{-6}$ %/ms per additional mm³ of the left LC volume (contrast T-D).

Table 6. Pupil dilations obtained during performance of the OB paradigm.
Overview of mean PDR data (with standard deviation) and statistical results gained from regression analyses.

		N HC/AD	HC (M (SD))	AD (M (SD))	R-Square	Regression Coefficient B	SE	*p*-value
Target vs. Standard	Amplitude (in %)	20/21	0.13 (0.06)	0.12 (0.06)	0.42	-0.02	0.02	ns
	Latency (in ms)	20/21	1095.90 (213.49)	1145.38 (161.38)	0.32	117.30	72.48	ns
	Slope (in %/ms)	20/21	$1.23*10^{-4}$ ($0.48*10^{-4}$)	$1.00*10^{-4}$ ($0.47*10^{-4}$)	0.41	$-2.81*10^{-5}$	$1.8*10^{-5}$	ns
Target vs. Distractor	Amplitude (in %)	20/21	0.14 (0.05)	0.11 (0.05)	0.44	-0.03	0.02	ns
	Latency (in ms)	20/21	1092.75 (199.03)	1124.90 (162.11)	0.25	97.24	70.79	ns
	Slope (in %/ms)	20/21	$1.31*10^{-4}$ ($0.45*10^{-4}$)	$0.96*10^{-4}$ ($0.41*10^{-4}$)	0.44	$-3.38*10^{-5}$	$1.7*10^{-5}$	ns

Note. HC = healthy controls; AD = Alzheimer's disease; M = mean; SD = standard deviation; OB = Oddball; SE = standard error; ns = not significant.
Linear regression analysis did not show significant group differences. The slope within the condition target vs. distractor indicates a group difference on trend level ($p = 0.05$).

Furthermore, waveform differences of the PDR were statistically tested by applying cluster-based random permutations to control for the multiple comparison problem (table 7). The contrast T-S condition evoked a PDR that is significantly larger in HC subjects compared to AD patients within the time window 700-942 ms after stimulus appearance ($p < 0.05$). The contrast T-D condition showed a similar difference with a larger PDR in HC subjects compared to AD patients within 700-1168 ms after stimulus appearance ($p < 0.01$).

A within-subject design of the cluster permutations analysed the difference between the individual physiological deflections after target detection from tonic baseline activity. Both groups indicated a significant PDR in the contrast T-S condition (HC: 459-3001 ms, $p \leq 0.001$; AD: 662-3001 ms, $p \leq 0.001$) and in the contrast T-D condition (HC: 411-3001 ms, $p \leq 0.001$; AD: 690-2475 ms, $p \leq 0.001$).

Table 7. Cluster-based random permutation test for PDR data (OB paradigm).

			N	Time window (in ms)	p-value
Target vs. Standard	HC vs. AD			700-942	<0.05
	Within-subject	HC	20	459-3001	≤0.001
		AD	21	662-3001	≤0.001
Target vs. Distractor	HC vs. AD			700-1168	<0.01
	Within-subject	HC	20	411-3001	≤0.001
		AD	21	690-2475	≤0.001

Note. OB = Oddball; HC = healthy controls; AD = Alzheimer's disease.
Statistics for the within-subject design was performed for the difference between the individual physiological deflections from the baseline.

3.2.4 Correlation analyses of oddball parameters

The correlation analyses of the LC volumes, behavioural and physiological parameters were performed by calculating Kendall's tau. The complete list of results is shown in appendix-table 2, split into halves containing either data measured in AD patients or in HC. For reasons of clarity, the following description of the results will

concentrate on a selection of relevant results only. Significant correlations with respect to the P3 and PDR parameters were mainly observed in data measured in the contrast T-S condition.

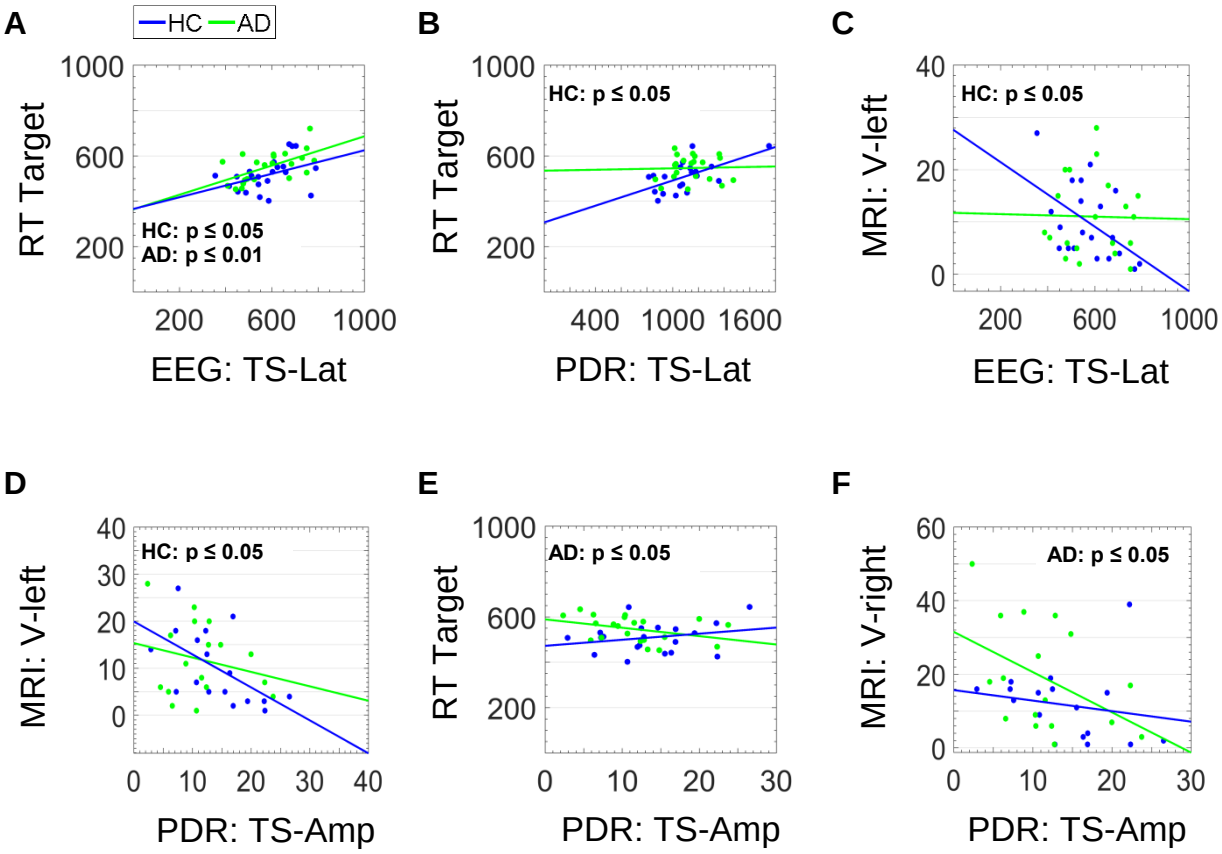

Figure 9. Correlations between parameters obtained in the OB paradigm.
Scatterplots are presented for selected, significant correlations either for both groups (A), for HC (B, C, D) or for AD patients (E, F). The lines indicate the least squares for each group and correlation.
The following abbreviations were used: TS = contrast target-standard; Lat = latency (in ms); RT = reaction time (in ms); V = volume (in mm^3); Amp = amplitude (in % dilation from baseline).

P3 parameters

In both groups, longer P3 latencies were significantly correlated with longer RTs after correct target identification (figure 9A; HC: $r_\tau = 0.32$, $p \leq 0.05$; AD: $r_\tau = 0.47$, $p \leq 0.01$). Within the group of HC it is noticeable that the P3 latencies were additionally related to the LC volume: longer latencies were more likely to be measured in healthy participants with smaller LC volumes in the left hemisphere (figure 9C, $r_\tau = -0.34$, $p \leq 0.05$). This effect did not become evident in AD patients.

PDR parameters

The relationship of PDR parameters with the RT was more diverse and depended on the investigated group of participants: in HC, longer PDR latencies were associated with a longer RT (figure 9B, r_τ = 0.39, $p \leq 0.05$), while there was not such a correlation in AD patients. In contrast, within the patient group a negative link attracted attention: smaller PDR amplitudes predicted longer RTs (figure 9E; r_τ = -0.33, $p \leq 0.05$).

LC volumes had significant correlations with the PDR in both groups. Smaller left LC volumes were associated with larger PDR amplitudes in HC (figure 9D, r_τ = -0.38, $p \leq 0.05$). AD patients, however, showed this relationship with respect to the right LC volume which was significantly smaller in patients with larger PDR amplitudes (figure 9F, r_τ = -0.38, $p \leq 0.05$). This result was also found for the parameter PDR slope: a larger slope was correlated with smaller LC volumes in the left hemisphere in HC (r_τ = -0.42, $p \leq 0.05$) and in the right hemisphere in AD patients (r_τ = -0.33, $p \leq 0.05$).

3.3 Attentional blink paradigm

All participants performed two versions of the AB paradigm: a dual task design to investigate the classic AB effect and a single task design to examine a stimulus detection task that is less demanding than the classical AB2 set-up. Both tasks were designed in a RSVP containing a set of numbers (distractors) with one respectively two letters (targets). To measure the functioning of the LC-NE system, the target accuracy in AB1 and the AB effect in AB2 (behavioural correlates), and the simultaneously recorded P3 and PDR (physiological correlates) were obtained during task performance.

3.3.1 Behavioural correlate: the attentional blink dual task

The performance of the classical AB2 paradigm was statistically evaluated in 21 AD patients and 24 HC subjects. The upper half of table 8 shows the mean accuracies (in per cent) for T1 and T2 separately per lag. Depicted in figure 10 are the mean

Table 8. Performance in attentional blink dual-target paradigm.

Presented are mean target identification rates (with standard deviation in parenthesis) and the statistical overview of the group comparison.

	N	T1 identification rate (in %)	T2 identification rate (in %)				
			Lag 1	Lag 2	Lag 3	Lag 5	Lag 7
HC	24	94.25 (4.65)	93.34 (7.63)	84.93 (14.11)	84.24 (17.51)	82.02 (18.02)	87.41 (12.53)
AD	21	73.10 (20.28)	54.88 (39.91)	43.84 (35.64)	46.89 (42.53)	55.35 (32.26)	63.70 (26.09)

		Estimate	95% Confidence Interval		SE	Global *p*-value
			Lower Bound	Upper Bound		
Intercept		102.10	0.08	204.13	51.66	$p < 0.05$
Lag	Lag 1 vs. Lag 7	-11.42	-27.87	5.02	8.23	ns
	Lag 2 vs. Lag 7	-22.65	-38.03	-7.27	7.70	
	Lag 3 vs. Lag 7	-18.57	-35.66	-1.49	8.55	
	Lag 5 vs. Lag 7	-8.74	-24.44	6.95	7.86	
HC vs. AD		21.78	6.90	36.66	7.33	$p < 0.001$
Lag*group interaction	Lag 1 vs. Lag 7	17.87	-4.50	40.23	11.20	ns
	Lag 2 vs. Lag 7	22.21	1.29	43.12	10.48	
	Lag 3 vs. Lag 7	17.82	-5.41	41.06	11.63	
	Lag 5 vs. Lag 7	5.57	-15.78	26.91	10.68	

Note. HC = healthy controls; AD = Alzheimer's disease; SE = standard error; ns = not significant.
All statistical values are based on mixed-model regression analysis.

identification rates for T2 after correct T1 identification and in relation to the individual lag categories.

Group effects on the T2 identification rate in relationship with the individual lag categories were tested by calculating a mixed-model regression analysis. Fixed effects were the categories “lag” with five levels (lag 1, 2, 3, 5, 7), “group” with 2 levels (AD, HC) and the “lag*group” interaction. An overview of the statistical results is presented in the lower half of table 8. The regression analysis revealed that there is a significant main effect of the predictor “group” ($p < 0.001$): control subjects achieve, on average, 21.78 % higher accuracy rates compared to AD patients. However, the five lags did not show group-dependent effects on the T2 accuracy rate. Additionally, there was no main effect of the predictor “lag”.

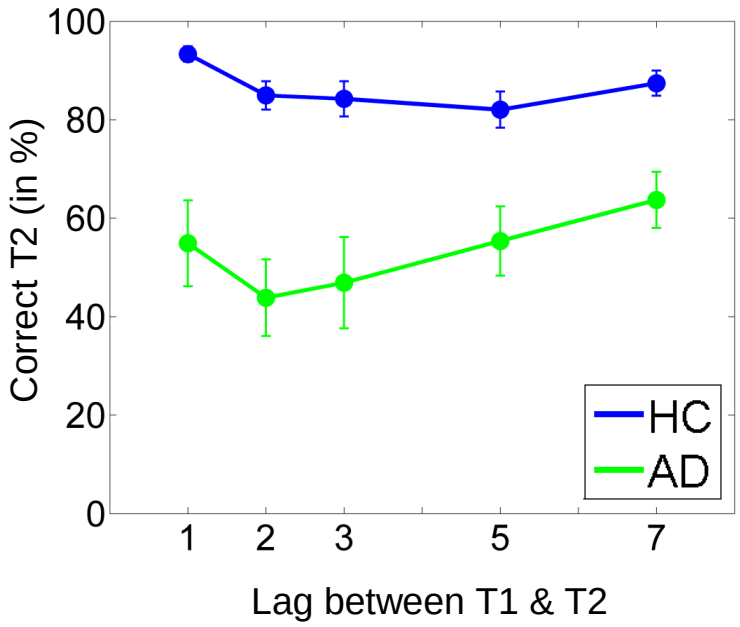

Figure 10. Behavioral results of the AB2 paradigm.
Mean accuracies for T2 identification rates after correct T1 identification are presented in relation to the distance between T1 and T2. Error bars indicate the SEM.

The MRI covariate of the left LC volume significantly predicted the T2 accuracy (intercept: 0.70, 95% confidence interval lower bound: 0.16, 95% confidence interval upper bound: 1.23, SE=0.27, $p < 0.05$). From this regression estimation derived that the T2 identification rate increased 0.70 % for each mm^3 of the left LC volume.

Within each group, the fixed effect of the predictor “lag” with five levels (lag 1, 2, 3, 5, 7) was tested by using a mixed-model regression analysis. The statistical results are summarized in table 9, with the data assigned to the HC in the upper half and to the AD patients in the lower half. Healthy control subjects indicated a significant effect of the five lag categories on the corresponding target identification rates ($p < 0.01$). According to pairwise comparisons, there was the trend ($p = 0.05$) for a higher T2 accuracy at lag 1 (M: 93.34 %, SD: 7.63) compared to lag 5 (M: 82.02 %, SD: 18.02). The group of AD patients does not show differential effects of the individual lag categories on the T2 accuracy.

Table 9. Statistics of the performance obtained in the AB2 paradigm.

Group: HC		Estimate	95% Confidence Interval		Global *p*-value
			Lower Bound	Upper Bound	
Intercept		118.14	87.06	149.22	$p < 0.001$
Lag*	Lag 1 vs. Lag 7	5.93	-0.05	11.90	$p < 0.01$
	Lag 2 vs. Lag 7	-2.48	-9.80	4.84	
	Lag 3 vs. Lag 7	-3.17	-11.58	5.25	
	Lag 5 vs. Lag 7	-5.39	-13.86	3.08	

Group: AD		Estimate	95% Confidence Interval		Global *p*-value
			Lower Bound	Upper Bound	
Intercept		259.18	144.35	374.00	$p < 0.001$
Lag	Lag 1 vs. Lag 7	-8.82	-29.50	11.86	ns
	Lag 2 vs. Lag 7	-19.87	-38.80	-0.93	
	Lag 3 vs. Lag 7	-16.82	-37.60	3.96	
	Lag 5 vs. Lag 7	-8.36	-25.97	9.26	

Note. HC = healthy controls; AD = Alzheimer's disease; ns = not significant.
* Pairwise comparisons show a difference between lag 1 and lag 5 on trend level (mean difference: 11.31, p=0.05). No further statistical difference is found.
All statistical values are based on mixed-model regression analysis.

3.3.2 Behavioural correlate: the attentional blink single task

Performance of the AB1 task required to distinguish target trials from non-target trials and if appropriate, to identify a target stimulus. The investigated parameter was the accuracy of correct responses in per cent. The data of 23 AD patients and 24 HC were considered for the statistical analyses. Figure 11 shows group comparisons of the achieved accuracies separately for target (A) and non-target (B) trials. As expected, the accuracy rates of non-target trials indicated a very low variance in both the AD (M: 95.91 %, SD: 5.03) and HC (M: 94.70 %, SD: 8.22) group. Therefore, the assumption of a normal distribution was not met and this parameter was excluded from statistical group comparisons.

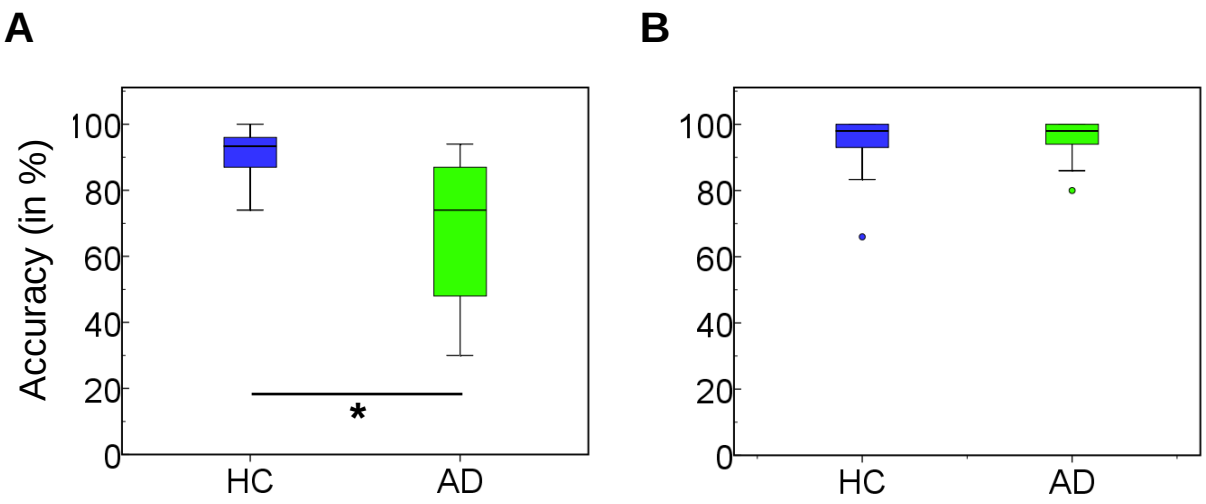

Figure 11. Accuracies achieved in the AB1 paradigm.
Accuracy levels are presented for AD patients and HC in target trials (A) and non-target trials (B). The central line indicates the median, the bottom and top edges of the box highlight the 25th and 75th percentiles, respectively, and the whiskers extend to the most extreme data points. The circles mark the outliers.
* $p \leq .001$ significant group difference according to linear regression analysis.

A linear regression analysis was calculated to predict the target identification rate based on the groups AD and HC. The measured mean data and the including statistics are represented in table 10. Significant group effects on the target identification rate were found ($p \leq 0.001$) and manifested in T1 accuracies that were estimated to decrease about 21.99 % in AD patients compared to those measured in HC. The MRI covariates did not predict the observed target accuracy rate.

Table 10. Performance in the AB1 paradigm.
Presented are mean target identification rates (with standard deviation in parenthesis) and the statistical overview of the group comparison.

	N	Target identification rate (in %)	R-Square	Regression Coefficient B	SE	*p*-value
HC	24	90.63 (7.58)	0.53	-21.99	5.79	$p \leq .001$
AD	23	68.26 (21.47)				

Note. HC = healthy controls; AD = Alzheimer's disease; SE = standard error.

3.3.3 The electrophysiological P3 component

The P3 component was measured in response to the correct detection of target stimuli or in non-target trials, in a time window typically corresponding to target presentations. For statistical analyses the individual ERPs were calculated as contrast waveforms between target and non-target trials in 22 AD patients and 24 healthy participants. The resulting average EEG waveforms are depicted in figure 12 and show the mean values for amplitude (HC: M=3.69 µV, SD=2.49; AD: M=5.25 µV, SD=3.23), latency (HC: M=544.71 ms, SD=139.93; AD: M=457.73 ms, SD=96.81) and slope (HC: M=7.5x10^{-3} µV/ms, SD=5.9x10^{-3}; AD: M=11.8x10^{-3} µV/ms, SD=6.8x10^{-3}).

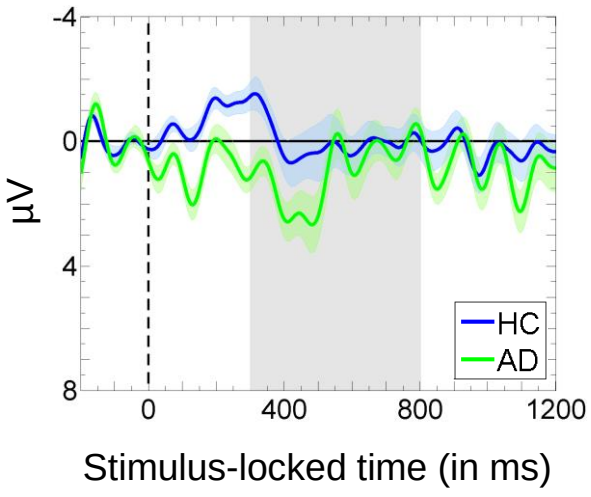

Figure 12. EEG waveforms acquired during performance of the AB1 paradigm.
Data are averaged over the centroparietal electrodes CPz, Pz and POz. The dashed line indicates the appearance of the target. The grey rectangle highlights the defined analysis window for the P3b component (300-800 ms). The shaded color areas show the SEM for each waveform.

Visual data inspection revealed that the EEG waveforms obtained during performance of the AB1 task did not contain robust P3 components. Therefore, a within-subject design of the cluster-based random permutations was used to evaluate the individual quality of the electrophysiological responses. Only six AD patients showed significant positive deflections within 357-517 ms ($p \leq 0.01$) and 91-163 ms ($p \leq 0.05$) after correct stimulus detection. Within the group of HC, however, no statistically relevant deflection (positive or negative) was detected. A group comparison performed via cluster-based random permutations did not show significant differences between the electrophysiological responses in AD patients and in HC. Further statistical evaluation of group differences measured by regression analyses is not reported.

3.3.4 The pupil dilation response

The PDR was calculated in response to correct target detection or in non-target trials, in a time window typically corresponding to target presentations. Contrast waveforms between target and non-target trials were calculated in 21 AD patients and 20 HC. The resulting waveform is represented in figure 13 and mean amplitudes, latencies and slopes derived from the PDR are noted in table 11.

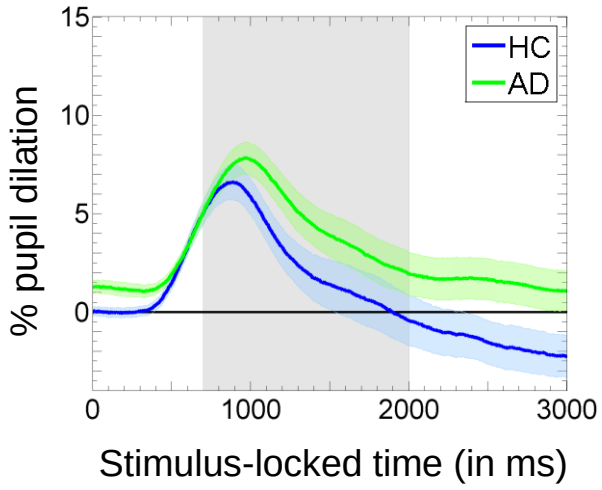

Figure 13. Pupil dilations acquired during performance of the AB1 paradigm.
Data are represented in response to target detection. The grey rectangle highlights the defined analysis window for the PDR (700-2000 ms). The shaded color areas show the SEM for each waveform.

A linear regression analysis was used to evaluate the effect of the different groups of participants on the PDR (table 11). As statistics showed, there was no significant group effect on the investigated parameters. Furthermore, the covariates describing the LC volume did not predict the PDR.

All parameters obtained from the PDR were also statistically tested by applying cluster-based random permutations. According to this test, there was no group difference between pupillary deflections in response to target detection. A within-subject design of the cluster permutations analysed the difference between the individual physiological deflections from tonic baseline activity. AD patients revealed significant positive deflections within 1-1907 ms ($p \leq 0.01$) and the HC group showed a significant PDR within 433-1324 ms after target detection ($p \leq 0.01$).

Table 11. Pupillary responses obtained from the AB1 paradigm.
Presented are mean data (with standard deviations) and the statistical overview of a group comparison between AD patients (n=21) and controls (n=20).

	Amplitude (in %)	Latency (in ms)	Slope (in %/ms)
HC (M (SD))	0.07 (0.04)	864.55 (138.63)	$0.8x10^{-4}$ ($0.4x10^{-4}$)
AD (M (SD))	0.09 (0.04)	1001.86 (218.26)	$0.9x10^{-4}$ ($0.4x10^{-4}$)
R-Square	0.13	0.33	0.08
Regression Coefficient B	0.02	108.49	$1.13x10^{-5}$
SE	0.02	76.53	$1.8x10^{-5}$
p-value	ns	ns	ns

Note. AB = Attentional blink; AD = Alzheimer's disease; HC = healthy controls; M = mean; SD = standard deviation; SE = standard error; ns = not significant.
Linear regression analysis did not show significant group differences.

3.3.5 Correlation analyses of attentional blink parameters

The correlation analyses of the LC volumes, behavioural and physiological parameters were performed by calculating Kendall's tau. The complete list of results is shown in the appendix-table 3, split into halves containing either data measured in

AD patients or in HC. For reasons of clarity, the following description of the results will concentrate on a selection of relevant correlations only (figure 14).

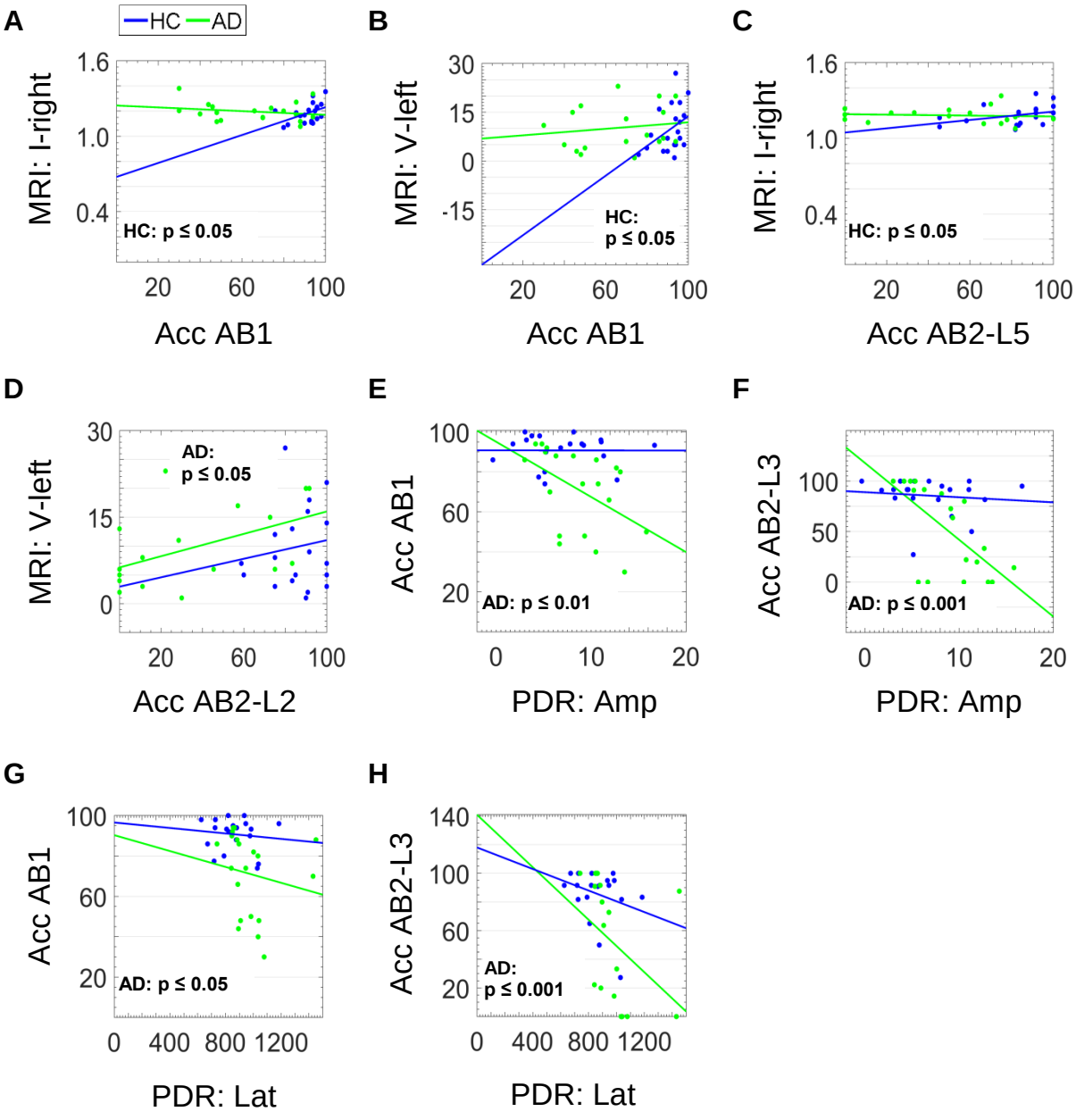

Figure 14. Correlations between parameters obtained in the AB paradigm.
Scatterplots are presented for selected, significant correlations within the group of HC (A-C) and within the AD group (D-H). The lines indicate the least squares for each group and correlation.
The following abbreviations were used: Acc = accuracy (in %); I = intensity (in arbitrary units); V = volume (in mm^3); L1-7 = Lag 1-7; Amp = amplitude (in % dilation from baseline); Lat = latency (in ms).

Behavioural parameters

Accuracy rates obtained in the classic AB2 paradigm indicated a significant relationship with structural MRI data. Healthy control subjects were more likely to score higher T2 accuracies at lag 5 in case the right LC intensity is high (figure 14C, $r_\tau = 0.35$, $p \leq 0.05$). AD patients did not show this effect at lag 5, but a similar correlation at lag 2: high accuracy rates were mainly accomplished by subjects with large LC volumes in the left hemisphere (figure 14D, $r_\tau = 0.37$, $p \leq 0.05$). Control subjects did not indicate a significant lag 2 correlation. On trend level, however, higher lag 2 accuracy rates were achieved by HC with high LC intensities in the right hemisphere ($r_\tau = 0.30$, $p = 0.08$).

The target identification rate measured in the AB1 paradigm did not reveal any significant correlations with the LC volume or the PDR in AD patients. Within the control group, higher accuracy rates were associated with both high LC intensities in the right hemisphere (figure 14A, $r_\tau = 0.39$, $p \leq 0.05$) and with larger LC volumes in the left hemisphere (figure 14B, $r_\tau = 0.35$, $p \leq 0.05$).

PDR parameters

Significant correlations with respect to the PDR parameters were only found in AD patients. Larger amplitudes were linked to a lower target identification rate in both the AB1 (figure 14E, $r_\tau = -0.44$, $p \leq 0.01$) and the AB2 at lag 3 (figure 14F, $r_\tau = -0.58$, $p \leq 0.001$). A similar relationship was estimated for the PDR latency. Patients with AD indicated longer latencies when accuracy rates were lower in AB1 (figure 14G, $r_\tau = -0.36$, $p \leq 0.05$) and in AB2 at lag 3 (figure 14H, $r_\tau = -0.57$, $p \leq 0.001$).

Statistical analyses did not reveal any significant correlations between PDR parameters and structural MRI parameters (see complete list of correlations in appendix-table 3).

4. Discussion

This chapter discusses the results of the current thesis and evaluates to what extent the investigated parameters might be used as correlates for NE deficiency in early AD patients.

4.1 Locus coeruleus volumes

Structural measures of the LC nucleus were used as covariates in lineal regression analyses. In this way, potential effects of LC volumes on the investigated behavioural and physiological correlates were investigated. Statistical evaluation of the obtained structural MRI parameters did not reveal significant differences in LC volumes or intensities between AD patients and HC. This finding is unexpected since previous studies reported smaller LC nuclei in AD patients (Betts, Cardenas-Blanco*, et al.*, 2019; Kelly *et al.*, 2017; Olivieri *et al.*, 2019; Takahashi *et al.*, 2015). Elaborating on possible explanations for the present outcome leads to the question if the used MRI method and thus, the calculated LC volumes, could be inaccurate.

Here, data were acquired by using neuromelanin-sensitive MRI scans. This approach is based on the magnetic nature of neuromelanin which accumulates in noradrenergic LC neurons (Baker *et al.*, 1989; Wakamatsu *et al.*, 2015). Until today, this rather indirect volumetric measure represents the only *in vivo* approach for detecting structural dimensions of the LC nucleus. The accumulated concentration of neuromelanin in LC neurons varies across the lifespan (Manaye *et al.*, 1995; Mann & Yates, 1974) which needs to be considered when evaluating the corresponding MRI scans. Because the neuromelanin concentration could not have reached its maximum yet, it does not represent a suitable marker for neuronal density in young adults. However, the rate of neuromelanin accumulation in LC neurons remains stable between 50 and 80 years old (Liu *et al.*, 2019; Manaye *et al.*, 1995). This finding led to the conclusion that older participants produce neuromelanin signals that potentially correspond to the actual number of LC neurons. For this reason, it is assumed that MRI scans obtained in the present study provide reliable LC volumes in HC and do not falsify conclusions.

However, it is important to keep in mind that the present MRI data did not show significant differences between AD patients and HC. A recent study shed light on the question how LC contrasts are sensitive to changes in AD. Betts, Cardenas-Blanco*, et al.* (2019) measured MRI LC contrast ratios in eleven patients with AD-dementia, 16 individuals with AD-MCI, 21 with subjective cognitive decline and 25 HC. Additional correlation analyses between LC contrast, CSF amyloid and tau were calculated in 44 subjects. The study showed that AD-dementia patients indicated decreased LC contrasts in comparison with HC, while patients with AD-MCI and subjective cognitive decline had LC contrasts similar to those in HC. Furthermore, smaller LC contrasts were found in subjects with larger levels of CSF amyloid. This relationship was not found with CSF tau. These findings clearly point to a direct association between LC contrasts and AD pathology, but this relationship was restricted to AD-dementia and did not occur in AD-MCI (Betts, Cardenas-Blanco*, et al.*, 2019). In contrast to the present study, Betts' study strictly divided their group of participants according to the clinical state of AD. Here, individuals with AD-dementia and AD-MCI were both comprised in one clinical patient group. This approach might have diminished potential LC contrast differences between the AD group and HC, because subjects with AD-MCI indicate similar LC contrasts as HC (Betts, Cardenas-Blanco*, et al.*, 2019).

Furthermore, neuromelanin-sensitive MRI is a relatively young imaging technique and to date, there is no consistent standard method for calculating structural dimensions of the LC. This situation needs to be considered when comparing MRI data obtained in different studies. Two commonly calculated parameters are volumetric measures (Castellanos *et al.*, 2015) and contrast intensities relative to a surrounding reference tissue (Betts, Cardenas-Blanco*, et al.*, 2019; Keren *et al.*, 2015; Takahashi *et al.*, 2015). The present study analysed neuromelanin-sensitive MRI data by integrating both signal intensity and volumes to obtain a measure of LC degeneration. A previously published LC atlas mask (Keren *et al.*, 2009) was used to automatically localize the LC nucleus. This limited the risks of intra- and inter-rater variability. Then a Gaussian mixture model was applied on voxel intensities within the atlas defined ROI to classify three types of tissue. The Gaussian distribution of high mean intensity was ascribed to the hyperintense LC region, low mean intensity derived from the surrounding tissue and intermediate intensity represented partial volume effects. Advantage of this approach was that it

decreased the possibility of including partial volume effects into the calculated LC intensities. This could have resulted in a measure of LC degeneration that differs from previously obtained LC intensities/volumes.

In addition, it is important to note that some studies split the individual LC masks into three segments that were analysed separately. Disease-dependent neuronal loss was particularly found in the rostral segment of the LC (Betts, Cardenas-Blanco*, et al.*, 2019; German *et al.*, 1992; Theofilas *et al.*, 2017), while the caudal portion was still intact (Betts, Cardenas-Blanco*, et al.*, 2019; German *et al.*, 1992) or demonstrated only slight decreases (Theofilas *et al.*, 2017). The current study, however, did not distinguish certain segments of the LC region for analyses. This difference could explain why this study lacked any group differences in LC dimensions.

Eventually, it needs to be considered that there is also another MRI study reporting inconsistent results concerning structural LC changes in AD. Miyoshi *et al.* (2013) did not find significantly reduced LC signal intensities in AD patients compared to HC. Locus coeruleus neurons could possibly be preserved in early stages of AD (Busch, Bohl, & Ohm, 1997). The researchers suggested that this would explain the similar LC volumes in the performed group comparison (Miyoshi *et al.*, 2013). This result, however, needs to be handled with care because the size of the AD group was very small as they only included six subjects.

In summary, neuromelanin-sensitive MRI is a relatively young imaging technique that does not provide a consistent standard analysis of LC volumes, yet. Therefore, it remains challenging to compare measures of LC neuron loss due to AD between different studies. The current study used a novel approach to obtain LC hyperintensities. The advantage was that it minimized the risk of including partial volume effects into the calculation of voxel intensities ascribed to the LC. Other studies split the LC into three segments or defined different inclusion criteria for the patient group. These aspects could have contributed to the incongruent outcome of the current analysis. The reliability of the reported structural MRI data should therefore not be doubted although the expected group differences were not found.

4.2 Behavioural correlates

4.2.1 Visual 3-stimulus oddball paradigm

Performance of the visual 3-stimulus OB paradigm produced inconsistent behavioural effects. The target accuracy was significantly lower in AD patients compared to HC, while the RT did not differ between both groups. Structural LC volumes did not have effects on the investigated group differences. Most previous studies investigating participants with pharmacologically induced NE deficiency (Coull *et al.*, 1995; Lovelace, Duncan, & Kaye, 1996) or AD patients (Polich & Corey-Bloom, 2005; Tsolaki *et al.*, 2017) showed that decreased target accuracies are accompanied by increased RTs. The unexpected outcome in this study was a comparable RT in AD patients and HC. However, the patients' fast response occurred at the expense of the target accuracy. A previous study found a similar behavioural pattern in response to an auditory 2-stimulus OB paradigm. Brown *et al.* (2015) reported that a pharmacologically decreased NE concentration in young adults did not affect the RT but decreased the perceptual sensitivity. These findings indicate that a decreased NE concentration associated with early AD might account for poor stimulus evaluation but does not necessarily affect the speed of information processing. This can result in a RT that is comparable to the RT in older HC. In more progressive stages of a malfunctioning LC-NE system, neuron loss shows a more severe impact as target accuracies and RT are both decreased in patients with moderate AD (e.g. Polich & Corey-Bloom, 2005; Tsolaki *et al.*, 2017).

This consideration leads to the question if previous AD studies reporting slower RTs in AD patients measured patient groups with more severe stages of LC-NE system degeneration. The following considerations suppose that progressive dementia is accompanied by progressive degeneration of the LC. The current study mainly included subjects with early AD-dementia that were clinically diagnosed according to the same inclusion criteria (McKhann *et al.*, 2011) as for instance patients in the Polich and Corey-Bloom (2005) study. However, the report of Polich and Corey-Bloom (2005) does not provide any additional information concerning the patients' cognitive state. Tsolaki *et al.* (2017) reveal more details as they report the MMSE score achieved by the investigated AD patients. They had, on average, a smaller MMSE than the AD patients included into the present study. The crucial

impact of varying cognitive states becomes even clearer when considering Tsolaki's further results. The research group reported decreased target accuracies combined with steady RTs in AD-MCI patients performing an auditory OB paradigm. This outcome is very similar to the present finding. Possibly, the AD-MCI patients' cognitive abilities had a positive impact on the average RT obtained in this study.

Another conceivable explanation for the similar RT in AD patients and HC can be found in the setup of the OB paradigm. The task difficulty is controlled by varying the stimulus presentation time. Previous studies including AD patients showed a presentation time of for instance 100 ms (Polich & Corey-Bloom, 2005) or 150 ms (Tsolaki *et al.*, 2017). In this study setup, all stimuli were presented within a time window of 500 ms to take account of the relatively slow PDR that was measured simultaneously. Presumably, this adjustment decreased the task difficulty compared to the OB paradigms presented in the Polich and Corey-Bloom (2005) and Tsolaki *et al.* (2017) studies. Earlier experiments investigated the effect of task difficulty on the RT in healthy, young adults (Kim *et al.*, 2008) and in AD patients (Polich & Corey-Bloom, 2005). The outcome was that easier OB designs were associated with shorter RTs, while harder task conditions resulted in longer RTs. The similar RT achieved by AD patients and HC in this study argues for an OB paradigm setup that did not exceed the patients' perceptual processing demands. This explanation needs to be regarded with suspicion since the decreased target accuracy in AD patients indicates an insufficient response to environmental changes.

The present findings show that the target accuracy obtained in a visual 3-stimulus OB paradigm represents a behavioural correlate of the LC-NE system with characteristic alterations in AD patients. The according target RT appears to be less sensitive to neurodegenerative processes occurring early in the course of the disease. The conclusion is that the parameter RT is not a robust and reliable behavioural correlate for investigating malfunctions of the LC-NE system.

4.2.2 The attentional blink single task

The AB1 paradigm was introduced to examine a less demanding stimulus detection task than the classic AB2 paradigm. The task involved both trials without any target stimulus and trials including a single target. Accuracies obtained in non-target trials were similar in AD patients (96 %) and in HC (95 %). This finding can be explained

by the low difficulty level of trials requiring no target identification. But the evaluation of target trials revealed significant group effects on accuracy rates: target identification was approximately 22 % lower in AD patients as in HC. The patient group supposedly suffered from an impaired ability to select and evaluate relevant incoming information (e.g.: reviewed by Parasuraman & Haxby, 1993; reviewed by Perry & Hodges, 1999). In the present study this effect was enhanced since stimuli had been presented within a RSVP stream. All stimuli appeared for not longer than 120 ms and in direct succession (no ISI). New incoming stimuli could have overwritten previous stimuli before they were consolidated into working memory store. Thus, the RSVP task design potentially impeded the perception of relevant information in AD patients.

The present outcome, though, is not in line with a previous study investigating a very similar approach. In addition to a classic AB2 paradigm, Peters *et al.* (2012) also presented a single target condition of the experiment to their participants. All parameters were chosen similar to the current study with the exception of a target presentation in contrast colour. The researchers reported that the task performance did not significantly differ between AD patients and the control group. This outcome can potentially be explained by the simplified task conditions. Highlighting target stimuli in different colours than distractors results in more effective visual perception (von Wright, 1972). The different outcomes obtained in the present study and in Peters *et al.* (2012) study show that AD patients significantly benefit from easing target detection in a visual AB1 paradigm.

The regression analyses revealed that neither LC volumes nor LC intensities were significant predictors for the observed target accuracy. This indicates that LC dimensions were not necessarily relevant determinants for the task performance. Nevertheless, the accuracy rate obtained in the current AB1 paradigm represents a behavioural parameter with characteristic alterations in AD patients. Correlation analyses between task performance and LC structures reveal to what extent these data can be used as a marker for degeneration of the LC-NE system (see chapter 4.5).

4.2.3 The attentional blink dual task

The patient group achieved significantly lower T2 accuracy rates as HC in all lag categories. The number of intervening distractors between T1 and T2 did not reveal group-dependent effects on T2 identification. Thus, the measured group differences did not provide evidence for AD-specific differences in the degree of "lag 1 sparing", AB effect and gradual improvement of attention after the blink period. This outcome is unexpected since previous studies reported a significantly reduced ability to deal with two concurrent targets in participants with AD. Peters *et al.* (2012) investigated the magnitude of the classic AB in 18 healthy, older subjects and 18 AD patients by presenting an AB paradigm with similar parameters as with the current study. Distractors were displayed as numbers and two characters represented target stimuli. The patient group indicated a more pronounced and prolonged AB effect than healthy elderly. As the distance between both targets increased, the performance of AD patients approximated the performance of control subjects. This outcome had previously been confirmed by two other studies examining the stimulus processing disturbances in either a classical RSVP task with AD-dementia patients (Kavcic & Duffy, 2003) or an RSVP task requiring visuospatial orientation with AD-MCI subjects (Perry & Hodges, 2003). The suggestion is that the limited processing capacity in AD results from an enhanced inter-target competition due to decreased allocation of NE (Kavcic & Duffy, 2003). The current study, though, did not replicate the finding of an elongated AB effect in AD patients in comparison with HC. To find a possible explanation, it is important to evaluate the quality of the applied AB2 paradigm in this study.

Within group analyses showed a significant effect of lag latencies on target accuracy in HC. According to this result, the identification of T2 strongly depended on the number of intervening distractors between both targets. At lag 1, T2 accuracy was almost identical with T1 accuracy (T1: 94% vs. T2: 93%) which argues for the previously described "lag 1 sparing". This phenomenon of preserved accuracies occurs when there is no intervening distractor between T1 and T2 (Potter *et al.*, 1998). As expected, T2 accuracy clearly decreased at a T1-T2 distance of 240 ms and this attentional deficit is referred to as AB effect (Raymond, Shapiro, & Arnell, 1992). Jolicoeur (1999a) suggested that this deficit shows the largest occurrence when both targets are presented with a temporal distance in the range of 200-500

ms. After this time window, the performance of T2 identification gradually recovers. Here, the described attentional deficit period elongated until 600 ms at lag 5 when HC even had the lowest T2 accuracy. According to pairwise comparisons, there was a trend (p = 0.05) for a lower T2 accuracy at lag 5 compared to lag 1. This finding emphasizes the preserved visual attention when there is no intervening stimulus in contrast to the deficit occurring after the perception of distracting events. At lag 7, or at a distance of 840 ms between T1 and T2 presentation, was the expected gradual recovery as T2 accuracy increased to 87%. However, the presented AB2 paradigm did not include the complete recovery time period back to T1 accuracy level. The delayed AB period points to an increased release of NE in response to T1 processing and a subsequent elongated refractory period (Warren *et al.*, 2009). This finding can be the result of a high level of task difficulty. Although the current results indicated a slightly elongated attention deficit that did not completely recover within the investigated time window, the applied experiment still elicited important hallmarks of an AB paradigm: “lag 1 sparing”, the AB effect and the subsequent gradual improvement of attention.

Peters *et al.* (2012) presented distractors and both targets for duration of 120 ms each. In contrast to the current study, both target characters appeared in a different colour than distractors. This modification was used in an attempt to ease target selection. Results obtained in HC showed that T2 accuracy at lag 1 was similar to the corresponding lag category in the present study: 94% vs. 93%. Thus, visual attention within the time window of “lag 1 sparing” seems to be independent of parameters assisting stimulus selection. But the comparison of further results demonstrates that the described simplification of the AB paradigm (Peters *et al.*, 2012) showed an effect in later lag categories: a weaker AB effect at lag 3 and earlier recovery from the attention deficit. The differences between both findings are supposedly the result of the more difficult task parameters in the current study since targets and distractors were presented in the same colour.

In AD patients, however, the experiment failed to elicit the important hallmarks of AB paradigms. The indicated “lag 1 sparing” followed by the AB and the subsequent recovery at lag 7 do not reveal statistically significant influence of varying intervening distractors between T1 and T2. A potential explanation is that the chosen task parameters raised the paradigm difficulty to a level that could not be accomplished by AD patients. Here, all T2 accuracy rates were remarkably lower as

the accuracy measured in AD patients by Peters *et al.* (2012). Three patients were excluded from analyses because they did not attain the minimum number of a single correct T2 identification. Furthermore, the relatively high standard deviation (see table 8) calculated in the AD group shows that individual T2 accuracy rates had large variations. Some patients did not exceed the minimum number of correct T2 identifications so that the occurrence of floor effects may be assumed. Prior to this study, the AB2 procedure had been tested in an unpublished pilot study with three AD patients and five control subjects. Based on these pilot results, it was decided to elongate the usually applied stimulus presentation time to keep the experiment feasible for AD patients. As suggested by Peters *et al.* (2012), all stimuli were displayed for 120 ms, but the appearance of targets was not highlighted by a contrast colour. Possibly this was the decisive factor that increased the task difficulty to a level that could not be accomplished by all AD patients. Therefore, it needs to be considered to what extent the current results of the AB2 paradigm may be comparable with those of HC or other studies investigating AD patients.

Regression analyses revealed a significant effect of LC volumes on correct T2 identifications, which shows the important role of the LC-NE system for task performance. Target accuracies obtained in this AB2 paradigm, though, are not suited to function as a correlate for degeneration of the LC-NE system. The presented AB2 paradigm induced floor effects in early AD patients at such a rate that there was no significant AB effect in the patient group. Adaptation of task parameters, for instance highlighting target stimuli in contrast colours, might produce evaluable results that allow sound comparisons with control groups.

4.3 Physiological correlates

4.3.1 The electrophysiological P3 component

The electrophysiological P3 elicited by a visual 3-stimulus oddball paradigm

Both contrast waveforms of the electrophysiological P3 did not reveal any significant group differences in amplitude, latency or slope. Structural LC parameters did not

clearly have effects on this result, but there was a trend for the left LC intensity predicting amplitude and slope. This result is quite unexpected since most previous OB paradigms reliably elicited P3 components with significantly lower amplitudes and prolonged latencies in AD patients (for instance: Cecchi *et al.*, 2015; Morrison *et al.*, 2018; Parra *et al.*, 2012). To test the quality of the OB paradigm presented here, additional within-subject analyses were carried out. Cluster statistics performed on individual waveforms in each group showed positive, target-induced deflections from about 400 ms after target occurrence. This effect was significant in both groups and allows the conclusion that the presented OB paradigm reliably elicited P3 components. Thus, the neurophysiological processes that are involved in P3 generation were activated in AD patients and HC. Elaborating on other reasons why the current outcome was against the expectations, leads to the question if the analysis method was a causal factor. But as assessed by cluster-based random permutations, the electrophysiological deflections were also similar in both groups when analysed independently of the investigated parameters amplitude, latency and slope. It is known that the selection of the analysed EEG electrodes has important influence on the outcome of data evaluation. Here, the studies were mainly based on waveforms that had been measured in the three centroparietal electrodes. These were identified as the location with the most prominent disease-related changes (Cecchi *et al.*, 2015). Based on this finding, the assumption is that potential electrophysiological changes in AD patients should be present in these electrodes. The investigated parameters do therefore not solely explain the deviant outcome of this study.

The current study differed in one detail to previously published studies. Most of them were mainly based on waveforms elicited by single stimuli rather than contrast waveforms as in this study. However, calculations of contrast waveforms were already used in a previous study with older participants and conclusions were comparable to those gained from target-induced deflections only (Iragui *et al.*, 1993). Analysing contrast waveforms is probably advantageous against single component analysis because by subtracting the electrophysiological response evoked by standards, tonic LC activity and sensory processing components are excluded from the investigated signal (Polich & Corey-Bloom, 2005). The resulting contrast waveform represents the pure phasic LC response only so that conclusions provide higher informative values.

Results from previous studies did not reveal consistent outcomes when investigating P3 amplitudes and latencies. Exceptional cases were reported in terms of missing latency (Juckel *et al.*, 2008; Lee *et al.*, 2013) or amplitude (Chen *et al.*, 2015; Papadaniil *et al.*, 2016; Pedroso *et al.*, 2012) differences between patients and HC. As it is suggested by the currently obtained amplitude and latency, early AD patients might hold some compensatory mechanism that enables a sufficient and fast activation of brain regions that are involved in P3 generation. Recently, it was suggested that the mere loss of NE due to LC degeneration is not the key contributor to AD pathogenesis, it is rather the loss of the integrity of the entire NE system (Gannon & Wang, 2018). This theory is supported by studies manipulating the LC-NE system. Pharmacologically reduced NE levels in humans or animals were associated with latencies (C. C. Duncan & Kaye, 1987; Joseph & Sitaram, 1989; Lovelace, Duncan, & Kaye, 1996) and amplitudes (Pineda & Swick, 1992) that were similar to those measured in control subjects. In these experiments neuronal connections to target brain regions stayed intact. Other animal studies accomplished LC neuron damage and thereby disturbed information processing. This manipulation resulted in reduced P3 components (Ehlers & Chaplin, 1992; Pineda, Foote, & Neville, 1989). Thus, the loss of NE might not necessarily result in altered electrophysiological responses as long as the rate of information processing can somehow be compensated in early stages of the disease.

These observations did certainly not result in comparable performances of AD patients and HC in this study. Although stable P3 amplitudes in AD patients suggested a constant amount of attentional resources focussing on task demands, the patient group achieved lower target accuracy rates. It seems that the allocation of NE is not sufficient to enable the correct evaluation of the environment in the same rate as in HC. A possible reason is that AD patients have an elongated refractory period that explains lower accuracies but would not necessarily take an effect on the P3 which was only analysed in trials with correct accuracy. According to this interpretation, the investigated P3 waveforms pertained to trials that were not presented within refractory periods.

However, conclusive evidence for these theories cannot be provided by the data available in this study. Further experiments focussing on the neurobiological alterations in AD patients are necessary. The outcome of the current analyses suggests that the electrophysiological P3 evoked during performance of a visual 3-

stimulus OB paradigm is not sufficiently sensitive to neurodegenerative alterations in early AD. Furthermore, the fact that LC volumes do not significantly predict group effects supports the conclusion that the P3 does not show group differences reflecting LC degeneration. The early disease-related NE deficiency cannot reliably be established by this physiological correlate of the LC-NE system.

The electrophysiological P3 elicited by the attentional blink paradigm (single task mode)

In both groups, the performance of the AB1 paradigm did not elicit robust P3 components. Within-subject analyses were calculated to evaluate the individual quality of the electrophysiological responses per group. Statistics did not reveal any significant deflection after stimulus identification in HC. This result suggests that identifying a single target stimulus within a RSVP stream does not sufficiently stimulate the LC-NE system. In this case the neural network does not allocate sufficient cognitive resources that are relevant for P3 generation. In accordance with the relatively high target accuracy of 91 % in healthy elderly, it is likely that the level of task difficulty was too low. The recruited neural activation has been too small to elicit robust positive deflections after calculating difference waveforms.

In six AD patients, within-subject analyses showed significant positive deflections within 357-517 ms ($p \leq 0.01$) after correct stimulus detection which accounts for the occurrence of P3 components. Conversely it means that 16 AD patients did not elicit any significant deflection which largely diminished the effect of six patients with P3 component after group average. Given the theory that the low task difficulty did not elicit sufficient neural resources to generate a P3 component, this would mean that around 73% of the AD patients coped with the task. However, according to the behavioural evaluation it appears that more AD patients faced difficulties as it is indicated by the relatively low target accuracy of 68 %. This incidence emphasizes that a low task difficulty cannot be the only reason for a limited P3 generation.

Analyses of ERP components are not subject to a uniform standard and the selection of the investigated electrodes has effects on the outcome of signal analyses. Here, the most positive deflection was found in the POz electrode which was part of the three centroparietal electrodes averaged for signal analysis. A similar AB1 paradigm was previously performed by young participants and the researchers

analysed the topography of the obtained electrophysiological deflections (Kranczioch, Debener, & Engel, 2003). The P3 component was reported to be maximal at the central midline in close spatial proximity to the Cz electrode. A comparison with Kranczioch's study suggests that young subjects produce rather centrally located P3 components while older subjects/AD patients show maximum deflections at parietal locations. However, an argument against this theory is the previously reported observation that the spatial topography of the P3 slightly shifts to frontal areas in association with normal ageing (Horvath *et al.*, 2018).

Since both groups failed to generate a robust P3 component, statistical analyses did not continue to calculate comprehensive group comparisons. This study showed that the AB1 paradigm, respectively the presentation of a single target within a RSVP stream, does not reliably activate the neural network that is involved in P3 generation. In conclusion, this parameter is not suited to function as a correlate for degeneration of the LC-NE system.

4.3.2 The pupil dilation response

The pupil dilation response elicited by a visual 3-stimulus oddball paradigm

In both contrasts, the regression analysis of the PDR did not show significant group differences in amplitude or latency. The slope indicated the trend for a lower average value in AD patients compared to HC subjects. This finding was based on the conservative approach of investigating predefined parameters (amplitude, latency and slope) rather than the entire waveform. To take account of more modern statistics controlling for the multiple comparison problem when investigating the obtained waveforms, additional analyses were performed. Cluster-based random permutations revealed a significantly smaller PDR in AD patients. This could be confirmed for both contrasts and supports the previously described trend for a smaller slope in the patient group. Additionally calculated within-subject analyses were carried out to test the quality of the presented OB paradigm to induce robust PDRs. Cluster statistics investigated individual waveforms measured within both groups and revealed positive, target-induced deflections from about 500 ms (HC) respectively 650 ms (AD) after target occurrence. This effect was significant in both

groups and allows the conclusion that the presented OB paradigm reliably elicited the neurophysiological processes that are involved in controlling the PDR.

To date, there are no comparable studies with AD patients investigating the PDR elicited by an OB paradigm. However, one report described the PDR in subjects at risk for developing AD, patients with AD and HC during performance of a cognitive task requiring goal-directed search and memory (Dragan *et al.*, 2017). The parameter of interest was the rate of changes in pupil size after stimulus onset (pupil response velocity) and represents a parameter that is similar to the currently investigated slope. Dragan *et al.* (2017) reported that the elicited pupillary response decreased with age and, in particular, with AD-related cognitive impairment. This effect was elicited by stimulus onset rather than mnemonic processes. On account of this observation, the researchers proposed that the observed pupillary changes were mediated by the LC-NE system. Although pupil sizes were obtained during performance of a memory task, the study allows conclusions that are comparable to the current theories that were also examined in the context of the LC-NE system. It is important to note that Dragan's result is based on the small sample size of nine patients with AD, and the inclusion criteria for AD patients were limited to cognitive tests and behavioural symptoms rather than biomarker-evidenced diagnostics. The result still supports the current outcome that cognitive processes mediated by the LC-NE system produce smaller pupillary changes in AD patients compared to those in healthy subjects.

Previous studies suggested that pupillary responses modulated by mental effort might be used as a correlate for cognitive decline (Ahern & Beatty, 1979; Beatty, 1982; Granholm *et al.*, 1996; van Der Meer *et al.*, 2010). Increasing pupil diameters are linked to increasing cognitive demands and inversely related to individual cognitive abilities. According to this theory, patients with impaired cognitive abilities show larger PDRs to maintain behavioural performances (Granholm *et al.*, 1996; Granholm *et al.*, 2017). Granholm *et al.* (2017) investigated this effect in AD-MCI patients indicating different stages of cognitive impairment during performance of a digit span task. Patients with moderate cognitive impairment showed larger PDRs while maintaining the same behavioural performance as HC. The authors concluded that task-induced increased pupil diameters represent the physiological outcome of a compensatory mechanism. Alternating processing loads revealed that this effect was limited to low and moderate levels of cognitive load. Pupil dilations

dropped off in all subjects that were beyond their cognitive capacity. Additionally, the compensatory mechanism found its natural limitation in patients with severe cognitive impairment, and resulted in decreased pupil diameters and poor task performances. These compensatory mechanisms are potentially mediated by interactions between the anterior attention system and the LC-NE system (Aston-Jones & Cohen, 2005b; Coull *et al.*, 1999; Sara, 2009). Hence, a dysfunctional LC-NE system likely manifests in failing compensation and smaller PDRs in AD patients. The current study presumably supports this theory. Inclusion of MRI covariates to regression analyses showed that the measured variance of LC volumes across groups significantly predicted amplitude, latency and slope during performance of the OB paradigm. This study investigated patients with early AD-dementia and it might be regarded as a continuation of the previously described experiments with AD-MCI patients by Granholm *et al.* (2017). The currently observed smaller PDRs and decreased behavioural accuracy in AD patients are in line with Granholm's (2017) theory: performance of the OB paradigm probably exceeded the compensatory capacities of the patient group so that pupil diameters and cognitive abilities (accuracies) dropped.

The current results show that the PDR obtained during performance of an OB paradigm represents a physiological marker that is sensitive for degenerative changes of the LC-NE system in the course of early AD. Evaluation of the PDR should be based on the analysis of the entire pupillary deflection from baseline by using statistics correcting for the multiple comparison problem. Alternatively, the slope of the target-induced pupil dilation is proposed to be a promising correlate for NE deficiency in AD patients. Repeating the experiments with a larger number of participants could demonstrate if the trend for a decreased PDR slope in patients turns into statistically significant differences.

The pupil dilation response elicited by the attentional blink paradigm (single task mode)

The PDR, analysed in terms of amplitude, latency and slope, and elicited during performance of the AB1 paradigm did not differ between AD patients and HC. Additionally, a statistical evaluation of the entire waveform was performed by applying cluster-based random permutations. This approach confirmed the previous finding and did not show any group differences of pupillary deflections in response to target detection. To test the ability of the AB1 paradigm to reliably induce stimulus-

related pupil dilations, additional within-subject analyses were calculated for each group. As revealed by cluster statistics the individual pupil sizes significantly dilated about 430 ms (HC) respectively immediately (AD) after target detection. Therefore, it is assumed that the presented AB1 paradigm reliably stimulated neurophysiological processes resulting in distinct PDRs.

To date, none of the previous studies investigated the PDR elicited by an AB1 paradigm in AD patients. The data clearly show that the AB1 paradigm elicited individual PDRs, but it did not induce PDRs that were sensitive to early neurodegeneration in AD. This was unexpected because the patients' cognitive abilities (accuracies) significantly dropped in comparison with HC. According to the previously described theory corroborated by Granholm *et al.* (2017) poor task performances are associated with decreased pupil sizes and are the result of failed compensation mechanisms. If this theory is translated to the current study it suggests that a potential compensation mechanism was not adequately efficient in AD patients. Some neural processes sufficiently induced a PDR, but they were not able to produce satisfactory cognitive abilities.

This study clearly showed that the PDR obtained during performance of the AB1 paradigm is not sensitive for disease-related changes in early AD and is not suggested to be used as a marker for degeneration of the LC-NE system.

4.4 Correlation analyses: parameters obtained during performance of the oddball paradigm

Since the objective of this study is to identify markers being sensitive to the degeneration of LC-NE system, correlations between LC volumes/intensities and the investigated behavioural and physiological parameters are of particular interest.

4.4.1 Correlations with LC volumes/intensities

The group of HC showed that smaller LC volumes were associated with longer P3 latencies, larger PDR amplitudes and larger slopes. In AD patients, a similar result became evident: smaller LC volumes were correlated with larger PDR amplitudes and slopes, but missed any significant relationship with EEG parameters.

Experiments with monkeys provided evidence for a significant positive correlation of pupil diameters with LC tonic activity and behavioural performance (Joshi *et al.*, 2016; Rajkowski, 1993). Additionally, pharmacological manipulations indicated that increased pupil diameters are associated with enhanced activity of the LC-NE system (Hou *et al.*, 2005; Minzenberg *et al.*, 2008). These outcomes point to a functional relationship between the LC and pupillary responses: more activity of LC neurons may supposedly result in larger PDRs. Unfortunately previous studies focus on fMRI data rather than investigating correlations of structural LC volumes with physiological data. There are indications that there is a functional relationship of the LC and the PDR in young adults. Murphy *et al.* (2014) assessed brain activity during performance of a 2-stimulus OB task by using combined pupillometry and fMRI. The study included 14 young participants (age range: 21-48 years) and primary focused the analyses of BOLD activity on the ROI containing the LC. Comparable to the current study, Murphy *et al.* (2014) localized the LC by using the standardized atlas mask published by Keren *et al.* (2009). The study revealed a strong positive correlation between target-induced LC activity and the PDR. Additional analyses excluded primary visual cortex activation from the signal and showed a largely preserved relationship between PDR and LC activity (Murphy *et al.*, 2014).

This outcome suggests that the LC nucleus plays an important role in controlling the PDR and therefore, structural measures of the LC may also be correlated with PDRs. Based on this assumption the current results are unexpected: in this study, smaller LC volumes were associated with larger PDR amplitudes (in both groups) and with longer P3 latencies (in HC). To date, no study reported the relationship between LC volumes/intensities and PDRs in AD patients so that the reliability of the current outcome cannot be proven. Hämmerer *et al.* (2018) investigated to what extent age-dependent alterations of the LC account for cognitive decline in ageing. Younger and older participants performed a memory task to activate the LC-NE system. Intensities of the LC were acquired by neuromelanin-sensitive MRI scans. Additionally, the PDR was obtained as a potential marker of LC activity. It should be noted that there were no age differences in mean LC intensity or volume. The researchers reported two main outcomes of this study. On the one hand, older subjects indicated poorer memory performance, especially in response to emotionally salient stimuli, in correlation with smaller LC intensities. This outcome was not evident in young participants and showed that LC intensities might explain

age-dependent alterations in memory performance (Hämmerer *et al.*, 2018). On the other hand, larger PDRs were observed after perceiving salient stimuli (in both groups) and showed, on trend level, a correlation with stronger LC intensities (in older participants). The missing significance of the latter result was quite unexpected and the authors considered small statistical power as a potential explanation (Hämmerer *et al.*, 2018). This study showed that the initially assumed correlation of large LC volumes with increased PDRs could not be significantly demonstrated in older participants. In contrast, the current study indicates that smaller LC volumes were associated with larger PDRs in a comparable group of individuals (HC). Further experiments including structural MRI measurements should evaluate if these results are based on small statistical power, methodological weaknesses or structural alterations related to ageing and AD.

In summary, the current findings show that the electrophysiological P3 component is not associated with structural LC measures in AD patients. Additionally, it did not show disease-dependent alterations when comparing deflections in HC and in AD patients. This parameter is therefore not recommended to be used as marker for LC degeneration in AD patients. The obtained group differences of the PDR slope did not turn into significant alterations, but indicated the trend for a lower average value in AD patients. Although the current results revealed odd correlations between LC volumes and the PDR, they suggest that there is a significant link between these parameters. Before the slope could be used as physiological correlate in early AD patients, further analyses are necessary to investigate the nature of this relationship and indicate to what extent these correlations are specific for AD.

4.4.2 Other correlations

In this study, longer RTs were obtained when subjects indicated longer P3 latencies (both groups), longer PDR latencies (HC) and smaller PDR amplitudes (AD). This relationship is in line with previous findings. Nieuwenhuis, Aston-Jones, and Cohen (2005) proposed that the electrophysiological P3 is a result of phasic bursts of NE in response to stimulus evaluation and decision making. According to their theory of LC function, the P3 component should be correlated with behavioural parameters such as accuracy and RT. This theory was further investigated by Kamp and Donchin (2015) who obtained both the P3 component and PDR in an OB paradigm in young

participants. The authors reported that targets (“infrequents”) elicited P3 latencies that were correlated with RT, while P3 amplitudes did not show significant correlations with behaviour. The current study demonstrated that this finding is also evident in older subjects and in AD patients. While P3 latencies indicated significant relationships with RT in both groups, P3 amplitudes were not associated with the behavioural responses RT and accuracy. These outcomes suggest that the degree of allocated cognitive resources, measured in terms of amplitudes (van Dinteren *et al.*, 2014), does not affect the RT. It is rather the speed of signal processing, reflected by the latency (van Dinteren *et al.*, 2014), that has direct influence on the time necessary for response execution.

Kamp and Donchin (2015) revealed inconsistent findings regarding PDR parameters since both amplitude and latency were significantly related to RTs. The outcome of the present study shows that this relationship differs in aged and diseased individuals. Older subjects associated longer latencies with longer RTs, while in AD patients smaller amplitudes correlated with longer RTs. A possible explanation is that older subjects show longer RTs because they need more time to recruit relevant neural resources. This delay could be an adaptation to maintain behavioural accuracies on an almost perfect level (99.58 %, SD = 1.59). This correlation was not found in AD patients which might contribute to the significant decrease of accuracy (94.79 %, SD = 12.62, $p < 0.05$) in this group. Patients with AD potentially possess reduced neural resources which resulted in smaller PDR amplitudes and eventually longer RTs.

To summarize, the outcomes of this study show that behavioural parameters obtained during performance of a visual OB paradigm indicated restricted relationships with the LC-NE system. The parameter “accuracy” lacks any link with structural MRI data or physiological parameters. Although correlation analyses did not reveal a direct association of RTs with LC volumes/intensities in AD patients and in HC, the current results revealed that this behavioural parameter is strongly linked to physiological responses that are controlled by the LC-NE system (e.g. de Gee *et al.*, 2017; Murphy *et al.*, 2014; reviewed by Nieuwenhuis, Aston-Jones, & Cohen, 2005).

4.5 Correlation analyses: parameters obtained during performance of the attentional blink paradigms

4.5.1 Correlations with LC volumes/intensities

In the AB2 paradigm, HC were likely to achieve better task performances at lag 2 (on trend level) and lag 5 (significant) when they had higher LC intensities. The patient group showed a similar correlation at lag 2 when they had higher accuracy rates in association with larger LC volumes. Performance of the AB1 paradigm revealed that accuracies in HC were significantly better when the LC intensity was higher and the LC volume was larger. No correlation between LC measures and AB1 performance was found in the AD group.

These correlations of behavioural accuracies in the AB1 and AB2 paradigms were in accordance with previous findings. Human studies (Gilzenrat et al., 2010; reviewed by Nieuwenhuis, Aston-Jones, & Cohen, 2005) and those with monkeys (Aston-Jones et al., 1994; Clayton et al., 2004) reported a correlation of high performance levels with phasic activation of LC neurons. During task performance NE is released from the LC nucleus and increases the neuronal sensitivity for relevant information (e.g. target stimuli). At the same time, irrelevant information processing appears to be inhibited. These findings can be translated to the here presented visual stimulus detection tasks that also recruited the LC-NE system. Larger LC volumes indicate a larger storage of NE (Aston-Jones & Cohen, 2005b; Heneka *et al.*, 2010). Thus, participants benefited from a NE-mediated facilitation of the local “signal-to-noise” ratio, resulting in improved stimulus discrimination (Sara, 2009). Based on these assumptions, the present outcome of positive relationships between task performance and LC volumes/intensities is a consistent finding. This study shows that an equivalent correlation is also evident in AD patients performing the AB2 paradigm. Patients had better behavioural performances when they indicated larger LC volumes. This outcome suggests that AD patients take advantage of the functionality of the LC-NE system. Statistical analyses revealed that in both groups the NE-mediated improvement of target detection was particularly relevant at lag 2 respectively 240 ms after target presentation. This time point corresponds well with the occurrence of the AB effect. The phenomenon was previously observed

when both targets were presented with a temporal distance in the range of 200-500 ms (Jolicoeur, 1999a). Within the group of HC, an additional positive correlation between LC intensities and task performance was found at lag 5 or 600 ms after target occurrence. Thus, the potentially task-improving effects of NE occurred after the temporal frame of the AB when the performance of T2 identification typically recovers. However, in the present study the task performance at lag 5 was not significantly improved towards the performance at lag 2. Here, the described attentional deficit period appeared elongated compared to a similar experiment (Peters *et al.*, 2012). It should be taken into consideration that the presented AB2 paradigm indicated a level of task difficulty that was too high to reveal NE-mediated improved stimulus detection rates at lag 5.

Furthermore, there were no significant relationships between LC volumes and PDRs obtained during performance of the AB1 paradigm. Up to date, no studies investigated correlations between structural LC measures and PDRs in AD patients. Comparable approaches focused their research on the activity of the brain region containing the LC nucleus. The maximum pupil amplitude represents the proportion of NE release (reviewed by Beatty & Lucero-Wagoner, 2000), while the baseline pupil diameter is associated with tonic LC activity (Gilzenrat *et al.*, 2010; Rajkowski, 1993). This suggests that the LC nucleus plays an important role in controlling the PDR and therefore, it stands to reason that there should be a correlation between both parameters. Based on this assumption, the present finding of not any relationship between LC volumes and PDRs was unexpected. It is noteworthy that previous studies based their conclusions on data from OB paradigms (Gilzenrat *et al.*, 2010; Murphy *et al.*, 2014) and memory tasks (Hämmerer *et al.*, 2018) rather than AB1 paradigms, and none of these studies investigated AD patients. Therefore, it remains unclear if the present result represents a reliable outcome.

In summary, the investigated correlation analyses showed that it is mainly the AB2 paradigm that produced behavioural data significantly related to structural LC measures. These behavioural data were also sensitive to disease-related changes of the LC nucleus, but floor effects in AD patients give rise to justified doubts about the validity of the test results. Based on the current study, this parameter is therefore not suggested as correlate for degeneration of the NE system. The AB1 paradigm produced behavioural data that were associated with the LC nucleus in HC, but not in early AD patients. Because of the importance of the LC-NE system for task

performance and the detected group differences, it is concluded that the accuracy in an AB1 paradigm represents a reliable marker for norepinephrine deficiency. In contrast, PDR parameters obtained from this paradigm are not appropriate candidates as correlates for LC degeneration.

4.5.2 Other correlations

Data obtained in HC did not show significant correlations beyond the previously described relationships with structural LC measures. Within the group of AD patients, lower accuracies in both the AB1 paradigm and the AB2 paradigm were significantly associated with larger amplitudes and longer latencies of the PDR.

The described relationship points to an inefficient, delayed allocation of neural resources in AD patients. This correlation was quite unexpected since increased pupil diameters were proposed to be associated with enhanced activity of the LC-NE system (Minzenberg *et al.*, 2008) and therefore, with good behavioural performances (Kamp & Donchin, 2015). Reduced LC-NE system activity, as found in AD patients, typically results in decreased PDRs (Hou *et al.*, 2005) and poor behavioural performances (Tsolaki *et al.*, 2017). A supposable explanation for the current finding is the theory that PDRs modulated by mental effort represent an indicator for cognitive decline (Ahern & Beatty, 1979; Beatty, 1982; Granholm *et al.*, 1996; van Der Meer *et al.*, 2010). Increasing pupil diameters are linked to increasing cognitive demands and inversely related to individual cognitive abilities. Patients with impaired cognitive abilities show larger PDRs to maintain behavioural performances (Granholm *et al.*, 1996; Granholm *et al.*, 2017). But the here investigated patients were not able to compensate the disease-related impaired cognition which manifested in bad task performances. In case compensation mechanisms fail, the PDR typically decreases in AD patients (Dragan *et al.*, 2017; Granholm *et al.*, 2017). At this juncture it cannot be explained why the present study did not replicate this finding.

4.6 Limitations and future directions

As statistical analyses revealed, there were no significant differences in LC volumes or intensities between AD patients and HC. This finding possibly weakened the conclusions regarding differential effects of LC volumes. The consequences of LC degeneration on the investigated behavioural and physiological correlates would have become more evident if the group differences between LC volumes were significant. In spite of this limitation, this study showed that behavioural performances obtained in OB and AB1 paradigms as well as the PDR during performance of the OB paradigm were reliably decreased in early AD patients. Previous studies revealed that these parameters are mainly controlled by the functioning of the NE system (for instance: R. M. Krebs *et al.*, 2018; Murphy *et al.*, 2014). This suggests that alterations in these parameters reflect disease-related changes of the LC nucleus. However, this conclusion is based on theoretical assumptions since the LC activity is measured rather indirectly in form of these parameters. Unequivocal evidence for a causal relationship between LC degeneration and alterations of LC parameters can be provided by fMRI.

The applied AB2 paradigm needs to be revised in three respects. In the first place, the task difficulty appears to be too high when target and standard stimuli were presented in the same colour. This resulted in floor effects and considerably reduced the amount of evaluable trials especially in the AD group. A reliable group comparison with sound conclusions about the usability of the AB2 paradigm as marker for LC-NE degeneration was not possible. Future studies investigating AD patients are supposed to ease target selection by highlighting target stimuli in contrast colours. Second, the presented number of lags was not sufficient to evoke the complete recovery of task performance. The group of HC failed to produce accuracies that were significantly higher at longer lags compared to those at shorter lags. But according to the criteria postulated by MacLean and Arnell (2012), evaluation of the AB effect requires a complete recovery of the AB. Further experiments with older participants should therefore present a longer maximum temporal distance between T1 and T2 than 840 ms. And third, the number of 20 trials per lag category was too low to ensure reliable analyses of physiological parameters obtained during performance of the AB2 paradigm. This fact, though, had been considered already prior to the start of this study and it had been accepted to keep

the experimental procedure feasible for AD patients. Participation in all experiments took between five and six hours per subject (incl. preparing of EEG acquisition) and increasing the number of trials would have exhausted the patients too much.

To ensure a high quality standard, strict inclusion criteria were applied for the selection of all participants. The intake of any medication affecting the NE system resulted in exclusion from this study but patients did not stop taking AD-related medication, such as acetylcholinesterase inhibitors (AChEI). This manipulation of the cholinergic system might have had effects on the investigated parameters. Improved visual selective attention (Foldi, White, & Schaefer, 2005) and reduced P3 components (Chang *et al.*, 2014; Katada *et al.*, 2003; Werber *et al.*, 2003) were previously observed in response to cholinergic treatment. Thus, including AD patients taking AChEIs might lead to conclusions that reflect the cognitive-behavioral effects of the medication. As proofed by the established literature, there is no consistent solution how to deal with this issue. Many studies do not provide any information about the participants' AD-related medication (for instance: Cecchi *et al.*, 2015; Dragan *et al.*, 2017; Granholm *et al.*, 2017). Other cohorts (for instance: Peters *et al.*, 2012; Tsolaki *et al.*, 2017) as well as the present AD patients continued the intake of AChEIs. This decision was based on the consideration that a sudden discontinuation of medication intake could affect the patients' well-being.

Eventually, it cannot be excluded that small statistical power could have contributed to unexpected outcomes of this study. The group sizes of 26 respectively 24 subjects was possibly not sufficient to reveal significant disease-dependent alterations in all parameters.

Potential effects of the cholinergic system are not unequivocally excluded. To proof conclusive evidence for a noradrenergic regulation of the investigated parameters, prospective studies should repeat the experiments after the intake of a selective β-receptor antagonist like propranolol. A randomized and placebo-controlled within-subject design with healthy, older participants is expected to reveal changes of behavioural and physiological parameters that are similar to the described alterations in AD patients. In young subjects, a manipulation with propranolol significantly modulated correlates of the LC-NE system like the electrophysiological P3 component (de Rover *et al.*, 2015) and the performance obtained in an AB2 paradigm (de Martino, Strange, & Dolan, 2008). Currently, effects of these noradrenergic manipulations have not been reported in healthy, older

participants with sufficient sample sizes. Findings from these studies could provide an important requirement for further pharmacological interventions that are based on β-receptor agonists. In this way, those parameters that were sensitive for LC-NE system degeneration in the present study could serve as correlates proving the effectiveness of new drugs for treating AD.

Appendix

Appendix-list 1.

Intake of the following active substances affecting the NE system was considered as exclusion criterion for this study.

- Amphetamine
- Atenolol
- Atomoxetine
- Bambuterol
- Befunolol
- Betaxolol
- Bisoprolol
- Brimonidine
- Bunazosin
- Carteolol
- Carvedilol
- Celiprolol
- Chlorprothixen
- Clenbuterol
- Clozapine
- Dobutamine
- Doxazosin
- Duloxetine
- Ephedrine
- Epinephrine
- Ergotamine
- Esmolol
- Etilefrine
- Fenoterol
- Formoterol
- Guanfacine
- Indacaterol
- Indoramin
- Levobunolol
- Methyldopa
- Methylphenidate
- Metipranolol
- Metoprolol
- Mianserin
- Mirtazapine
- Moclobemide
- Modafinil
- Naphazoline
- Olanzapine
- Olodaterol
- Orciprenaline
- Paliperidone
- Perazine
- Phenoxybenzamine
- Phentolamine
- Phenylephrine
- Phenylephrine
- Prazosin
- Propranolol
- Quetiapine
- Reproterol
- Risperidone
- Salbutamol
- Salmeterol
- Sertindole
- Sotalol
- Terazosin
- Terbutaline
- Tetryzoline
- Thioridazin
- Timolol
- Tramazoline
- Tranylcypromine
- Trimazosin
- Urapidil
- Venlafaxine
- Vilanterol
- Ziprasidone

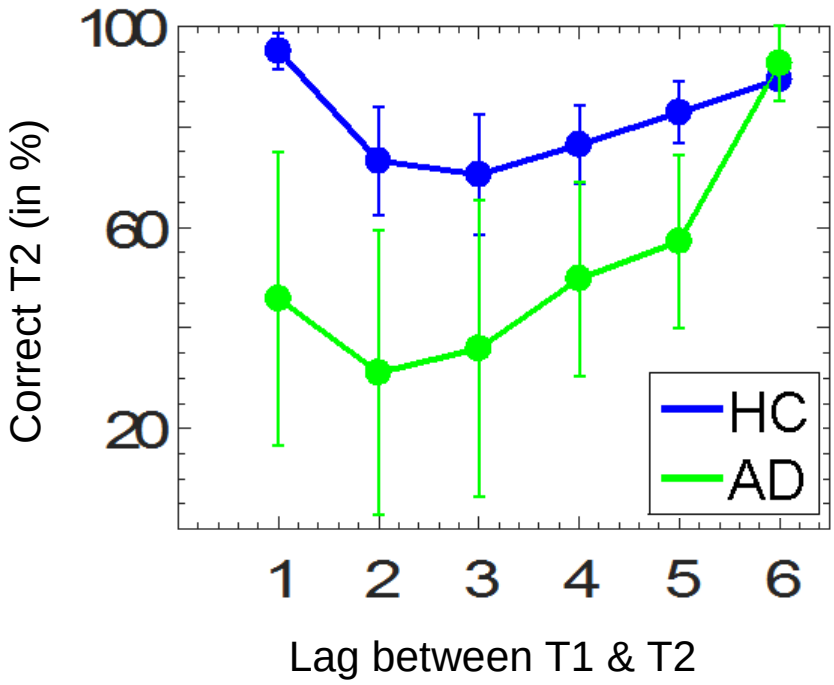

Appendix-figure 1. Behavioral results of the AB2 task acquired within the preceding pilot study. The accuracy of correct T2 identification (with SEM) is represented in relation to the distance between T1 and T2.

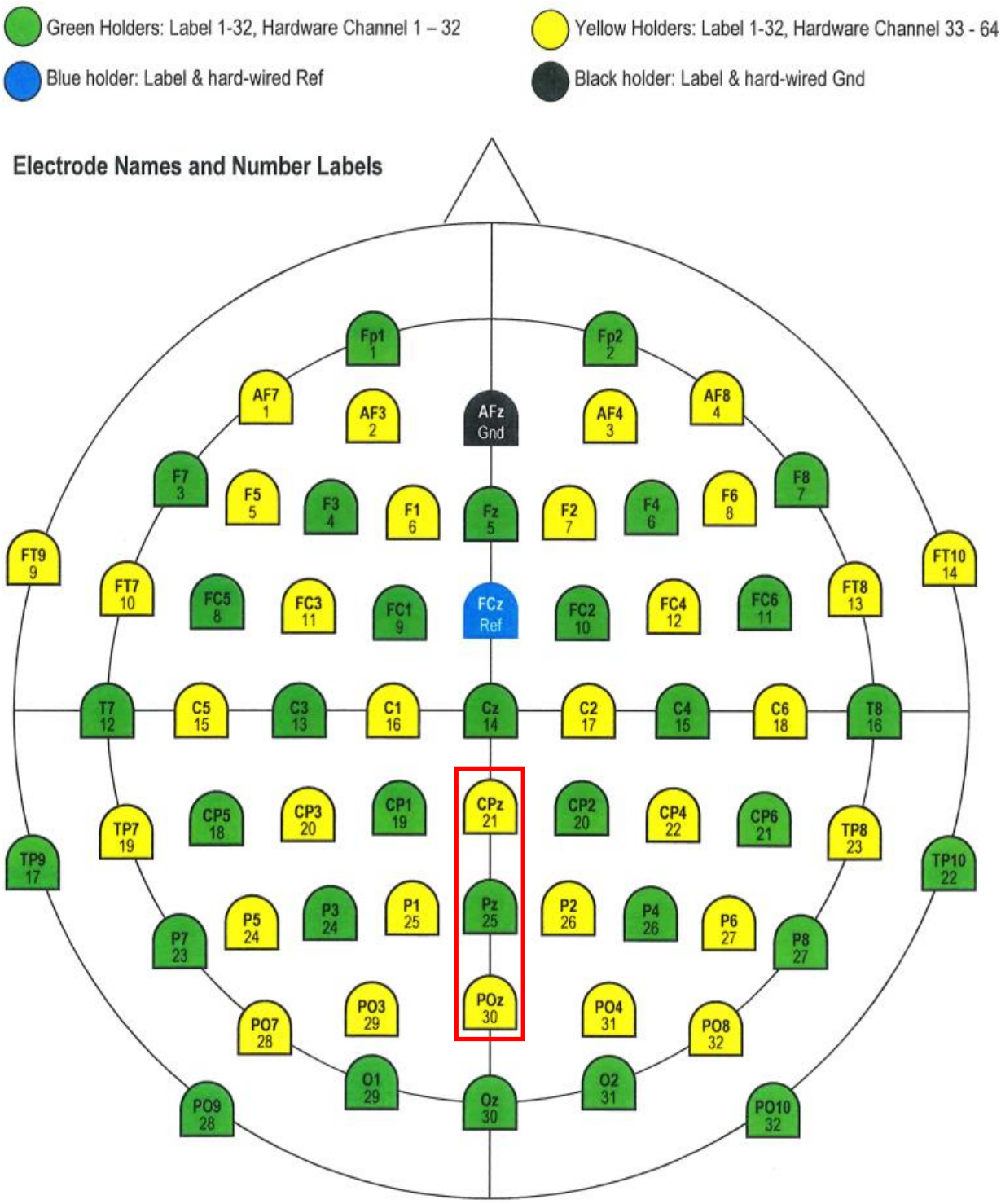

Appendix-figure 2. Electroencephalographic montage indicating the applied electrode positions. Electrodes were placed according to the international 10-20 localization system. The red rectangle highlights the 3 centroparietal electrodes that were averaged and statistically analysed in this study.

The figure was modified from Brain Products GmbH, Germany, September 2017.

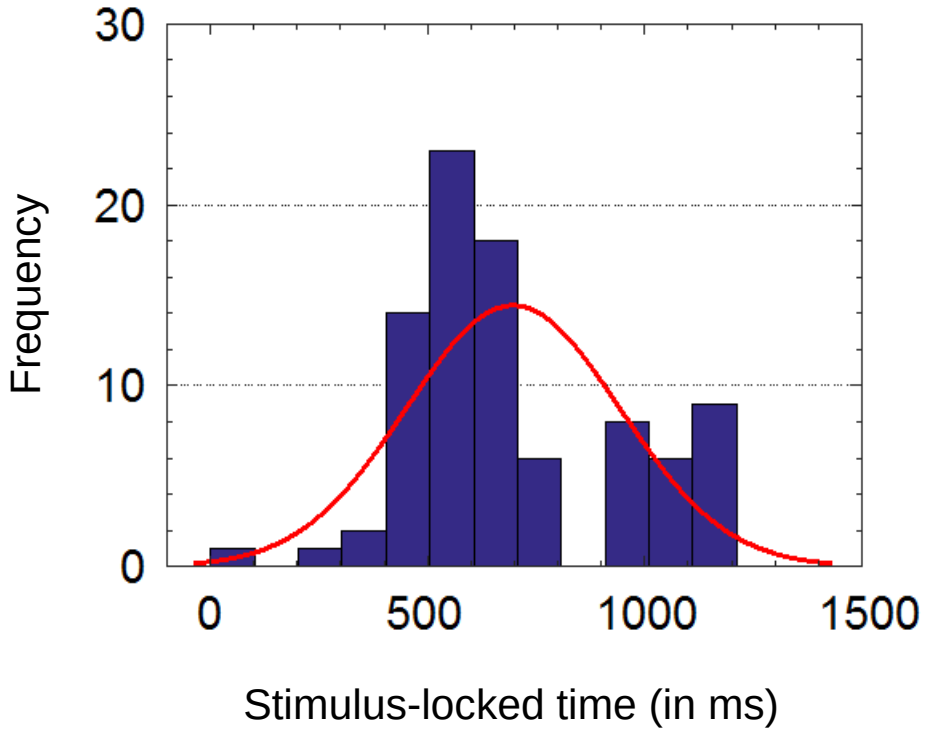

***Appendix-figure 3*.** Histogram showing the time values of the most positive EEG deflections after stimulus presentation within the OB paradigm. Data were summed for both groups and both conditions. The red curve indicates the probability distribution.
Based on this bimodal distribution pattern, the analysis window for parameterization of ERP components was set to 300-800 ms.

Appendix-table 1.
Average data that were assumed to calculate inverse transformations of the target accuracy.

Group	Age	Education	Gender	Left LC intensity	Right LC intensity	Left LC volume	Right LC volume
HC	70	15	male	1.15	1.15	10	10
AD	70	15	male	1.15	1.15	10	10

Appendix-equation 1.
The following inverse transformation accounts for a subject's regression coefficient and target accuracy in the HC group.

Regression equation:

$$\begin{aligned} \boldsymbol{R} = \ & \boldsymbol{-8.04\ (intercept) + 1 * 1.15\ (group) - 70 * 0.02\ (age) - 15} \\ & \boldsymbol{* 0.08\ (education) + 0 * 0.24\ (gender) + 1.15} \\ & \boldsymbol{* 3.97\ (left\ LC\ intensity) + 1.15 * 3.56\ (right\ LC\ intensity) + 10} \\ & \boldsymbol{* 0.01\ (left\ LC\ volume) + 10 * 0.04\ (right\ LC\ volume) = -0.33} \end{aligned}$$

Regression coefficient:

$$\sqrt{\boldsymbol{R(Accuracy)}} = \boldsymbol{-0.33}$$

$$<=> \boldsymbol{R(Accuracy) = (-0.33)^2 = 0.11}$$

$$\boldsymbol{Target\ accuracy = 100 - 0.11 = 99.89\%}$$

Appendix-equation 2.
This inverse transformation accounts for a subject's regression coefficient and target accuracy in the AD group.

Regression equation:

$$\begin{aligned} \boldsymbol{R} = \ & \boldsymbol{-8.04\ (intercept) + 2 * 1.15\ (group) - 70 * 0.02\ (age) - 15} \\ & \boldsymbol{* 0.08\ (education) + 0 * 0.24\ (gender) + 1.15} \\ & \boldsymbol{* 3.97\ (left\ LC\ intensity) + 1.15 * 3.56\ (right\ LC\ intensity) + 10} \\ & \boldsymbol{* 0.01\ (left\ LC\ volume) + 10 * 0.04\ (right\ LC\ volume) = 0.82} \end{aligned}$$

Regression coefficient:

$$\sqrt{\boldsymbol{R(Accuracy)}} = \boldsymbol{0.82}$$

$$<=> \boldsymbol{R(Accuracy) = (0.82)^2 = 0.67}$$

$$Target\ accuracy = 100 - 0.67 = 99.33\%$$

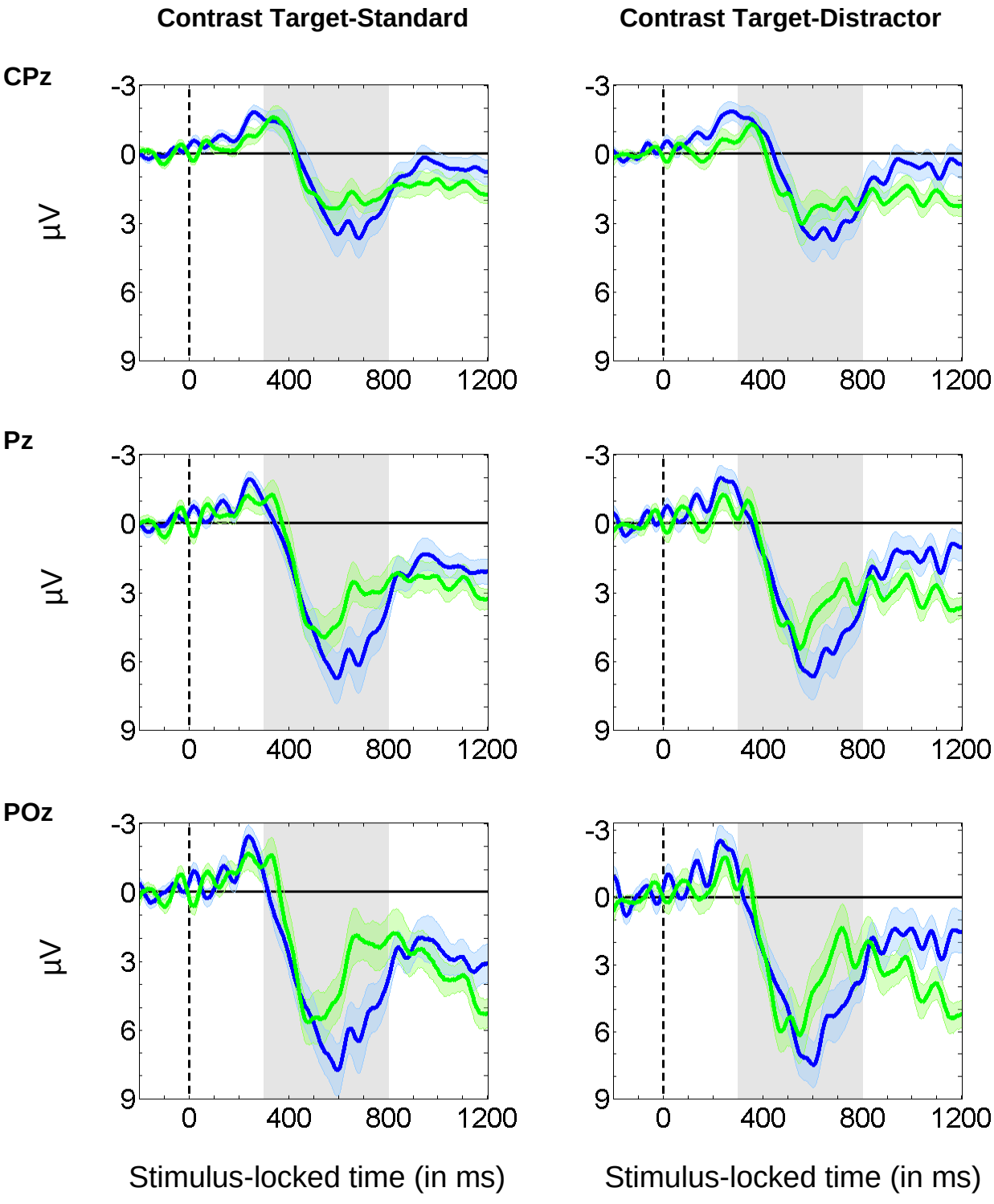

Appendix-figure 4. Centroparietal EEG waveforms acquired during performance of the OB paradigm. Data from the presented electrodes CPz, Pz and POz were averaged for both contrasts, target vs. standard, and target vs. distractor. Thereby the multiple comparison problem was reduced.
The dashed line indicates appearance of the stimulus. The grey rectangle highlights the defined analysis window for the P3b component (300-800 ms). The shaded color areas show the SEM for each waveform.

Appendix-table 2.

Correlations between behavioral and functional parameters gained from the OB paradigm. The upper diagonal displays data from HC and the lower diagonal data from the AD group.

	EEG: TS-Amp	EEG: TD-Amp	EEG: TS-Lat	EEG: TD-Lat	EEG: TS-Slo	EEG: TD-Slo	PDR: TS-Amp	PDR: TD-Amp	PDR: TS-Lat	PDR: TD-Lat	PDR: TS-Slo	PDR: TD-Slo	Acc Target	RT Target	MRI: I-left	MRI: I-right	MRI: V-left	MRI: V-right
EEG: TS-Amp		0.73**	0.17	0.04	0.76**	0.71**	0.15	0.11	0.22	0.16	0.03	0.03	-0.23	0.26	-0.23	-0.08	-0.05	-0.06
EEG: TD-Amp	0.71**		0.18	0.08	0.65**	0.84**	0.18	0.14	0.27	0.21	0.06	0.06	-0.20	0.31*	-0.15	-0.06	-0.05	-0.18
EEG: TS-Lat	-0.18	-0.09		0.71**	-0.07	0.05	0.40*	0.39*	0.31	0.26	0.31	0.31	0.010	0.32*	-0.04	-0.13	-0.34*	-0.26
EEG: TD-Lat	-0.17	-0.20	0.70**		-0.15	-0.08	0.28	0.24	0.16	0.14	0.16	0.16	-0.03	0.46**	-0.02	-0.19	-0.17	-0.28
EEG: TS-Slo	0.80**	0.60**	-0.38*	-0.30		0.74**	-0.01	-0.05	0.06	0.01	-0.07	-0.07	-0.22	0.16	-0.20	-0.07	-0.01	-0.05
EEG: TD-Slo	0.58**	0.71**	-0.32*	-0.48**	0.66**		0.19	0.15	0.20	0.15	0.10	0.10	-0.15	0.21	-0.11	-0.04	-0.09	-0.14
PDR: TS-Amp	-0.14	-0.17	-0.20	0.03	0.01	-0.15		0.90**	0.37*	0.36*	0.78**	0.60**	0.04	0.18	0.09	-0.12	-0.38*	-0.20
PDR: TD-Amp	-0.11	-0.22	-0.15	-0.04	-0.02	-0.15	0.74**		0.33*	0.32	0.76**	0.66**	0.04	0.10	0.14	-0.19	-0.43*	-0.28
PDR: TS-Lat	0.06	-0.04	-0.21	-0.22	0.11	0.10	0.29	0.47**		0.72**	0.15	0.10	0.20	0.39*	0.16	-0.10	-0.06	-0.14
PDR: TD-Lat	0.04	-0.06	-0.32	-0.22	0.14	0.08	0.24	0.46**	0.84**		0.16	-0.02	0.23	0.30	0.10	-0.16	-0.20	-0.08
PDR: TS-Slo	-0.14	-0.17	-0.13	0.12	-0.04	-0.22	0.83**	0.59**	0.11	0.07		0.70**	0.01	-0.02	0.08	-0.04	-0.42*	-0.14
PDR: TD-Slo	-0.16	-0.22	-0.15	0.05	-0.09	-0.22	0.83**	0.78**	0.27	0.4	0.79**		0.01	-0.12	0.18	-0.01	-0.27	-0.26
Acc Target	0.12	0.10	-0.23	-0.09	0.17	0.12	0.25	0.11	0.01	0.00	0.31	0.22		-0.14	0.13	-0.14	0.02	-0.32
RT Target	-0.02	-0.01	0.47**	0.30	-0.10	-0.09	-0.33*	-0.23	0.06	0.05	-0.35*	-0.28	-0.29		-0.09	-0.03	0.01	-0.02
MRI: I-left	0.00	0.03	0.00	-0.06	-0.04	0.00	-0.03	-0.13	-0.06	-0.11	-0.03	-0.09	-0.21	-0.07		-0.14	-0.13	-0.31*
MRI: I-right	0.05	0.11	0.18	0.00	0.02	0.17	-0.04	0.12	0.22	0.21	-0.10	0.02	-0.05	0.26	-0.03		0.22	0.18
MRI: V-left	-0.04	-0.01	-0.03	-0.05	-0.03	0.04	-0.16	-0.11	0.07	0.12	-0.20	-0.03	-0.07	0.21	0.01	0.04		0.17
MRI: V-right	0.00	0.07	-0.04	-0.05	-0.02	0.11	-0.38*	-0.22	-0.18	-0.07	-0.33*	-0.26	-0.12	-0.02	-0.00	0.03	0.27	

Note. HC = healthy controls; AD = Alzheimer's disease; TS = contrast target-standard; Amp = amplitude; TD = contrast target-distractor; Lat = latency; Slo = slope; Acc = accuracy; RT = reaction time; I = intensity; V = volume. Data indicate correlation coefficients according to Kendall's tau. ** significant at $p \leq 0.01$; * significant at $p \leq 0.05$.

Appendix-table 3.

Correlations between behavioral and functional parameters gained from the AB paradigm. The upper diagonal displays data from HC and the lower diagonal data from the AD group.

	PDR: Amp	PDR: Lat	PDR: Slope	Acc AB1	Acc AB2-L1	Acc AB2-L2	Acc AB2-L3	Acc AB2-L5	Acc AB2-L7	MRI: I-left	MRI: I-right	MRI: V-left	MRI: V-right
PDR: Amp		0.30	0.85**	-0.08	0.02	-0.12	-0.13	0.08	0.05	0.34	-0.27	-0.32	-0.04
PDR: Lat	0.35*		0.15	-0.06	0.03	0.04	-0.14	-0.01	-0.17	0.12	0.07	-0.35	0.01
PDR: Slope	0.73**	0.09		-0.01	-0.02	-0.09	-0.11	0.09	0.08	0.31	-0.24	-0.20	-0.07
Acc AB1	-0.44**	-0.36*	-0.36*		0.04	0.40**	0.25	0.36*	0.23	0.07	0.39*	0.35*	0.01
Acc AB2-L1	-0.39*	-0.31	-0.31	0.50**		0.16	0.00	0.07	0.29	0.08	0.02	-0.04	-0.07
Acc AB2-L2	-0.34*	-0.36*	-0.28	0.62**	0.53**		0.50**	0.39*	0.35*	0.25	0.30	0.12	-0.19
Acc AB2-L3	-0.58**	-0.57**	-0.42*	0.72**	0.53**	0.68**		0.34*	0.26	-0.08	0.21	0.17	-0.14
Acc AB2-L5	-0.52**	-0.49**	-0.41*	0.61**	0.58**	0.53**	0.70**		0.40*	0.12	0.35*	-0.06	-0.24
Acc AB2-L7	-0.20	-0.22	-0.11	0.43**	0.23	0.25	0.37*	0.52**		0.20	0.18	0.22	-0.26
MRI: I-left	-0.18	0.01	-0.18	-0.01	-0.06	0.02	0.06	-0.11	-0.37*		-0.13	-0.14	-0.23
MRI: I-right	0.09	-0.10	0.14	-0.24	-0.11	0.03	-0.18	-0.23	-0.19	0.07		0.19	0.12
MRI: V-left	0.04	0.05	-0.05	0.11	0.19	0.37*	0.20	0.15	-0.05	-0.02	0.00		0.11
MRI: V-right	0.07	0.12	-0.07	-0.01	0.30	0.16	0.00	0.06	-0.09	0.01	-0.05	0.05	

Note. AB = Attentional blink; HC = healthy controls; AD = Alzheimer's disease; Amp = amplitude; Lat = latency; Acc = accuracy; L1-7 = Lag 1-7; I = intensity; V = volume. Data indicate correlation coefficients according to Kendall's tau.

** significant at $p \leq 0.01$; * significant at $p \leq 0.05$.

References

Ahern, S., & Beatty, J. (1979). Pupillary responses during information processing vary with Scholastic Aptitude Test scores. *Science, 205*(4412), 1289-1292. doi: 10.1126/science.472746

Ahnaou, A., Walsh, C., Manyakov, N. V., Youssef, S. A., & Drinkenburg, W. H. (2019). Early Electrophysiological Disintegration of Hippocampal Neural Networks in a Novel Locus Coeruleus Tau-Seeding Mouse Model of Alzheimer's Disease. *Neural Plast, 2019*, 6981268. doi: 10.1155/2019/6981268

Albert, M. S., DeKosky, S. T., Dickson, D., Dubois, B., Feldman, H. H., Fox, N. C., . . . Phelps, C. H. (2011). The diagnosis of mild cognitive impairment due to Alzheimer's disease: Recommendations from the National Institute on Aging-Alzheimer's Association workgroups on diagnostic guidelines for Alzheimer's disease. *Alzheimer's & Dementia, 7*(3), 270-279. doi: 10.1016/j.jalz.2011.03.008

Alexinsky, T., Aston-Jones, G., Rajkowski, J., & Revay, R. (1990). *Physiological correlates of adaptive behavior in a visual discrimination task in monkeys.* Paper presented at the Society for Neuroscience Abstracts.

Alnæs, D., Sneve, M. H., Espeseth, T., Endestad, T., van de Pavert, S. H. P., & Laeng, B. (2014). Pupil size signals mental effort deployed during multiple object tracking and predicts brain activity in the dorsal attention network and the locus coeruleus. *J Vis, 14*(4), 1-1. doi: 10.1167/14.4.1

Alzheimer's Association Report. (2015). 2015 Alzheimer's disease facts and figures. *Alzheimer's & Dementia, 11*(3), 332-384. doi: 10.1016/j.jalz.2015.02.003

Ardekani, B. A., Choi, S. J., Hossein-Zadeh, G.-A., Porjesz, B., Tanabe, J. L., Lim, K. O., . . . Begleiter, H. (2002). Functional magnetic resonance imaging of brain activity in the visual oddball task. *Cognitive Brain Research, 14*(3), 347-356. doi: 10.1016/S0926-6410(02)00137-4

Arnsten, A. F., Steere, J. C., & Hunt, R. D. (1996). The contribution of alpha 2-noradrenergic mechanisms of prefrontal cortical cognitive function. Potential significance for attention-deficit hyperactivity disorder. *Arch Gen Psychiatry, 53*(5), 448-455. doi: 10.1001/archpsyc.1996.01830050084013

Aston-Jones, G., & Cohen, J. D. (2005a). Adaptive gain and the role of the locus coeruleus–norepinephrine system in optimal performance. *Journal of Comparative Neurology, 493*(1), 99-110. doi: 10.1002/cne.20723

Aston-Jones, G., & Cohen, J. D. (2005b). An Integrative Theory of Locus-Coeruleus-Norepinephrine Function: Adaptive Gain and Optimal Performance. *Annual Review of Neuroscience, 28*(1), 403-450. doi: 10.1146/annurev.neuro.28.061604.135709

Aston-Jones, G., Rajkowski, J., & Cohen, J. D. (1999). Role of locus coeruleus in attention and behavioral flexibility. *Biol Psychiatry, 46*(9), 1309-1320. doi: 10.1016/S0006-3223(99)00140-7

Aston-Jones, G., Rajkowski, J., Kubiak, P., & Alexinsky, T. (1994). Locus coeruleus neurons in monkey are selectively activated by attended cues in a vigilance task. *The Journal of Neuroscience, 14*(7), 4467-4480. doi: 10.1523/jneurosci.14-07-04467.1994

Aston-Jones, G., Rajkowski, J., Lu, W., Zhu, Y., Cohen, J. D., & Morecraft, R. J. (2002). Prominent projections from the orbital prefrontal cortex to the locus coeruleus in monkey. *Soc. Neurosci. Abstr., 28*(86), 9. doi: 10.3389/fncom.2012.0000

Aston-Jones, G., Segal, M., & Bloom, F. E. (1980). Brain aminergic axons exhibit marked variability in conduction velocity. *Brain research, 195*(1), 215-222. doi: 10.1016/0006-8993(80)90880-x

Baker, K. G., Törk, I., Hornung, J.-P., & Halasz, P. (1989). The human locus coeruleus complex: an immunohistochemical and three dimensional reconstruction study. *Exp. Brain Res, 77*, 257-270. doi: 10.1007/BF00274983

Bancher, C., Brunner, C., Lassmann, H., Budka, H., Jellinger, K., Wiche, G., . . . Wisniewski, H. (1989). Accumulation of abnormally phosphorylated τ precedes the formation of

neurofibrillary tangles in Alzheimer's disease. *Brain research, 477*(1-2), 90-99. doi: 10.1016/0006-8993(89)91396-6

Beatty, J. (1982). Task-evoked pupillary responses, processing load, and the structure of processing resources. *Psychological Bulletin, 91*(2), 276. doi: 10.1016/0006-8993(89)91396-6

Beatty, J., & Lucero-Wagoner, B. (2000). The pupillary system. In J. T. Cacioppo, L. G. Tassinary, & G. G. Berntson (Eds.), *Handbook of psychophysiology* (Vol. 2, pp. 142-162): Cambridge University Press.

Benarroch, E. E. (2009). The locus ceruleus norepinephrine system. Functional organization and potential clinical significance. *Neurology, 73*(20), 1699-1704. doi: 10.1212/WNL.0b013e3181c2937c

Berridge, C. W., & Waterhouse, B. D. (2003). The locus coeruleus–noradrenergic system: modulation of behavioral state and state-dependent cognitive processes. *Brain Research Reviews, 42*(1), 33-84. doi: 10.1016/S0165-0173(03)00143-7

Betts, M. J., Cardenas-Blanco, A., Kanowski, M., Jessen, F., & Duzel, E. (2017). In vivo MRI assessment of the human locus coeruleus along its rostrocaudal extent in young and older adults. *Neuroimage, 163*, 150-159. doi: 10.1016/j.neuroimage.2017.09.042

Betts, M. J., Cardenas-Blanco, A., Kanowski, M., Spottke, A., Teipel, S. J., Kilimann, I., . . . Duzel, E. (2019). Locus coeruleus MRI contrast is reduced in Alzheimer's disease dementia and correlates with CSF Abeta levels. *Alzheimers Dement (Amst), 11*, 281-285. doi: 10.1016/j.dadm.2019.02.001

Betts, M. J., Kirilina, E., Otaduy, M. C. G., Ivanov, D., Acosta-Cabronero, J., Callaghan, M. F., . . . Hammerer, D. (2019). Locus coeruleus imaging as a biomarker for noradrenergic dysfunction in neurodegenerative diseases. *Brain, 142*(9), 2558-2571. doi: 10.1093/brain/awz193

Birkl, C., Langkammer, C., Haybaeck, J., Ernst, C., Stollberger, R., Fazekas, F., & Ropele, S. (2014). Temperature-induced changes of magnetic resonance relaxation times in the human brain: a postmortem study. *Magn Reson Med, 71*(4), 1575-1580. doi: 10.1002/mrm.24799

Bledowski, C., Prvulovic, D., Hoechstetter, K., Scherg, M., Wibral, M., Goebel, R., & Linden, D. E. (2004). Localizing P300 generators in visual target and distractor processing: a combined event-related potential and functional magnetic resonance imaging study. *J Neurosci, 24*(42), 9353-9360. doi: 10.1523/JNEUROSCI.1897-04.2004

Bolton, D. A. E., & Staines, W. R. (2014). Attention-based modulation of tactile stimuli: A comparison between prefrontal lesion patients and healthy age-matched controls. *Neuropsychologia, 57*, 101-111. doi: 10.1016/j.neuropsychologia.2014.03.003

Borodovitsyna, O., Flamini, M., & Chandler, D. (2017). Noradrenergic Modulation of Cognition in Health and Disease. *Neural Plasticity, 2017*, 14. doi: 10.1155/2017/6031478

Bougrain, L., Saavedra, C., & Ranta, R. (2012). *Finally, what is the best filter for P300 detection?* TOBI Workshop lll- Tools for Brain-Computer Interaction. Würzburg, Germany.

Braak, E., Braak, H., & Mandelkow, E.-M. (1994). A sequence of cytoskeleton changes related to the formation of neurofibrillary tangles and neuropil threads. *Acta Neuropathologica, 87*(6), 554-567. doi: 10.1007/BF00293315

Braak, H., & Braak, E. (1991). Neuropathological stageing of Alzheimer-related changes. *Acta Neuropathol, 82*(4), 239-259. doi: 10.1007/BF00308809

Braak, H., & Del Tredici, K. (2011). The pathological process underlying Alzheimer's disease in individuals under thirty. *Acta Neuropathologica, 121*(2), 171-181. doi: 10.1007/s00401-010-0789-4

Braak, H., Thal, D. R., Ghebremedhin, E., & Del Tredici, K. (2011). Stages of the pathologic process in Alzheimer disease: age categories from 1 to 100 years. *Journal of Neuropathology & Experimental Neurology, 70*(11), 960-969. doi: 10.1097/NEN.0b013e318232a379

Broadbent, D. E., & Broadbent, M. H. (1987). From detection to identification: response to multiple targets in rapid serial visual presentation. *Percept Psychophys, 42*(2), 105-113. doi: 10.3758/bf03210498

Brown, S. B. R. E., van der Wee, N. J. A., van Noorden, M. S., Giltay, E. J., & Nieuwenhuis, S. (2015). Noradrenergic and cholinergic modulation of late ERP responses to deviant stimuli. *Psychophysiology, 52*(12), 1620-1631. doi: 10.1111/psyp.12544

Bugiani, O., Murrell, J. R., Giaccone, G., Hasegawa, M., Ghigo, G., Tabaton, M., . . . Ghetti, B. (1999). Frontotemporal Dementia and Corticobasal Degeneration in a Family with a P301S Mutation in Tau. *Journal of Neuropathology & Experimental Neurology, 58*(6), 667-677. doi: 10.1097/00005072-199906000-00011

Busch, C., Bohl, J., & Ohm, T. G. (1997). Spatial, Temporal and Numeric Analysis of Alzheimer Changes in the Nucleus Coeruleus. *Neurobiol Aging, 18*(4), 401-406. doi: 10.1016/S0197-4580(97)00035-3

Carrión, R. E., & Bly, B. M. (2008). The effects of learning on event-related potential correlates of musical expectancy. *Psychophysiology, 45*(5), 759-775. doi: 10.1111/j.1469-8986.2008.00687.x

Casey, B. J., Forman, S. D., Franzen, P., Berkowitz, A., Braver, T. S., Nystrom, L. E., . . . Noll, D. C. (2001). Sensitivity of prefrontal cortex to changes in target probability: A functional MRI study. *Human Brain Mapping, 13*(1), 26-33. doi: doi:10.1002/hbm.1022

Cassidy, C. M., Zucca, F. A., Girgis, R. R., Baker, S. C., Weinstein, J. J., Sharp, M. E., . . . Horga, G. (2019). Neuromelanin-sensitive MRI as a noninvasive proxy measure of dopamine function in the human brain. *Proc Natl Acad Sci U S A, 116*(11), 5108-5117. doi: 10.1073/pnas.1807983116

Castellanos, G., Fernández-Seara, M. A., Lorenzo-Betancor, O., Ortega-Cubero, S., Puigvert, M., Uranga, J., . . . Pastor, M. A. (2015). Automated Neuromelanin Imaging as a Diagnostic Biomarker for Parkinson's Disease. *Movement Disorders, 30*(7), 945-952. doi: 10.1002/mds.26201

Cecchi, M., Moore, D. K., Sadowsky, C. H., Solomon, P. R., Doraiswamy, P. M., Smith, C. D., . . . Fadem, K. C. (2015). A clinical trial to validate event-related potential markers of Alzheimer's disease in outpatient settings. *Alzheimers Dement (Amst), 1*(4), 387-394. doi: 10.1016/j.dadm.2015.08.004

Chang, Y. S., Chen, H. L., Hsu, C. Y., Tang, S. H., & Liu, C. K. (2014). Parallel improvement of cognitive functions and P300 latency following donepezil treatment in patients with Alzheimer's disease: a case-control study. *J Clin Neurophysiol, 31*(1), 81-85. doi: 10.1097/01.wnp.0000436899.48243.5e

Chen, L., Zhou, Y., Liu, L., Zhang, X., Zhang, H., & Liu, S. (2015). Cortical event-related potentials in Alzheimer's disease and frontotemporal lobar degeneration. *Journal of the neurological sciences, 359*(1-2), 88-93. doi: 10.1016/j.jns.2015.10.040

Chun, M. M., & Potter, M. C. (1995). A Two-Stage Model for Multiple-Target Detection in Rapid Serial Visual Presentation. *Journal of Experimental Psychology-Human Perception and Performance, 21*(1), 109-127. doi: Doi 10.1037/0096-1523.21.1.109

Cipriani, G., Dolciotti, C., Picchi, L., & Bonuccelli, U. (2011). Alzheimer and his disease: a brief history. *Neurological Sciences, 32*(2), 275-279. doi: 10.1007/s10072-010-0454-7

Clavaguera, F., Bolmont, T., Crowther, R. A., Abramowski, D., Frank, S., Probst, A., . . . Staufenbiel, M. (2009). Transmission and spreading of tauopathy in transgenic mouse brain. *Nature cell biology, 11*(7), 909-913. doi: 10.1038/ncb1901

Clayton, E. C., Rajkowski, J., Cohen, J. D., & Aston-Jones, G. (2004). Phasic Activation of Monkey Locus Ceruleus Neurons by Simple Decisions in a Forced-Choice Task. *The Journal of Neuroscience, 24*(44), 9914-9920. doi: 10.1523/jneurosci.2446-04.2004

Cohen, J. D., Botvinick, M., & Carter, C. S. (2000). Anterior cingulate and prefrontal cortex: who's in control? *nature neuroscience, 3*(5), 421. doi: 10.1038/74783

Corbetta, M., Miezin, F. M., Dobmeyer, S., Shulman, G. L., & Petersen, S. E. (1991). Selective and divided attention during visual discriminations of shape, color, and speed: functional anatomy by positron emission tomography. *J Neurosci, 11*(8), 2383-2402. doi: 10.1523/jneurosci.11-08-02383

Corbetta, M., Patel, G., & Shulman, G. L. (2008). The Reorienting System of the Human Brain: From Environment to Theory of Mind. *Neuron, 58*(3), 306-324. doi: 10.1016/j.neuron.2008.04.017

Coull, J. T., Buchel, C., Friston, K. J., & Frith, C. D. (1999). Noradrenergically mediated plasticity in a human attentional neuronal network. *Neuroimage, 10*(6), 705-715. doi: 10.1006/nimg.1999.0513

Coull, J. T., Middleton, H. C., Robbins, T. W., & Sahakian, B. J. (1995). Clonidine and diazepam have differential effects on tests of attention and learning. *Psychopharmacology (Berl), 120*(3), 322-332. doi: 10.1007/BF02311180

Dahl, M. J., Mather, M., Düzel, S., Bodammer, N. C., Lindenberger, U., Kühn, S., & Werkle-Bergner, M. (2019). Locus coeruleus integrity preserves memory performance across the adult life span. *bioRxiv*, 332098. doi: 10.1101/332098

Dahlström, A., & Fuxe, K. (1964). Evidence for the Existence of Monoamine-Containing Neurons in the Central Nervous System. I. Demonstration of Monoamines in the Cell Bodies of Brain Stem Neurons. *Acta Physiol Scand, 62*(232), Suppl., 1-55.

de Gee, J. W., Colizoli, O., Kloosterman, N. A., Knapen, T., Nieuwenhuis, S., & Donner, T. H. (2017). Dynamic modulation of decision biases by brainstem arousal systems. *Elife, 6*, e23232. doi: 10.7554/eLife.23232.001

de Martino, B., Strange, B. A., & Dolan, R. J. (2008). Noradrenergic neuromodulation of human attention for emotional and neutral stimuli. *Psychopharmacology, 197*(1), 127-136. doi: 10.1007/s00213-007-1015-5

de Rover, M., Brown, S. B. R. E., Band, G. P., Giltay, E. J., van Noorden, M. S., van der Wee, N. J. A., & Nieuwenhuis, S. (2015). Beta receptor-mediated modulation of the oddball P3 but not error-related ERP components in humans. *Psychopharmacology, 232*(17), 3161-3172. doi: 10.1007/s00213-015-3966-2

Debener, S., Makeig, S., Delorme, A., & Engel, A. K. (2005). What is novel in the novelty oddball paradigm? Functional significance of the novelty P3 event-related potential as revealed by independent component analysis. *Cognitive Brain Research, 22*(3), 309-321. doi: 10.1016/j.cogbrainres.2004.09.006

Del Tredici, K., & Braak, H. (2013). Dysfunction of the locus coeruleus–norepinephrine system and related circuitry in Parkinson's disease-related dementia. *J Neurol Neurosurg Psychiatry, 84*(7), 774-783. doi: 10.1136/jnnp-2011-301817

Dell'Acqua, R., Jolicoeur, P., Pesciarelli, F., Job, R., & Palomba, D. (2003). Electrophysiological evidence of visual encoding deficits in a cross-modal attentional blink paradigm. *Psychophysiology, 40*(4), 629-639. doi: 10.1111/1469-8986.00064

Dell'Acqua, R., Pascali, A., Jolicoeur, P., & Sessa, P. (2003). Four-dot masking produces the attentional blink. *Vision Res, 43*(18), 1907-1913. doi: 10.1016/s0042-6989(03)00308-0

Desimone, R., & Duncan, J. (1995). Neural mechanisms of selective visual attention. *Annu Rev Neurosci, 18*, 193-222. doi: 10.1146/annurev.ne.18.030195.001205

Devilbiss, D. M., & Waterhouse, B. D. (2004). The Effects of Tonic Locus Ceruleus Output on Sensory-Evoked Responses of Ventral Posterior Medial Thalamic and Barrel Field Cortical Neurons in the Awake Rat. *The Journal of Neuroscience, 24*(48), 10773-10785. doi: 10.1523/jneurosci.1573-04.2004

Dickter, C. L., & Kieffaber, P. D. (2014). *EEG Methods for the Psychological Sciences*: SAGE Publications. ISBN: 9781446283004.

Donchin, E. (1981). Surprise!... Surprise? *Psychophysiology, 18*(5), 493-513. doi: 10.1111/j.1469-8986.1981.tb01815.x

Donchin, E., & Coles, M. G. H. (1988). Is the P300 Component a Manifestation of Context Updating. *Behavioral and Brain Sciences, 11*(3), 357-374. doi: 10.1017/S0140525x00058027

Dragan, M. C., Leonard, T. K., Lozano, A. M., McAndrews, M. P., Ng, K., Ryan, J. D., . . . Hoffman, K. L. (2017). Pupillary responses and memory-guided visual search reveal age-related and Alzheimer's-related memory decline. *Behavioural Brain Research, 322*, 351-361. doi: 10.1016/j.bbr.2016.09.014

Duncan, C. C., & Kaye, W. H. (1987). Effects of clonidine on event-related potential measures of information processing. *Electroencephalography and clinical neurophysiology, 40*, Suppl., 527-531.

Duncan, J., Martens, S., & Ward, R. (1997). Restricted attentional capacity within but not between sensory modalities. *Nature, 387*(6635), 808-810. doi: 10.1038/42947

Dusek, P., Madai, V. I., Huelnhagen, T., Bahn, E., Matej, R., Sobesky, J., . . . Wuerfel, J. (2019). The choice of embedding media affects image quality, tissue R2 (*) , and susceptibility behaviors in post-mortem brain MR microscopy at 7.0T. *Magn Reson Med, 81*(4), 2688-2701. doi: 10.1002/mrm.27595

Dux, P. E., & Marois, R. (2009). The attentional blink: a review of data and theory. *Atten Percept Psychophys, 71*(8), 1683-1700. doi: 10.3758/APP.71.8.1683

Ehlers, C. L., & Chaplin, R. (1992). Long latency event related potentials in rats: the effects of changes in stimulus parameters and neurochemical lesions. *Journal of Neural Transmission/General Section JNT, 88*(1), 61-75. doi: 10.1007/BF01245037

Einhauser, W., Stout, J., Koch, C., & Carter, O. (2008). Pupil dilation reflects perceptual selection and predicts subsequent stability in perceptual rivalry. *Proc Natl Acad Sci U S A, 105*(5), 1704-1709. doi: 10.1073/pnas.0707727105

Evans, K. K., & Treisman, A. (2005). Perception of Objects in Natural Scenes: Is It Really Attention Free? *Journal of Experimental Psychology: Human Perception and Performance, 31*(6), 1476-1492. doi: 10.1037/0096-1523.31.6.1476

Feinstein, D. L., Heneka, M. T., Gavrilyuk, V., Dello Russo, C., Weinberg, G., & Galea, E. (2002). Noradrenergic regulation of inflammatory gene expression in brain. *Neurochem Int, 41*(5), 357-365. doi: 10.1016/s0197-0186(02)00049-9

Fernandes, P., Regala, J., Correia, F., & Gonçalves-Ferreira, A. J. (2012). The human locus coeruleus 3-D stereotactic anatomy. *Surgical and Radiologic Anatomy, 34*(10), 879-885. doi: 10.1007/s00276-012-0979-y

Field, A. P. (2009). *Discovering statistics using SPSS*(3rd ed.): SAGE. ISBN: 9781412977524.

Fjell, A. M., Walhovd, K. B., & Reinvang, I. (2005). Age-dependent changes in distribution of P3a/P3b amplitude and thickness of the cerebral cortex. *NeuroReport, 16*(13), 1451-1454. doi: 10.1097/01.wnr.0000177011.44602.17

Foldi, N. S., Lobosco, J. J., & Schaefer, L. A. (2002). The Effect of Attentional Dysfunction in Alzheimer's Disease: Theoretical and Practical Implications. *Semin Speech Lang, 23*(02), 139-150. doi: 10.1055/s-2002-24990

Foldi, N. S., White, R. E. C., & Schaefer, L. A. (2005). Detecting effects of donepezil on visual selective attention using signal detection parameters in Alzheimer's disease. *International Journal of Geriatric Psychiatry, 20*(5), 485-488. doi: doi:10.1002/gps.1319

Foote, S. L., Bloom, F. E., & Aston-Jones, G. (1983). Nucleus locus ceruleus: new evidence of anatomical and physiological specificity. *Physiological Reviews, 63*(3), 844-914. doi: 10.1152/physrev.1983.63.3.844

Friedman, D., Hakerem, G., Sutton, S., & Fleiss, J. L. (1973). Effect of stimulus uncertainty on the pupillary dilation response and the vertex evoked potential. *Electroencephalography and clinical neurophysiology, 34*(5), 475-484. doi: 10.1016/0013-4694(73)90065-5

Gannon, M., Che, P., Chen, Y., Jiao, K., Roberson, E. D., & Wang, Q. (2015). Noradrenergic dysfunction in Alzheimer's disease. *Frontiers in Neuroscience, 9*, 220. doi: 10.3389/fnins.2015.00220

Gannon, M., & Wang, Q. (2018). Complex noradrenergic dysfunction in Alzheimer's disease: Low norepinephrine input is not always to blame. *Brain research, in press* doi: 10.1016/j.brainres.2018.01.001

German, D. C., Manaye, K. F., White, C. L., 3rd, Woodward, D. J., McIntire, D. D., Smith, W. K., . . . Mann, D. M. (1992). Disease-specific patterns of locus coeruleus cell loss. *Ann Neurol, 32*(5), 667-676. doi: 10.1002/ana.410320510

German, D. C., Walker, B. S., Manaye, K. F., Smith, W. K., Woodward, D. J., & North, A. J. (1988). The human locus coeruleus: computer reconstruction of cellular distribution.

The Journal of Neuroscience, 8(5), 1776-1788. doi: 10.1523/JNEUROSCI.08-05-01776

Gilzenrat, M. S., Nieuwenhuis, S., Jepma, M., & Cohen, J. D. (2010). Pupil diameter tracks changes in control state predicted by the adaptive gain theory of locus coeruleus function. *Cognitive, Affective, & Behavioral Neuroscience, 10*(2), 252-269. doi: 10.3758/cabn.10.2.252

Giorgi, F. S., Ryskalin, L., Ruffoli, R., Biagioni, F., Limanaqi, F., Ferrucci, M., . . . Fornai, F. (2017). The Neuroanatomy of the Reticular Nucleus Locus Coeruleus in Alzheimer's Disease. *Frontiers in Neuroanatomy, 11*, 8. doi: 10.3389/fnana.2017.00080

Giorgi, F. S., Saccaro, L. F., Galgani, A., Busceti, C. L., Biagioni, F., Frati, A., & Fornai, F. (2019). The role of Locus Coeruleus in neuroinflammation occurring in Alzheimer's disease. *Brain Research Bulletin, 153*, 47-58. doi: 10.1016/j.brainresbull.2019.08.007

Goedert, M. (2015). Alzheimer's and Parkinson's diseases: The prion concept in relation to assembled Aβ, tau, and α-synuclein. *Science, 349*(6248), 1255555. doi: 10.1126/science.1255555

Gompf, H. S., Mathai, C., Fuller, P. M., Wood, D. A., Pedersen, N. P., Saper, C. B., & Lu, J. (2010). Locus coeruleus (LC) and anterior cingulate cortex sustain wakefulness in a novel environment. *J Neurosci, 30*(43), 14543-14551. doi: 10.1523/JNEUROSCI.3037-10.2010

Granholm, E. L., Asarnow, R. F., Sarkin, A. J., & Dykes, K. L. (1996). Pupillary responses index cognitive resource limitations. *Psychophysiology, 33*(4), 457-461. doi: 10.1111/j.1469-8986.1996.tb01071.x

Granholm, E. L., Panizzon, M. S., Elman, J. A., Jak, A. J., Hauger, R. L., Bondi, M. W., . . . Kremen, W. S. (2017). Pupillary responses as a biomarker of early risk for Alzheimer's disease. *Journal of Alzheimer's Disease, 56*(4), 1419-1428. doi: 10.3233/JAD-161078

Grill-Spector, K., Henson, R., & Martin, A. (2006). Repetition and the brain: neural models of stimulus-specific effects. *Trends Cogn Sci, 10*(1), 14-23. doi: 10.1016/j.tics.2005.11.006

Gross, J., Schmitz, F., Schnitzler, I., Kessler, K., Shapiro, K., Hommel, B., & Schnitzler, A. (2004). Modulation of long-range neural synchrony reflects temporal limitations of visual attention in humans. *Proc Natl Acad Sci U S A, 101*(35), 13050-13055. doi: 10.1073/pnas.0404944101

Grudzien, A., Shaw, P., Weintraub, S., Bigio, E., Mash, D. C., & Mesulam, M. M. (2007). Locus coeruleus neurofibrillary degeneration in aging, mild cognitive impairment and early Alzheimer's disease. *Neurobiol Aging, 28*(3), 327-335. doi: 10.1016/j.neurobiolaging.2006.02.007

Halliday, R., Naylor, H., Brandeis, D., Callaway, E., Yano, L., & Herzig, K. (1994). The effect of D-amphetamine, clonidine, and yohimbine on human information processing. *Psychophysiology, 31*(4), 331-337. doi: 10.1111/j.1469-8986.1994.tb02441.x

Hämmerer, D., Callaghan, M. F., Hopkins, A., Kosciessa, J., Betts, M., Cardenas-Blanco, A., . . . Dolan, R. J. (2018). Locus coeruleus integrity in old age is selectively related to memories linked with salient negative events. *Proceedings of the National Academy of Sciences, 115*(9), 2228-2233. doi: 10.1073/pnas.1712268115

Hammerschmidt, T., Kummer, M. P., Terwel, D., Martinez, A., Gorji, A., Pape, H.-C., . . . Heneka, M. T. (2013). Selective Loss of Noradrenaline Exacerbates Early Cognitive Dysfunction and Synaptic Deficits in APP/PS1 Mice. *Biol Psychiatry, 73*(5), 454-463. doi: 10.1016/j.biopsych.2012.06.013

Han, S. W., Eaton, H. P., & Marois, R. (2018). Functional Fractionation of the Cingulo-opercular Network: Alerting Insula and Updating Cingulate. *Cerebral Cortex*, bhy130-bhy130. doi: 10.1093/cercor/bhy130

Hawkins, H. L., Hillyard, S. A., Luck, S. J., Mouloua, M., Downing, C. J., & Woodward, D. P. (1990). Visual attention modulates signal detectability. *J Exp Psychol Hum Percept Perform, 16*(4), 802-811. doi: 10.1037//0096-1523.16.4.802

Heath, T. P., Melichar, J. K., Nutt, D. J., & Donaldson, L. F. (2006). Human taste thresholds are modulated by serotonin and noradrenaline. *Journal of Neuroscience, 26*(49), 12664-12671. doi: 10.1523/JNEUROSCI.3459-06

Hedges, D., Janis, R., Mickelson, S., Keith, C., Bennett, D., & Brown, B. L. (2016). P300 Amplitude in Alzheimer's Disease:A Meta-Analysis and Meta-Regression. *Clinical EEG and Neuroscience, 47*(1), 48-55. doi: 10.1177/1550059414550567

Heneka, M., Nadrigny, F., Regen, T., Martinez-Hernandez, A., Dumitrescu-Ozimek, L., Terwel, D., . . . Kummer, M. P. (2010). Locus ceruleus controls Alzheimer's disease pathology by modulating microglial functions through norepinephrine. *Proceedings of the National Academy of Sciences, 107*(13), 6058-6063. doi: 10.1073/pnas.0909586107

Heneka, M., Ramanathan, M., Jacobs, A., Dumitrescu-Ozimek, L., Bilkei-Gorzo, A., Debeir, T., . . . Staufenbiel, M. (2006). Locus Ceruleus degeneration promotes Alzheimer pathogenesis in amyloid precursor protein 23 transgenic mice. *J Neurosci, 26*, 1343-1354. doi: 10.1523/JNEUROSCI.4236-05.2006

Henson, R. N. A., & Rugg, M. D. (2003). Neural response suppression, haemodynamic repetition effects, and behavioural priming. *Neuropsychologia, 41*(3), 263-270. doi: 10.1016/S0028-3932(02)00159-8

Herscovitch, P., Markham, J., & Raichle, M. (1983). Brain blood flow measured with intravenous H215O. I. Theory and error analysis. *Journal of Nuclear Medicine, 24*(9), 782-789.

Hillstrom, A. P., Shapiro, K. L., & Spence, C. (2002). Attentional limitations in processing sequentially presented vibrotactile targets. *Percept Psychophys, 64*(7), 1068-1082. doi: 10.3758/bf03194757

Hommel, B., Kessler, K., Schmitz, F., Gross, J., Akyurek, E., Shapiro, K., & Schnitzler, A. (2006). How the brain blinks: towards a neurocognitive model of the attentional blink. *Psychol Res, 70*(6), 425-435. doi: 10.1007/s00426-005-0009-3

Horvath, A., Szucs, A., Csukly, G., Sakovics, A., Stefanics, G., & Kamondi, A. (2018). EEG and ERP biomarkers of Alzheimer's disease: a critical review. *Front Biosci (Landmark Ed), 23*, 183-220. doi: 10.2741/4587

Hou, R., Freeman, C., Langley, R., Szabadi, E., & Bradshaw, C. (2005). Does modafinil activate the locus coeruleus in man? Comparison of modafinil and clonidine on arousal and autonomic functions in human volunteers. *Psychopharmacology, 181*(3), 537-549. doi: 10.1007/s00213-005-0013-8

Huang, W. J., Chen, W. W., & Zhang, X. (2015). The neurophysiology of P 300-an integrated review. *Eur Rev Med Pharmacol Sci, 19*(8), 1480-1488.

Iba, M., McBride, J. D., Guo, J. L., Zhang, B., Trojanowski, J. Q., & Lee, V. M.-Y. (2015). Tau pathology spread in PS19 tau transgenic mice following locus coeruleus (LC) injections of synthetic tau fibrils is determined by the LC's afferent and efferent connections. *Acta Neuropathologica, 130*(3), 349-362. doi: 10.1007/s00401-015-1458-4

Iragui, V. J., Kutas, M., Mitchiner, M. R., & Hillyard, S. A. (1993). Effects of aging on event-related brain potentials and reaction times in an auditory oddball task. *Psychophysiology, 30*(1), 10-22. doi: 10.1111/j.1469-8986.1993.tb03200.x

Isaak, M. I., Shapiro, K. L., & Martin, J. (1999). The attentional blink reflects retrieval competition among multiple rapid serial visual presentation items: Tests of an interference model. *Journal of Experimental Psychology: Human Perception and Performance, 25*(6), 1774-1792. doi: 10.1037/0096-1523.25.6.1774

Ivanova, S., Rajkowski, J., Silakov, V., Watanabe, T., & Aston-Jones, G. (1997). Local chemomanipulations of locus coeruleus (LC) activity in monkeys alter cortical event-related potentials (ERPs) and task performance. *Soc Neurosci Abst, 23*, 1587.

Jack, C. R., Jr., Albert, M. S., Knopman, D. S., McKhann, G. M., Sperling, R. A., Carrillo, M. C., . . . Phelps, C. H. (2011). Introduction to the recommendations from the National Institute on Aging-Alzheimer's Association workgroups on diagnostic guidelines for Alzheimer's disease. *Alzheimers Dement, 7*(3), 257-262. doi: 10.1016/j.jalz.2011.03.004

Jacobs, H. I., Becker, A., Kwong, K., Uquillas, F. d. O., Sperling, R. A., & Johnson, K. A. (2018). Locus coeruleus signal intensity is associated with entorhinal tau pathology at higher levels of amyloid burden. *Alzheimer's & Dementia: The Journal of the Alzheimer's Association, 14*(7), P509-P510. doi: 10.1016/j.jalz.2018.06.490

Jardanhazi-Kurutz, D., Kummer, M. P., Terwel, D., Vogel, K., Thiele, A., & Heneka, M. T. (2011). Distinct adrenergic system changes and neuroinflammation in response to induced locus ceruleus degeneration in APP/PS1 transgenic mice. *Neuroscience, 176*, 396-407. doi: 10.1016/j.neuroscience.2010.11.052

Jenkins, P. O., Mehta, M. A., & Sharp, D. J. (2016). Catecholamines and cognition after traumatic brain injury. *Brain, 139*(9), 2345-2371. doi: 10.1093/brain/aww128

Jentsch, J. D., Aarde, S. M., & Seu, E. (2009). Effects of atomoxetine and methylphenidate on performance of a lateralized reaction time task in rats. *Psychopharmacology (Berl), 202*(1-3), 497-504. doi: 10.1007/s00213-008-1181-0

Jepma, M., & Nieuwenhuis, S. (2011). Pupil diameter predicts changes in the exploration–exploitation trade-off: Evidence for the adaptive gain theory. *Journal of Cognitive Neuroscience, 23*(7), 1587-1596. doi: 10.1162/jocn.2010.21548

Jiang, S., Qu, C., Wang, F., Liu, Y., Qiao, Z., Qiu, X., . . . Yang, Y. (2015). Using event-related potential P300 as an electrophysiological marker for differential diagnosis and to predict the progression of mild cognitive impairment: a meta-analysis. *Neurological Sciences, 36*(7), 1105-1112. doi: 10.1007/s10072-015-2099-z

Jolicoeur, P. (1999a). Concurrent response-selection demands modulate the attentional blink. *Journal of Experimental Psychology: Human Perception and Performance, 25*(4), 1097-1113. doi: 10.1037/0096-1523.25.4.1097

Jolicoeur, P. (1999b). Restricted attentional capacity between sensory modalities. *Psychon Bull Rev, 6*(1), 87-92. doi: 10.3758/bf03210813

Joseph, K., & Sitaram, N. (1989). The effect of clonidine on auditory P300. *Psychiatry research, 28*(3), 255-262. doi: 10.1016/0165-1781(89)90206-0

Joshi, S., Li, Y., Kalwani, R. M., & Gold, J. I. (2016). Relationships between Pupil Diameter and Neuronal Activity in the Locus Coeruleus, Colliculi, and Cingulate Cortex. *Neuron, 89*(1-14) doi: 10.1016/j.neuron.2015.11.028

Juckel, G., Clotz, F., Frodl, T., Kawohl, W., Hampel, H., Pogarell, O., & Hegerl, U. (2008). Diagnostic Usefulness of Cognitive Auditory Event-Related P300 Subcomponents in Patients With Alzheimers Disease? *Journal of Clinical Neurophysiology, 25*(3), 147-152. doi: 10.1097/WNP.0b013e3181727c95

Kahnt, T., & Tobler, P. N. (2013). Salience signals in the right temporoparietal junction facilitate value-based decisions. *J Neurosci, 33*(3), 863-869. doi: 10.1523/JNEUROSCI.3531-12.2013

Kalaria, R. N. (1989). Characterization of [125I]HEAT binding to alpha 1-receptors in human brain: assessment in aging and Alzheimer's disease. *Brain Res, 501*(2), 287-294. doi: 10.1016/0006-8993(89)90645-8

Kalaria, R. N., Andorn, A. C., Tabaton, M., Whitehouse, P. J., Harik, S. I., & Unnerstall, J. R. (1989). Adrenergic receptors in aging and Alzheimer's disease: increased beta 2-receptors in prefrontal cortex and hippocampus. *J Neurochem, 53*(6), 1772-1781. doi: 10.1111/j.1471-4159.1989.tb09242.x

Kalaria, R. N., Stockmeier, C. A., & Harik, S. I. (1989). Brain microvessels are innervated by locus ceruleus noradrenergic neurons. *Neurosci Lett, 97*(1-2), 203-208. doi: 10.1016/0304-3940(89)90164-x

Kalinin, S., Polak, P. E., Lin, S. X., Sakharkar, A. J., Pandey, S. C., & Feinstein, D. L. (2012). The noradrenaline precursor L-DOPS reduces pathology in a mouse model of Alzheimer's disease. *Neurobiol Aging, 33*(8), 1651-1663. doi: 10.1016/j.neurobiolaging.2011.04.012

Kamel, N., & Malik, A. S. (2014). *EEG/ERP Analysis: Methods and Applications*: CRC Press. ISBN: 9781482224719.

Kamp, S. M., & Donchin, E. (2015). ERP and pupil responses to deviance in an oddball paradigm. *Psychophysiology, 52*(4), 460-471. doi: 10.1111/psyp.12378

Katada, E., Sato, K., Sawaki, A., Dohi, Y., Ueda, R., & Ojika, K. (2003). Long-term effects of donepezil on P300 auditory event-related potentials in patients with Alzheimer's disease. *J Geriatr Psychiatry Neurol, 16*(1), 39-43. doi: 10.1177/0891988702250561

Katayama, J., & Polich, J. (1999). Auditory and visual P300 topography from a 3 stimulus paradigm. *Clin Neurophysiol, 110*(3), 463-468. doi: 10.1016/S1388-2457(98)00035-2

Kavcic, V., & Duffy, C. J. (2003). Attentional dynamics and visual perception: mechanisms of spatial disorientation in Alzheimer's disease. *Brain, 126*, 1173-1181. doi: 10.1093/brain/awg105

Keil, A., Bradley, M. M., Hauk, O., Rockstroh, B., Elbert, T., & Lang, P. J. (2002). Large-scale neural correlates of affective picture processing. *Psychophysiology, 39*(5), 641-649. doi: 10.1111/1469-8986.3950641

Kelly, S. C., He, B., Perez, S. E., Ginsberg, S. D., Mufson, E. J., & Counts, S. E. (2017). Locus coeruleus cellular and molecular pathology during the progression of Alzheimer's disease. *Acta Neuropathologica Communications, 5*(1), 8. doi: 10.1186/s40478-017-0411-2

Keren, N. I., Lozar, C. T., Harris, K. C., Morgan, P. S., & Eckert, M. A. (2009). In vivo mapping of the human locus coeruleus. *Neuroimage, 47*(4), 1261-1267. doi: 10.1016/j.neuroimage.2009.06.012

Keren, N. I., Taheri, S., Vazey, E. M., Morgan, P. S., Granholm, A.-C. E., Aston-Jones, G. S., & Eckert, M. A. (2015). Histologic validation of locus coeruleus MRI contrast in post-mortem tissue. *Neuroimage, 113*, 235-245. doi: 10.1016/j.neuroimage.2015.03.020

Kiat, J. E. (2018). Assessing cross-modal target transition effects with a visual-auditory oddball. *International Journal of Psychophysiology* doi: 10.1016/j.ijpsycho.2018.04.010

Kim, K. H., Kim, J. H., Yoon, J., & Jung, K.-Y. (2008). Influence of task difficulty on the features of event-related potential during visual oddball task. *Neuroscience Letters, 445*(2), 179-183. doi: 10.1016/j.neulet.2008.09.004

Kok, A. (2001). On the utility of P3 amplitude as a measure of processing capacity. *Psychophysiology, 38*(3), 557-577. doi: 10.1017/s0048577201990559

Kranczioch, C., Debener, S., & Engel, A. K. (2003). Event-related potential correlates of the attentional blink phenomenon. *Cognitive Brain Research, 17*(1), 177-187. doi: 10.1016/s0926-6410(03)00092-2

Kranczioch, C., Debener, S., Schwarzbach, J., Goebel, R., & Engel, A. K. (2005). Neural correlates of conscious perception in the attentional blink. *Neuroimage, 24*(3), 704-714. doi: 10.1016/j.neuroimage.2004.09.024

Krebs, N., Langkammer, C., Goessler, W., Ropele, S., Fazekas, F., Yen, K., & Scheurer, E. (2014). Assessment of trace elements in human brain using inductively coupled plasma mass spectrometry. *J Trace Elem Med Biol, 28*(1), 1-7. doi: 10.1016/j.jtemb.2013.09.006

Krebs, R. M., Fias, W., Achten, E., & Boehler, C. N. (2013). Picture novelty attenuates semantic interference and modulates concomitant neural activity in the anterior cingulate cortex and the locus coeruleus. *Neuroimage, 74*, 179-187. doi: 10.1016/j.neuroimage.2013.02.027

Krebs, R. M., Park, H. R. P., Bombeke, K., & Boehler, C. N. (2018). Modulation of locus coeruleus activity by novel oddball stimuli. *Brain Imaging and Behavior, 12*(2), 577-584. doi: 10.1007/s11682-017-9700-4

Kummer, M. P., Hammerschmidt, T., Martinez, A., Terwel, D., Eichele, G., Witten, A., . . . Heneka, M. T. (2014). Ear2 Deletion Causes Early Memory and Learning Deficits in APP/PS1 Mice. *The Journal of Neuroscience, 34*(26), 8845-8854. doi: 10.1523/JNEUROSCI.4027-13.2014

Lai, C.-L., Lin, R.-T., Liou, L.-M., & Liu, C.-K. (2010). The role of event-related potentials in cognitive decline in Alzheimer's disease. *Clinical Neurophysiology, 121*(2), 194-199. doi: 10.1016/j.clinph.2009.11.001

Langley, J., Huddleston, D. E., Liu, C. J., & Hu, X. (2017). Reproducibility of locus coeruleus and substantia nigra imaging with neuromelanin sensitive MRI. *Magnetic Resonance*

Materials in Physics, Biology and Medicine, 30(2), 121-125. doi: 10.1007/s10334-016-0590-z

Lee, M.-S., Lee, S.-H., Moon, E.-O., Moon, Y.-J., Kim, S., Kim, S.-H., & Jung, I.-K. (2013). Neuropsychological correlates of the P300 in patients with Alzheimer's disease. *Progress in Neuro-Psychopharmacology and Biological Psychiatry, 40*, 62-69. doi: 10.1016/j.pnpbp.2012.08.009

Liu, K. Y., Acosta-Cabronero, J., Cardenas-Blanco, A., Loane, C., Berry, A. J., Betts, M. J., . . . Hämmerer, D. (2019). In vivo visualization of age-related differences in the locus coeruleus. *Neurobiol Aging, 74*, 101-111. doi: 10.1016/j.neurobiolaging.2018.10.014

Liu, K. Y., Marijatta, F., Hammerer, D., Acosta-Cabronero, J., Duzel, E., & Howard, R. J. (2017). Magnetic resonance imaging of the human locus coeruleus: A systematic review. *Neurosci Biobehav Rev, 83*, 325-355. doi: 10.1016/j.neubiorev.2017.10.023

Lovelace, C., Duncan, C., & Kaye, W. (1996). *Effects of clonidine on event-related potential indices of auditory and visual information processing*. In *Psychophysiology* (Vol. 33, pp. S56-S56). 1010 VERMONT AVE NW SUITE 1100, WASHINGTON, DC 20005: SOC PSYCHOPHYSIOL RES

Luck, S. J. (1998). Sources of dual-task interference: Evidence from human electrophysiology. *Psychol Sci, 9*(3), 223-227. doi: 10.1111/1467-9280.00043

Luck, S. J. (2005). *An Introduction to the Event-related Potential Technique*. Cambridge, MA: MIT Press. ISBN: 9780262621960.

Luck, S. J., Vogel, E. K., & Shapiro, K. L. (1996). Word meanings can be accessed but not reported during the attentional blink. *Nature, 383*, 616. doi: 10.1038/383616a0

Luo, Y., Zhou, J., Li, M. X., Wu, P. F., Hu, Z. L., Ni, L., . . . Wang, F. (2015). Reversal of aging-related emotional memory deficits by norepinephrine via regulating the stability of surface AMPA receptors. *Aging Cell, 14*(2), 170-179. doi: 10.1111/acel.12282

Lykken, D. T. (1972). Range correction applied to heart rate and to GSR data. *Psychophysiology, 9*(3), 373-379. doi: 10.1111/j.1469-8986.1972.tb03222.x

Lyness, S. A., Zarow, C., & Chui, H. C. (2003). Neuron loss in key cholinergic and aminergic nuclei in Alzheimer disease: a meta-analysis. *Neurobiol Aging, 24*(1), 1-23. doi: 10.1016/s0197-4580(02)00057-x

MacLean, M. H., & Arnell, K. M. (2012). A conceptual and methodological framework for measuring and modulating the attentional blink. *Attention, Perception, & Psychophysics, 74*(6), 1080-1097. doi: 10.3758/s13414-012-0338-4

Manaye, K. F., McIntire, D. D., Mann, D. M., & German, D. C. (1995). Locus coeruleus cell loss in the aging human brain: a non-random process. *J Comp Neurol, 358*(1), 79-87. doi: 10.1002/cne.903580105

Mann, D. M., & Yates, P. O. (1974). Lipoprotein pigments--their relationship to ageing in the human nervous system. II. The melanin content of pigmented nerve cells. *Brain, 97*(3), 489-498. doi: 10.1093/brain/97.1.489

Manunta, Y., & Edeline, J. M. (2004). Noradrenergic induction of selective plasticity in the frequency tuning of auditory cortex neurons. *Journal of Neurophysiology, 92*(3), 1445-1463. doi: 10.1152/jn.00079.2004

Marcantoni, W. S., Lepage, M., Beaudoin, G., Bourgouin, P., & Richer, F. (2003). Neural correlates of dual task interference in rapid visual streams: an fMRI study. *Brain Cogn, 53*(2), 318-321. doi: 10.1016/s0278-2626(03)00134-9

Marchak, F., & Steinhauer, S. R. (2011). Fundamentals of Pupillary Measures and Eye Movements. 6 - Analysis of Pupillary Data. Retrieved from www.wpic.pitt.edu/research/biometrics/SPR%202011%20Workshop/SPR2011%20Workshop%20Pupil%20Analysis.ppt on 21. September 2017.

Maris, E., & Oostenveld, R. (2007). Nonparametric statistical testing of EEG- and MEG-data. *J Neurosci Methods, 164*(1), 177-190. doi: 10.1016/j.jneumeth.2007.03.024

Marois, R., & Ivanoff, J. (2005). Capacity limits of information processing in the brain. *Trends Cogn Sci, 9*(6), 296-305. doi: 10.1016/j.tics.2005.04.010

Marois, R., Yi, D. J., & Chun, M. M. (2004). The neural fate of consciously perceived and missed events in the attentional blink. *Neuron, 41*(3), 465-472. doi: 10.1016/S0896-6273(04)00012-1

Martens, S., Elmallah, K., London, R., & Johnson, A. (2006). Cuing and stimulus probability effects on the P3 and the AB. *Acta Psychol (Amst), 123*(3), 204-218. doi: 10.1016/j.actpsy.2006.01.001

Martens, S., Munneke, J., Smid, H., & Johnson, A. (2006). Quick minds don't blink: Electrophysiological correlates of individual differences in attentional selection. *Journal of Cognitive Neuroscience, 18*(9), 1423-1438. doi: 10.1162/jocn.2006.18.9.1423

Martens, S., & Wyble, B. (2010). The attentional blink: past, present, and future of a blind spot in perceptual awareness. *Neurosci Biobehav Rev, 34*(6), 947-957. doi: 10.1016/j.neubiorev.2009.12.005

McArthur, G., Budd, T., & Michie, P. (1999). The attentional blink and P300. *NeuroReport, 10*(17), 3691-3695.

McCarthy, G., Luby, M., Gore, J., & Goldman-Rakic, P. (1997). Infrequent events transiently activate human prefrontal and parietal cortex as measured by functional MRI. *J Neurophysiol, 77*(3), 1630-1634. doi: 10.1152/jn.1997.77.3.1630

McGinley, M. J., Vinck, M., Reimer, J., Batista-Brito, R., Zagha, E., Cadwell, C. R., . . . McCormick, D. A. (2015). Waking state: rapid variations modulate neural and behavioral responses. *Neuron, 87*(6), 1143-1161. doi: 10.1016/j.neuron.2015.09.012

McKhann, G. M., Knopman, D. S., Chertkow, H., Hyman, B. T., Jack, C. R., Jr., Kawas, C. H., . . . Phelps, C. H. (2011). The diagnosis of dementia due to Alzheimer's disease: recommendations from the National Institute on Aging-Alzheimer's Association workgroups on diagnostic guidelines for Alzheimer's disease. *Alzheimers Dement, 7*(3), 263-269. doi: 10.1016/j.jalz.2011.03.005

Michel, C. M. (2009). *Electrical Neuroimaging*: Cambridge University Press. ISBN: 9780521879798.

Minzenberg, M. J., Watrous, A. J., Yoon, J. H., Ursu, S., & Carter, C. S. (2008). Modafinil shifts human locus coeruleus to low-tonic, high-phasic activity during functional MRI. *Science, 322*(5908), 1700-1702. doi: 10.1126/science.1164908

Miyoshi, F., Ogawa, T., Kitao, S.-i., Kitayama, M., Shinohara, Y., Takasugi, M., . . . Kaminou, T. (2013). Evaluation of Parkinson Disease and Alzheimer Disease with the Use of Neuromelanin MR Imaging and 123I-Metaiodobenzylguanidine Scintigraphy. *American Journal of Neuroradiology, 34*(11), 2113-2118. doi: 10.3174/ajnr.A3567

Mohamed, N. V., Herrou, T., Plouffe, V., Piperno, N., & Leclerc, N. (2013). Spreading of tau pathology in Alzheimer's disease by cell-to-cell transmission. *European Journal of Neuroscience, 37*(12), 1939-1948. doi: 10.1111/ejn.12229

Mohanty, A., Gitelman, D. R., Small, D. M., & Mesulam, M. M. (2008). The spatial attention network interacts with limbic and monoaminergic systems to modulate motivation-induced attention shifts. *Cereb Cortex, 18*(11), 2604-2613. doi: 10.1093/cercor/bhn021

Moore, R. Y., & Bloom, F. E. (1979). Central Catecholamine Neuron Systems: Anatomy and Physiology of the Norepinephrine and Epinephrine Systems. *Annual Review of Neuroscience, 2*(1), 113-168. doi: 10.1146/annurev.ne.02.030179.000553

Morris, J. C., Heyman, A., Mohs, R. C., Hughes, J. P., van Belle, G., Fillenbaum, G., . . . Clark, C. (1989). The Consortium to Establish a Registry for Alzheimer's Disease (CERAD). Part I. Clinical and neuropsychological assessment of Alzheimer's disease. *Neurology, 39*(9), 1159-1165. doi: 10.1212/wnl.39.9.1159

Morrison, C., Rabipour, S., Knoefel, F., Sheppard, C., & Taler, V. (2018). Auditory Event-related Potentials in Mild Cognitive Impairment and Alzheimer's Disease. *Current Alzheimer Research, 15*(8), 702-715. doi: 10.2174/1567205015666180123123209

Mouton, P. R., Pakkenberg, B., Gundersen, H. J. G., & Price, D. L. (1994). Absolute number and size of pigmented locus coeruleus neurons in young and aged individuals. *Journal of Chemical Neuroanatomy, 7*(3), 185-190. doi: 10.1016/0891-0618(94)90028-0

Murphy, P. R., O'Connell, R. G., O'Sullivan, M., Robertson, I. H., & Balsters, J. H. (2014). Pupil diameter covaries with BOLD activity in human locus coeruleus. *Hum Brain Mapp, 35*(8), 4140-4154. doi: 10.1002/hbm.22466

Murphy, P. R., Robertson, I. H., Balsters, J. H., & O'Connell R, G. (2011). Pupillometry and P3 index the locus coeruleus-noradrenergic arousal function in humans. *Psychophysiology, 48*(11), 1532-1543. doi: 10.1111/j.1469-8986.2011.01226.x

Naidich, T. P., Duvernoy, H. M., Delman, B. N., Sorensen, A. G., Kollias, S. S., & Haacke, E. M. (2009). *Duvernoy's Atlas of the Human Brain Stem and Cerebellum: High-Field MRI, Surface Anatomy, Internal Structure, Vascularization and 3 D Sectional Anatomy*. Vienna: Springer ISBN: 9783211739716.

Navarra, R. L., Clark, B. D., Gargiulo, A. T., & Waterhouse, B. D. (2017). Methylphenidate enhances early-stage sensory processing and rodent performance of a visual signal detection task. *Neuropsychopharmacology, 42*(6), 1326. doi: 10.1038/npp.2016.267

Niendam, T. A., Laird, A. R., Ray, K. L., Dean, Y. M., Glahn, D. C., & Carter, C. S. (2012). Meta-analytic evidence for a superordinate cognitive control network subserving diverse executive functions. *Cognitive, Affective, & Behavioral Neuroscience, 12*(2), 241-268. doi: 10.3758/s13415-011-0083-5

Nieuwenhuis, S., Aston-Jones, G., & Cohen, J. D. (2005). Decision making, the P3, and the locus coeruleus-norepinephrine system. *Psychological Bulletin, 131*(4), 510-532. doi: 10.1037/0033-2909.131.4.510

Nieuwenhuis, S., De Geus, E. J., & Aston-Jones, G. (2011). The anatomical and functional relationship between the P3 and autonomic components of the orienting response. *Psychophysiology, 48*(2), 162-175. doi: 10.1111/j.1469-8986.2010.01057.x

Nieuwenhuis, S., Gilzenrat, M. S., Holmes, B. D., & Cohen, J. D. (2005). The role of the locus coeruleus in mediating the attentional blink: a neurocomputational theory. *Journal of Experimental Psychology: General, 134*(3), 291. doi: 10.1037/0096-3445.134.3.291

O'Connell, R. G., Balsters, J. H., Kilcullen, S. M., Campbell, W., Bokde, A. W., Lai, R., . . . Robertson, I. H. (2012). A simultaneous ERP/fMRI investigation of the P300 aging effect. *Neurobiol Aging, 33*(10), 2448-2461. doi: 10.1016/j.neurobiolaging.2011.12.021

Ohtsuka, C., Sasaki, M., Konno, K., Koide, M., Kato, K., Takahashi, J., . . . Terayama, Y. (2013). Changes in substantia nigra and locus coeruleus in patients with early-stage Parkinson's disease using neuromelanin-sensitive MR imaging. *Neuroscience Letters, 541*, 93-98. doi: 10.1016/j.neulet.2013.02.012

Olivieri, P., Lagarde, J., Lehericy, S., Valabrègue, R., Michel, A., Macé, P., . . . Sarazin, M. (2019). Early alteration of the locus coeruleus in phenotypic variants of Alzheimer's disease. *Annals of Clinical and Translational Neurology, 6*(7), 1345-1351. doi: 10.1002/acn3.50818

Oostenveld, R., Fries, P., Maris, E., & Schoffelen, J. M. (2011). FieldTrip: Open source software for advanced analysis of MEG, EEG, and invasive electrophysiological data. *Comput Intell Neurosci, 2011*, 156869. doi: 10.1155/2011/156869

Papadaniil, C. D., Kosmidou, V. E., Tsolaki, A., Tsolaki, M., Kompatsiaris, I. Y., & Hadjileontiadis, L. J. (2016). Cognitive MMN and P300 in mild cognitive impairment and Alzheimer's disease: A high density EEG-3D vector field tomography approach. *Brain research, 1648*, 425-433. doi: 10.1016/j.brainres.2016.07.043

Papesh, M. H., & Guevara Pinto, J. D. (2019). Spotting rare items makes the brain "blink" harder: Evidence from pupillometry. *Atten Percept Psychophys* doi: 10.3758/s13414-019-01777-6

Parasuraman, R., & Haxby, J. V. (1993). Attention and brain function in Alzheimer's disease: A review. *Neuropsychology, 7*(3), 242. doi: 10.1037/0894-4105.7.3.242

Pardo, J. V., Fox, P. T., & Raichle, M. E. (1991). Localization of a human system for sustained attention by positron emission tomography. *Nature, 349*(6304), 61-64. doi: 10.1038/349061a0

Pariyadath, V., & Eagleman, D. M. (2008). Brief subjective durations contract with repetition. *J Vis, 8*(16), 11-11. doi: 10.1167/8.16.11

Parra, M. A., Ascencio, L. L., Urquina, H. F., Manes, F., & Ibanez, A. M. (2012). P300 and neuropsychological assessment in mild cognitive impairment and Alzheimer dementia. *Front Neurol, 3*, 172. doi: 10.3389/fneur.2012.00172

Pedroso, R. V., Fraga, F. J., Corazza, D. I., Andreatto, C. A. A., de Melo Coelho, F. G., Costa, J. L. R., & Santos-Galduróz, R. F. (2012). P300 latency and amplitude in Alzheimer's disease: a systematic review. *Brazilian Journal of Otorhinolaryngology, 78*(4), 126-132. doi: 10.1590/S1808-86942012000400023

Perry, R. J., & Hodges, J. R. (1999). Attention and executive deficits in Alzheimer's disease. A critical review. *Brain, 122*(3), 383-404. doi: 10.1093/brain/122.3.383

Perry, R. J., & Hodges, J. R. (2003). Dissociation between top-down attentional control and the time course of visual attention as measured by attentional dwell time in patients with mild cognitive impairment. *European Journal of Neuroscience, 18*(2), 221-226. doi: 10.1046/j.1460-9568.2003.02754.x

Perry, R. J., Watson, P., & Hodges, J. R. (2000). The nature and staging of attention dysfunction in early (minimal and mild) Alzheimer's disease: relationship to episodic and semantic memory impairment. *Neuropsychologia, 38*(3), 252-271. doi: 10.1016/S0028-3932(99)00079-2

Pesciarelli, F., Kutas, M., Dell'Acqua, R., Peressotti, F., Job, R., & Urbach, T. P. (2007). Semantic and repetition priming within the attentional blink: An event-related brain potential (ERP) investigation study. *Biological Psychology, 76*(1), 21-30. doi: 10.1016/j.biopsycho.2007.05.003

Peters, F., Ergis, A. M., Gauthier, S., Dieudonne, B., Verny, M., Jolicoeur, P., & Belleville, S. (2012). Abnormal temporal dynamics of visual attention in Alzheimer's disease and in dementia with Lewy bodies. *Neurobiol Aging, 33*(5), 1012 e1011-1010. doi: 10.1016/j.neurobiolaging.2011.10.019

Pineda, J. A., Foote, S., & Neville, H. (1989). Effects of locus coeruleus lesions on auditory, long-latency, event-related potentials in monkey. *Journal of Neuroscience, 9*(1), 81-93. doi: 10.1523/jneurosci.09-01-00081

Pineda, J. A., & Swick, D. (1992). Visual P3-like potentials in squirrel monkey: Effects of a noradrenergic agonist. *Brain Research Bulletin, 28*(3), 485-491. doi: 10.1016/0361-9230(92)90051-x

Piquado, T., Isaacowitz, D., & Wingfield, A. (2010). Pupillometry as a Measure of Cognitive Effort in Younger and Older Adults. *Psychophysiology, 47*(3), 560-569. doi: 10.1111/j.1469-8986.2009.00947.x

Polich, J. (1989). Habituation of P300 from auditory stimuli. *Psychobiology, 17*(1), 19-28. doi: 10.3758/BF03337813

Polich, J. (1996). Meta-analysis of P300 normative aging studies. *Psychophysiology, 33*(4), 334-353. doi: 10.1111/j.1469-8986.1996.tb01058.x

Polich, J., & Corey-Bloom, J. (2005). Alzheimers Disease and P300: Review and Evaluation of Task and Modality. *Current Alzheimer Research, 2*(5), 515-525. doi: 10.2174/156720505774932214

Porter, G., Troscianko, T., & Gilchrist, I. D. (2007). Effort during visual search and counting: Insights from pupillometry. *The Quarterly Journal of Experimental Psychology, 60*(2), 211-229. doi: 10.1080/17470210600673818

Posner, M. I. (1992). Attention as a cognitive and neural system. *Current directions in psychological science, 1*(1), 11-14. doi: 10.1111/1467-8721.ep10767759

Posner, M. I., & Driver, J. (1992). The neurobiology of selective attention. *Curr Opin Neurobiol, 2*(2), 165-169. doi: 10.1016/0959-4388(92)90006-7

Posner, M. I., & Petersen, S. E. (1990). The attention system of the human brain. *Annual Review of Neuroscience, 13*(1), 25-42. doi: 10.1146/annurev.ne.13.030190.000325

Posner, M. I., Petersen, S. E., Fox, P. T., & Raichle, M. E. (1988). Localization of cognitive operations in the human brain. *Science, 240*(4859), 1627-1631. doi: 10.1126/science.3289116

Potter, M. C., Chun, M. M., Banks, B. S., & Muckenhoupt, M. (1998). Two attentional deficits in serial target search: The visual attentional blink and an amodal task-switch deficit. *Journal of Experimental Psychology: Learning, Memory, and Cognition, 24*(4), 979-992. doi: 10.1037/0278-7393.24.4.979

Qiyuan, J., Richer, F., Wagoner, B. L., & Beatty, J. (1985). The pupil and stimulus probability. *Psychophysiology, 22*(5), 530-534. doi: 10.1111/j.1469-8986.1985.tb01645.x

Raichle, M. E., Martin, W., Herscovitch, P., Mintun, M., & Markham, J. (1983). Brain blood flow measured with intravenous H215O. II. Implementation and validation. *Journal of Nuclear Medicine, 24*(9), 790-798.

Rajkowski, J. (1993). Correlations between locus coeruleus (LC) neural activity, pupil diameter and behavior in monkey support a role of LC in attention. *Soc. Neurosc., Abstract, Washington, DC, 1993*

Rajkowski, J., Kubiak, P., & Aston-Jones, G. (1994). Locus coeruleus activity in monkey: Phasic and tonic changes are associated with altered vigilance. *Brain Research Bulletin, 35*(5), 607-616. doi: 10.1016/0361-9230(94)90175-9

Rajkowski, J., Lu, W., Zhu, Y., Cohen, J., & Aston-Jones, G. (2000). Prominent projections from the anterior cingulate cortex to the locus coeruleus in Rhesus monkey. *Soc. Neurosci. Abstr., 26*(838), 15.

Raymond, J. E., Shapiro, K. L., & Arnell, K. M. (1992). Temporary suppression of visual processing in an RSVP task: an attentional blink? *J Exp Psychol Hum Percept Perform, 18*(3), 849-860. doi: 10.1037//0096-1523.18.3.849

Ritter, W., & Vaughan, H. G. (1969). Averaged evoked responses in vigilance and discrimination: a reassessment. *Science, 164*(3877), 326-328. doi: 10.1126/science.164.3877.326

Rolke, B., Heil, M., Streb, J., & Hennighausen, E. (2001). Missed prime words within the attentional blink evoke an N400 semantic priming effect. *Psychophysiology, 38*(2), 165-174. doi: 10.1111/1469-8986.3820165

Samuels, E. R., & Szabadi, E. (2008). Functional Neuroanatomy of the Noradrenergic Locus Coeruleus: Its Roles in the Regulation of Arousal and Autonomic Function Part I: Principles of Functional Organisation. *Current Neuropharmacology, 6*(3), 235-253. doi: 10.2174/157015908785777229

Sanei, S., & Chambers, J. A. (2007). *EEG Signal Processing*. United Kingdom: John Wiley & Sons. ISBN: 9780470025819.

Sara, S. J. (2009). The locus coeruleus and noradrenergic modulation of cognition. *Nature Reviews Neuroscience, 10*, 211. doi: 10.1038/nrn2573

Sasaki, M., Shibata, E., Tohyama, K., Takahashi, J., Otsuka, K., Tsuchiya, K., . . . Sakai, A. (2006). Neuromelanin magnetic resonance imaging of locus ceruleus and substantia nigra in Parkinson's disease. *NeuroReport, 17*(11), 1215-1218. doi: 10.1097/01.wnr.0000227984.84927.a7

Schindel, R., Rowlands, J., & Arnold, D. H. (2011). The oddball effect: Perceived duration and predictive coding. *J Vis, 11*(2), 17-17. doi: 10.1167/11.2.17

Schlotterer, G., Moscovitch, M., & Crapper-McLachlan, D. (1984). Visual processing deficits as assessed by spatial frequency contrast sensitivity and backward masking in normal ageing and Alzheimer's disease. *Brain, 107 (Pt 1)*, 309-325. doi: 10.1093/brain/107.1.309

Schröder, E., Kajosch, H., Verbanck, P., Kornreich, C., & Campanella, S. (2016). Methodological Considerations about the Use of Bimodal Oddball P300 in Psychiatry: Topography and Reference Effect. *Front Psychol, 7*, 1387. doi: 10.3389/fpsyg.2016.01387

Sergent, C., Baillet, S., & Dehaene, S. (2005). Timing of the brain events underlying access to consciousness during the attentional blink. *Nat Neurosci, 8*(10), 1391-1400. doi: 10.1038/nn1549

Servan-Schreiber, D., Printz, H., & Cohen, J. (1990). A network model of catecholamine effects: gain, signal-to-noise ratio, and behavior. *Science, 249*(4971), 892-895. doi: 10.1126/science.2392679

Shapiro, K., Schmitz, F., Martens, S., Hommel, B., & Schnitler, A. (2005). The neural correlates of temporal attention. *Manuscript submitted for publication*

Shapiro, K., Schmitz, F., Martens, S., Hommel, B., & Schnitzler, A. (2006). Resource sharing in the attentional blink. *NeuroReport, 17*(2), 163-166. doi: 10.1097/01.wnr.0000195670.37892.1a

Shibata, E., Sasaki, M., Tohyama, K., Kanbara, Y., Otsuka, K., Ehara, S., & Sakai, A. (2006). Age-related Changes in Locus Ceruleus on Neuromelanin Magnetic Resonance Imaging at 3 Tesla. *Magn Reson Med Sci., 5*(4), 197-200. doi: 10.2463/mrms.5.197

Shima, T., Sarna, T., Swartz, H. M., Stroppolo, A., Gerbasi, R., & Zecca, L. (1997). Binding of iron to neuromelanin of human substantia nigra and synthetic melanin: an electron paramagnetic resonance spectroscopy study. *Free Radic Biol Med, 23*(1), 110-119. doi: 10.1016/s0891-5849(96)00623-5

Shimohama, S., Taniguchi, T., Fujiwara, M., & Kameyama, M. (1986). Biochemical characterization of alpha-adrenergic receptors in human brain and changes in Alzheimer-type dementia. *J Neurochem, 47*(4), 1295-1301. doi: 10.1111/j.1471-4159.1986.tb00753.x

Siegle, G. J., Steinhauer, S. R., Carter, C. S., Ramel, W., & Thase, M. E. (2003). Do the Seconds Turn Into Hours? Relationships between Sustained Pupil Dilation in Response to Emotional Information and Self-Reported Rumination. *Cognitive Therapy and Research, 27*(3), 365-382. doi: 10.1023/a:1023974602357

Simson, R., Vaughan, H. G., & Ritter, W. (1977). The scalp topography of potentials in auditory and visual discrimination tasks. *Electroencephalography and clinical neurophysiology, 42*(4), 528-535. doi: 10.1016/0013-4694(77)90216-4

Sirvio, J., Jakala, P., Mazurkiewicz, M., Haapalinna, A., Riekkinen, P., Jr., & Riekkinen, P. J. (1993). Dose- and parameter-dependent effects of atipamezole, an alpha 2-antagonist, on the performance of rats in a five-choice serial reaction time task. *Pharmacol Biochem Behav, 45*(1), 123-129. doi: 10.1016/0091-3057(93)90095-b

Siuly, S., Li, Y., & Zhang, Y. (2017). *EEG Signal Analysis and Classification: Techniques and Applications*: Springer International Publishing. ISBN: 9783319476537.

Steinhauer, S. R., & Hakerem, G. (1992). The Pupillary Response in Cognitive Psychophysiology and Schizophrenia a. *Ann N Y Acad Sci, 658*(1), 182-204. doi: 10.1111/j.1749-6632.1992.tb22845.x

Sutton, S., Braren, M., Zubin, J., & John, E. (1965). Evoked-potential correlates of stimulus uncertainty. *Science, 150*(3700), 1187-1188. doi: 10.1126/science.150.3700.1187

Sutton, S., Tueting, P., Zubin, J., & John, E. R. (1967). Information delivery and the sensory evoked potential. *Science, 155*(3768), 1436-1439. doi: 10.1126/science.155.3768.1436

Swick, D., Pineda, J., & Foote, S. (1994). Effects of systemic clonidine on auditory event-related potentials in squirrel monkeys. *Brain Research Bulletin, 33*(1), 79-86. doi: 10.1016/0361-9230(94)90051-5

Szabadi, E. (2013). Functional neuroanatomy of the central noradrenergic system. *Journal of Psychopharmacology, 27*(8), 659-693. doi: 10.1177/0269881113490326

Szot, P., White, S. S., Greenup, J. L., Leverenz, J. B., Peskind, E. R., & Raskind, M. A. (2006). Compensatory Changes in the Noradrenergic Nervous System in the Locus Ceruleus and Hippocampus of Postmortem Subjects with Alzheimer's Disease and Dementia with Lewy Bodies. *The Journal of Neuroscience, 26*(2), 467-478. doi: 10.1523/jneurosci.4265-05.2006

Szot, P., White, S. S., Greenup, J. L., Leverenz, J. B., Peskind, E. R., & Raskind, M. A. (2007). Changes In Adrenoreceptors In The Prefrontal Cortex Of Subjects With Dementia: Evidence Of Compensatory Changes. *Neuroscience, 146*(1), 471-480. doi: 10.1016/j.neuroscience.2007.01.031

Takahashi, J., Shibata, T., Sasaki, M., Kudo, M., Yanezawa, H., Obara, S., . . . Terayama, Y. (2015). Detection of changes in the locus coeruleus in patients with mild cognitive impairment and Alzheimer's disease: High-resolution fast spin-echo T1-weighted imaging. *Geriatrics & Gerontology International, 15*(3), 334-340. doi: doi:10.1111/ggi.12280

Theofilas, P., Ehrenberg, A. J., Dunlop, S., Di Lorenzo Alho, A. T., Nguy, A., Leite, R. E. P., . . . Grinberg, L. T. (2017). Locus coeruleus volume and cell population changes during Alzheimer's disease progression: A stereological study in human postmortem brains with potential implication for early-stage biomarker discovery. *Alzheimer's & Dementia, 13*(3), 236-246. doi: 10.1016/j.jalz.2016.06.2362

Tona, K.-D., Keuken, M. C., de Rover, M., Lakke, E., Forstmann, B. U., Nieuwenhuis, S., & van Osch, M. J. P. (2017). In vivo visualization of the locus coeruleus in humans: quantifying the test–retest reliability. *Brain Structure and Function, 222*(9), 4203-4217. doi: 10.1007/s00429-017-1464-5

Trujillo Diaz, P., Summers, P., Ferrari, E., A. Zucca, F., Sturini, M., Mainardi, L., . . . Costa, A. (2016). Contrast mechanisms associated with neuromelanin-MRI: Neuromelanin-MRI Contrast. *Magn. Reson. Med., 78* doi: 10.1002/mrm.26584

Tse, P. U., Intriligator, J., Rivest, J., & Cavanagh, P. (2004). Attention and the subjective expansion of time. *Perception & psychophysics, 66*(7), 1171-1189. doi: 10.3758/BF03196844

Tsolaki, A. C., Kosmidou, V., Kompatsiaris, I., Papadaniil, C., Hadjileontiadis, L., Adam, A., & Tsolaki, M. (2017). Brain source localization of MMN and P300 ERPs in mild cognitive impairment and Alzheimer's disease: a high-density EEG approach. *Neurobiol Aging, 55*, 190-201. doi: 10.1016/j.neurobiolaging.2017.03.025

Turkington, C., & Mitchell, D. R. (2010). *The Encyclopedia of Alzheimer's Disease*: Infobase Publishing. ISBN: 9781438128580.

Usher, M., Cohen, J. D., Servan-Schreiber, D., Rajkowski, J., & Aston-Jones, G. (1999). The role of locus coeruleus in the regulation of cognitive performance. *Science, 283*(5401), 549-554. doi: 10.1126/science.283.5401.549

van Der Meer, E., Beyer, R., Horn, J., Foth, M., Bornemann, B., Ries, J., . . . Wartenburger, I. (2010). Resource allocation and fluid intelligence: Insights from pupillometry. *Psychophysiology, 47*(1), 158-169. doi: 10.1111/j.1469-8986.2009.00884.x

van Dinteren, R., Arns, M., Jongsma, M. L. A., & Kessels, R. P. C. (2014). P300 Development across the Lifespan: A Systematic Review and Meta-Analysis. *PLoS One, 9*(2), e87347. doi: 10.1371/journal.pone.0087347

van Rijn, H., Dalenberg, J. R., Borst, J. P., & Sprenger, S. A. (2012). Pupil dilation co-varies with memory strength of individual traces in a delayed response paired-associate task. *PLoS One, 7*(12), e51134. doi: 10.1371/journal.pone.0051134

Vaughan, H. G., & Ritter, W. (1970). The sources of auditory evoked responses recorded from the human scalp. *Electroencephalography and clinical neurophysiology, 28*(4), 360-367. doi: 10.1016/0013-4694(70)90228-2

Verleger, R., & Berg, P. (1991). The Waltzing Oddball. *Psychophysiology, 28*(4), 468-477. doi: doi:10.1111/j.1469-8986.1991.tb00733.x

Vogel, E. K., Luck, S. J., & Shapiro, K. L. (1998). Electrophysiological evidence for a postperceptual locus of suppression during the attentional blink. *Journal of Experimental Psychology: Human Perception and Performance, 24*(6), 1656-1674. doi: 10.1037/0096-1523.24.6.1656

von Wright, J. M. (1972). On the problem of selection in iconic memory. *Scand J Psychol, 13*(3), 159-171. doi: 10.1111/j.1467-9450.1972.tb00064.x

Wakamatsu, K., Tabuchi, K., Ojika, M., Zucca, F. A., Zecca, L., & Ito, S. (2015). Norepinephrine and its metabolites are involved in the synthesis of neuromelanin derived from the locus coeruleus. *Journal of Neurochemistry, 135*(4), 768-776. doi: 10.1111/jnc.13237

Warren, C. M., Breuer, A. T., Kantner, J., Fiset, D., Blais, C., & Masson, M. E. (2009). Target-distractor interference in the attentional blink implicates the locus coeruleus-norepinephrine system. *Psychon Bull Rev, 16*(6), 1106-1111. doi: 10.3758/PBR.16.6.1106

Watanabe, T., Tan, Z., Wang, X., Martinez-Hernandez, A., & Frahm, J. (2019). Magnetic resonance imaging of noradrenergic neurons. *Brain Struct Funct, 224*(4), 1609-1625. doi: 10.1007/s00429-019-01858-0

Waterhouse, B. D., & Woodward, D. J. (1980). Interaction of norepinephrine with cerebrocortical activity evoked by stimulation of somatosensory afferent pathways in the rat. *Experimental Neurology, 67*(1), 11-34. doi: 10.1016/0014-4886(80)90159-4

Werber, E. A., Gandelman-Marton, R., Klein, C., & Rabey, J. M. (2003). The clinical use of P300 event related potentials for the evaluation of cholinesterase inhibitors treatment

in demented patients. *J Neural Transm (Vienna), 110*(6), 659-669. doi: 10.1007/s00702-003-0817-9

Wickens, C., Kramer, A., Vanasse, L., & Donchin, E. (1983). Performance of concurrent tasks: a psychophysiological analysis of the reciprocity of information-processing resources. *Science, 221*(4615), 1080-1082. doi: 10.1126/science.6879207

Wierda, S. M., van Rijn, H., Taatgen, N. A., & Martens, S. (2012). Pupil dilation deconvolution reveals the dynamics of attention at high temporal resolution. *Proc Natl Acad Sci U S A, 109*(22), 8456-8460. doi: 10.1073/pnas.1201858109

Wolff, M. J., Scholz, S., Akyurek, E. G., & van Rijn, H. (2015). Two visual targets for the price of one? Pupil dilation shows reduced mental effort through temporal integration. *Psychon Bull Rev, 22*(1), 251-257. doi: 10.3758/s13423-014-0667-5

World-Health-Organization. (2017). *Global action plan on the public health response to dementia 2017–2025*. ISBN: 978-92-4-151348-7.

Yamamoto, M., Ficke, D. C., & Ter-Pogossian, M. M. (1982). Performance Study of PETT VI, a Positron Computed Tomograph with 288 Cesium Fluoride Detectors. *IEEE Transactions on Nuclear Science, 29*(1), 529-533. doi: 10.1109/TNS.1982.4335901

Zitnik, G. A., Clark, B. D., & Waterhouse, B. D. (2014). Effects of intracerebroventricular corticotropin releasing factor on sensory-evoked responses in the rat visual thalamus. *Brain research, 1561*, 35-47. doi: 10.1016/j.brainres.2014.02.048

Zylberberg, A., Oliva, M., & Sigman, M. (2012). Pupil dilation: a fingerprint of temporal selection during the "attentional blink". *Front Psychol, 3*, 316. doi: 10.3389/fpsyg.2012.00316

Danksagung

Großer Dank geht an meinen Doktorvater Priv.-Doz. Dr. Klaus Fließbach für die Vergabe des interessanten Themas dieser Doktorarbeit an mich. Seine Motivation, Diskussionsbereitschaft und konstruktiven Ratschläge waren mir eine hilfreiche Stütze bei der Umsetzung meines Promotionsprojektes.

Darüber hinaus möchte ich mich bei Prof. Dr. Michael Hofmann, Prof. Dr. Gerhard von der Emde und Prof. Dr. Tony Stöcker dafür bedanken, dass sie sich bereit erklärt haben, als Mitglieder meiner Prüfungskommission zu fungieren.

Mein Promotionsprojekt entstand im Deutschen Zentrum für Neurodegenerative Erkrankungen in Bonn mit Prof. Dr. Thomas Klockgether als Leiter der Klinischen Forschung. Zudem wurde die vorliegende Arbeit von der Deutschen Forschungsgemeinschaft (DFG) durch eine Sachbeihilfe (FL 715/3-1) gefördert. Ich bedanke mich für diese Möglichkeit sowie für die Bereitstellung eines optimalen wissenschaftlichen Arbeitsumfeldes. An dieser Stelle danke ich ebenfalls ganz herzlich all meinen Probanden für ihre Bereitschaft an meinen zeitintensiven und doch recht anstrengenden Experimenten teilzunehmen.

I would like to thank Dr. Hwee-Ling Lee for her helpful advice and for introducing me to data processing. Ganz besonders bedanken möchte ich mich auch bei Dr. Thomas Reber für seine Unterstützung bei der Erprobung alternativer Analysewege. An Dr. Leonie Weinhold aus dem Institut für Medizinische Biometrie, Informatik und Epidemiologie in Bonn geht mein Dank für ihre kompetente Beratung in statistischen Fragestellungen.

Ein großes Dankeschön richtet sich an Dr. Julia Bitzer für das Korrekturlesen dieser Arbeit, aber auch für ihre Freundschaft und die lustigen Abenteuer der letzten Jahre.

Zuletzt möchte ich mich von Herzen bei den wichtigsten Menschen in meinem Leben bedanken. Meine Eltern, mein Verlobter Boris sowie mein Schwiegervater in Spe gaben mir stets so viel Motivation, Kraft und Unterstützung. Durch Eure Liebe und fortwährenden Glauben an mich habe ich auch schwierige Zeiten gut überstanden.